RPP-ENV-58578, Rev. 0

Summary of the Natural System at Waste Management Area A/AX

Author Name:
A. J. Yonkofski, M. P. Bergeron
Washington River Protection Solutions, LLC
Richland, WA 99352
U.S. Department of Energy Contract DE-AC27-08RV14800

EDT/ECN: DCRF UC:
Cost Center: Charge Code:
B&R Code: Total Pages: 120

Key Words: WMA A/AX, natural system, vadose zone, hydrology, hydrogeology, groundwater, geology

Abstract: A summary of the natural system at Waste Management Area (WMA) A/AX, supporting the WMA A/AX Performance Assessment (PA). This report summarizes the previous data packages relating to the natural system of WMA A/AX. This report contains information relevant to the climate, location, geology, hydrology, and far-field vadose zone properties of WMA A/AX. This document is intended to provide a basis for discussion at the April 2015 PA scoping workshop.

APPROVED
By GE Bratton at 3:11 pm, Apr 09, 2015

DATE: Apr 13, 2015
HANFORD RELEASE

Release Approval Date Release Stamp

Approved For Public Release

RPP-ENV-58578
Revision 0

Summary of the Natural System at Waste Management Area A/AX

A. J. Yonkofski
M. P. Bergeron
Washington River Protection Solutions, LLC

Date Published
March 2015

Prepared for the U.S. Department of Energy
Office of River Protection

This page intentionally left blank.

EXECUTIVE SUMMARY

This document provides supporting information for the Natural System Working Session planned for April 1 and 2, 2015. This working session is one in a series sponsored by the U.S. Department of Energy's Office of River Protection and the State of Washington Department of Ecology. These working sessions are being used to solicit input from the working session participants and to obtain a common understanding concerning the scope, methods, and data to be used in the *Hanford Federal Facility Agreement and Consent Order* (Ecology et al. 1989).

Participating working session agency members include representatives from the U.S. Department of Energy, the U.S. Environmental Protection Agency, the U.S. Nuclear Regulatory Commission, and the State of Washington Department of Ecology as well as their contractors. Other participants in the working sessions include representatives of the tribal nations, other stakeholders groups, and members of the interested public.

The primary purpose of the Natural System Working Session is to provide a forum for detailed discussions of the important features, events, and processes related to the vadose zone and groundwater release that will need to be considered and used in the Performance Assessment for Waste Management Area A/AX. The desired outcome for this specific working session is to obtain a common understanding among working session participants concerning key features, events, and processes of the vadose zone and groundwater that will affect local-scale flow and contaminant transport processes at the Waste Management Area A/AX that will be considered the Post-Closure Performance Assessment Scenarios.

Topics that will be discussed in the working session and summarized in this document include the following.

- Geologic and Hydrogeologic Framework in the Region and the Hanford Site including:
  - Geologic history and setting
  - Major structural features
  - Major stratigraphic units
- Seismicity and other geologic hazards.
- Vadose Zone Flow and Transport System at the Waste Management Area A/AX including discussions concerning:
  - Hydrogeologic units and conditions
  - Factors affecting moisture movement in vadose zone
- Groundwater Flow and Transport System in vicinity of the Waste Management Area A/AX including discussions related to:
  - Major hydrogeologic units in groundwater
  - Flow conditions
  - Flow and transport properties at Waste Management Area A/AX.

TABLE OF CONTENTS

LIST OF FIGURES

LIST OF TABLES

LIST OF TERMS

Abbreviations and Acronyms

amsl	above mean sea level
bgs	below ground surface
BP	before present
CCU	Cold Creek unit
CERCLA	*Comprehensive Environmental Response, Compensation, and Liability Act of 1980*
CRBG	Columbia River Basalt Group
DOE	U.S. Department of Energy
DOE/RL	U.S. Department of Energy, Richland Operations Office
DQO	data quality objective
Ecology	State of Washington Department of Ecology
EIS	Environmental Impact Statement
EPA	U.S. Environmental Protection Agency
FEP	Features, Events, and Processes
FY	fiscal year
Hf	undifferentiated Hanford (formation)
HEIS	Hanford Environmental Information System
HFFACO	*Hanford Federal Facility Agreement and Consent Order*
IDF	Integrated Disposal Facility
MCL	maximum contaminant level
MPa	matric potential
NEPA	*National Environmental Policy Act of 1969*
PA	performance assessment
PNNL	Pacific Northwest National Laboratory
PUREX	Plutonium Uranium Extraction (Plant)
RCRA	*Resource Conservation and Recovery Act of 1976*
SST	single-shell tank
SST PA	DOE/ORP-2005-01, *Initial Single-Shell Tank System Performance Assessment for the Hanford Site*
STOMP	Subsurface Transport Over Multiple Phases (numeric code)
TC&WM	Tank Closure and Waste Management
UPR	unplanned release
WAC	*Washington Administrative Code*
WMA	waste management area
WTP	Waste Treatment Plant

Units

ft	foot
g	gram
gal	gallon
in.	inch
L	liter
m	meter
mg	milligram
mi^2	square mile
µg	microgram
pCi	picocurie

Hanford Formation Primary Geologic Units

CRBG	Columbia River Basalt Group
CCU	Cold Creek unit
CCU/R	undifferentiated CCU fine unit and/or Ringold Formation
H3/CCU/R	undifferentiated Hanford formation gravel and/or CCU gravel and/or Ringold Formation, unit A
H1 unit	upper gravel-dominated sequence
H2 unit	sand-dominated sequence
H3 unit	lower gravel-dominated sequence

1.0 INTRODUCTION

This document provides supporting information for the Natural System Working Session planned for April 1 and 2, 2015. This working session is one in a series sponsored by the U.S. Department of Energy's (DOE) Office of River Protection (ORP) and the State of Washington Department of Ecology (Ecology). These working sessions are being used to solicit input from the working session participants, and to obtain a common understanding concerning the scope, methods, and data to be used in the *Hanford Federal Facility Agreement and Consent Order* (HFFACO) (Ecology et al. 1989).

Participating working session agency members include representatives of the sponsoring organizations of the working sessions from DOE, the U.S. Environmental Protection Agency (EPA), the U.S. Nuclear Regulatory Commission, and Ecology as well as their contractors. Other participants in the working sessions include representatives of the tribal nations, other stakeholders groups, and members of the interested public.

The primary purpose of the Natural System Working Session is to provide a forum for discussion of three specific aspects of the Natural System at Waste Management Area (WMA) A/AX:

- **Regional and Local Hydrogeologic Framework** – Major geologic and hydrologic features, events, and processes (FEPs) within the regional framework that affect the WMA A/AX area

- **Local Vadose Zone System at WMA A/AX** – Flow and contaminant transport in unsaturated sediments within the vadose zone in vicinity of the WMA A/AX

- **Regional and Local Groundwater System** – Flow and contaminant transport in underlying unconfined aquifer system in vicinity of the WMA A/AX.

1.1 OBJECTIVE

The objective of this document is to combine published data with more recent information to provide the most current information related to flow and transport in the natural system (i.e., vadose zone and groundwater systems) beneath WMA A/AX.

The desired outcome for this specific working session is to obtain a common understanding among working session participants concerning the following.

- Geologic and Hydrogeologic Framework in the Region and the Hanford Site including:
    - Geologic history and setting
    - Major structural features
    - Major stratigraphic units
    - Seismicity and other geologic hazards.

- Vadose Zone Flow and Transport System at the WMA A/AX including discussions concerning:
  - Major hydrogeologic units and conditions
  - Extent of known contamination
  - Factors affecting moisture movement in vadose zone
  - Flow and transport properties of major units.

- Groundwater Flow and Transport System in vicinity of the WMA A/AX including discussions related to:
  - Major hydrogeologic units in groundwater
  - Flow conditions
  - Flow and transport properties at WMA A/AX.

1.2 SCOPE AND CONTENT OF REPORT

General topics that will be presented to facilitate technical discussions in the working session and summarized in this document include the following.

Section 1.0, Introduction – Describes the objectives and scope of this report.

Section 2.0, Background – Provides a brief summary of the WMA A/AX facilities.

Section 3.0, Major Features of the Natural System – Presents a general description of the major features of the natural system relevant to the WMA A/AX that include descriptions of the geology, history, stratigraphy, and structure framework of the Pasco basin, the Hanford Site, the Central Plateau, and the area in vicinity of the WMA A/AX.

Section 4.0, Vadose Zone System at Waste Management Area A/AX – Provides a discussion of conceptual models of moisture movement and contaminant transport in the vadose zone at WMA A/AX, major FEPs important to consider in conceptual models of the vadose zone during past site operations and after site closure, a brief summary of previous work, the factors affecting moisture movement, methods used to characterize moisture movement, and flow and transport parameter estimates that are recommended for use in a proposed cases for vadose zone flow and transport that should be considered in the WMA A/AX PA.

Section 5.0, Groundwater System at Waste Management Area A/AX – Provides a discussion of the key features and characteristics of the groundwater system at the Hanford Site with specific emphasis on the Central Plateau and the area in and around the WMA A/AX. Included in these descriptions are discussions of the major hydrogeologic units, their hydraulic properties, and the directions and rates of groundwater flow. This section also discusses the major FEPs important to consider in conceptual models of groundwater flow and transport in the past operations and after site closure, conceptual models of flow and contaminant transport in the groundwater system, and flow and transport parameter estimates that are recommended for use in proposed cases for groundwater flow and transport that should be considered in the WMA A/AX PA.

Section 6.0, References – Lists reference documents cited in this report.

This page intentionally left blank.

2.0 BACKGROUND INFORMATION

This Section provides an overview of the WMA A/AX. Waste Management Area A/AX (WMA A/AX or the 241-A and 241-AX Tank Farms), part of the single-shell tank (SST) system, is located in the Central Plateau (Figure 2-1), near the eastern edge of the 200 East Area (Figure 2-2). Major components of Waste Management Area A/AX include: 10 single-shell tanks (SSTs) used for waste retrieval and storage, and catch tanks, pipelines, pits and diversion boxes used to transfer waste to and from the single-shell tanks (Figure 2-3). The 241-A Tank Farm was constructed between 1954 and 1955. Six nominally 1,000,000 gallon SSTs in A Farm were designed for the storage of boiling waste generated from irradiated fuel reprocessing at the PUREX Plant. The 241-A tanks have three unique design features: airlift circulators for cooling the boiling wastes, an underground vessel ventilation header to remove condensate and volatiles, and laterals 10 ft beneath the tank for leak detection. The 241-A tanks were vented to an underground vessel ventilation header that connected to AX Farm and later to the 241-AY Tank Farm. The purpose of this ventilation header was to remove off-gas and water vapor from these tanks, which were often operated with the wastes at boiling conditions. The 241-A tanks were originally designed to contain liquid and solid wastes at a maximum temperature of 280 °F (RPP-10435, *Single-Shell Tank System Integrity Assessment Report*, pp. A-42). After installation of airlift circulators, the operating temperature limit was revised to a maximum of 300 °F at the tank bottom (RPP-10435, pp. A-54). Wastes at higher temperatures could cause buckling of the steel liner and/or structural damage to the concrete shell.

The 241-AX Tank Farm was constructed between 1963 and 1964 and contains four 1,000,000-gal capacity SSTs. The 241-AX tanks were originally designed to contain liquid and solid wastes at a maximum temperature of 350 °F (RPP-10435, pp. A-43). Wastes at higher temperatures could cause buckling of the steel liner and/or damage to the concrete shell. The 241-AX tanks were vented to an underground vessel ventilation header that connected to A Farm and later to the 241-AY Tank Farm. Like the A-Farm, the purpose of this ventilation header was to remove off-gas and water vapor from the tanks, which were often operated with the wastes at boiling conditions.

To support the transfer and storage of waste within WMA A/AX SSTs, there is a complex waste transfer system of pipelines (transfer lines), diversion boxes, vaults, valve pits, and other miscellaneous structures.

At least fifteen unplanned releases (UPRs) have occurred within or near WMA A/AX. The largest ones are associated with leaks in pipelines or diversion boxes, releases from inlet/outlet ports of the SSTs, or leaks from the SSTs. HNF-EP-0182, Rev. 223, *Waste Tank Summary Report for Month Ending October 31, 2006*, classified five tanks in WMA A/AX as assumed leakers (Figure 2-3): 241-A-103 [A-103], 241-A-104 [A-104], 241-A-105 [A-105], 241-AX-102 [AX-102], and 241-AX-104 [AX-104]. Tanks A-103, AX-102, and AX-104 were assumed to have leaked based on fluctuating waste levels in the 1970s and 1980s (HNF-EP-0182). Individual assessments have since concluded that these fluctuations in waste level were due to the waste properties and likely a combination of evaporation, gas release events, and a highly irregular waste surface within each tank (RPP-ASMT-42278, *Tank 241-A-103 Leak Assessment Report;* RPP-ASMT-42628, *Tank 241-AX-102 Integrity Assessment Report*; RPP-ASMT-57574, *Tank 241-AX-104 Integrity Assessment Report*). RPP-14430, *Subsurface Conditions Description of the C and A-AX Waste Management Area*, provides more detail on these UPR sites.

Figure 2-1. Hanford Site and its Location in Washington State

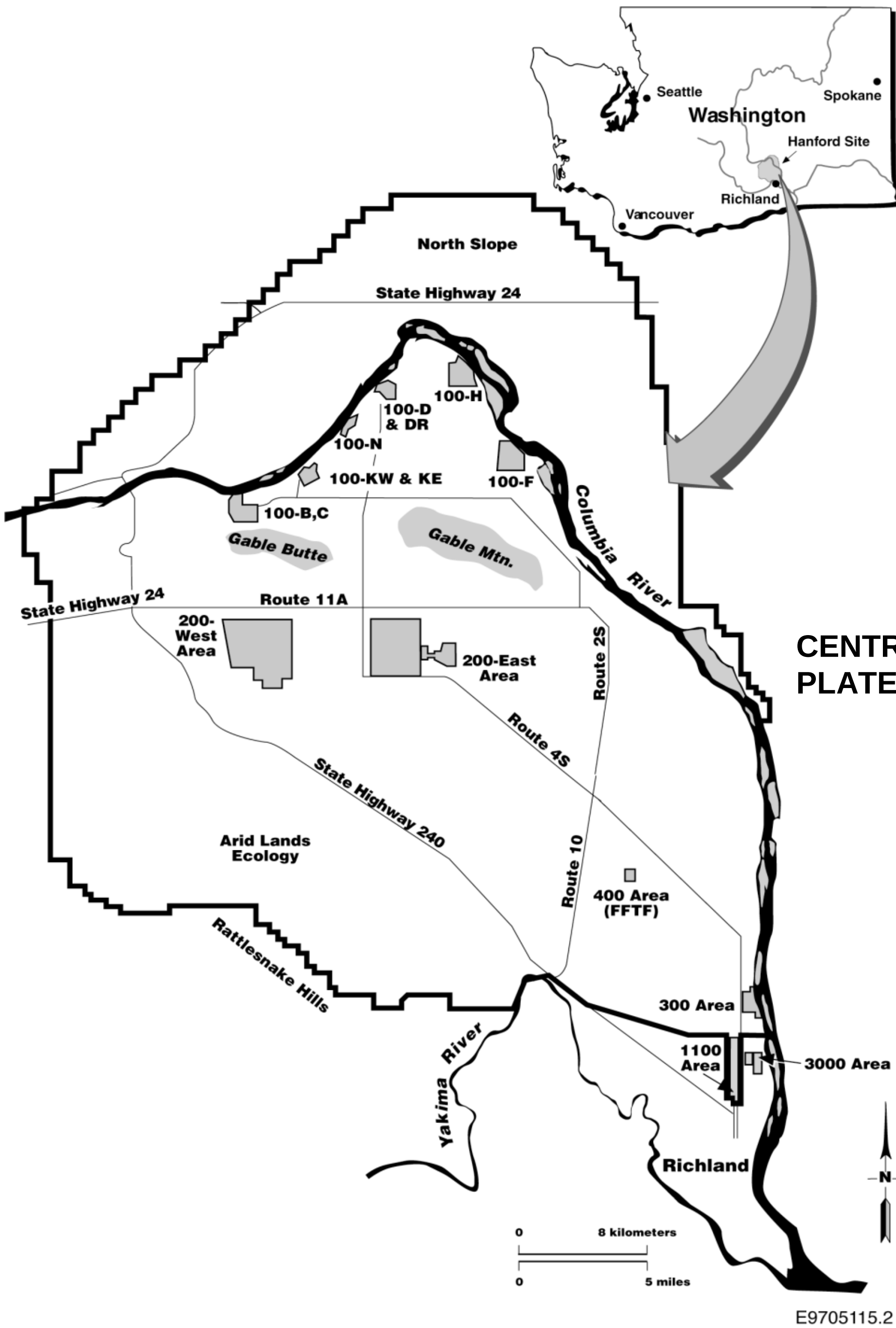

Figure 2-2. Facilities in the 200 Areas of Hanford's Central Plateau

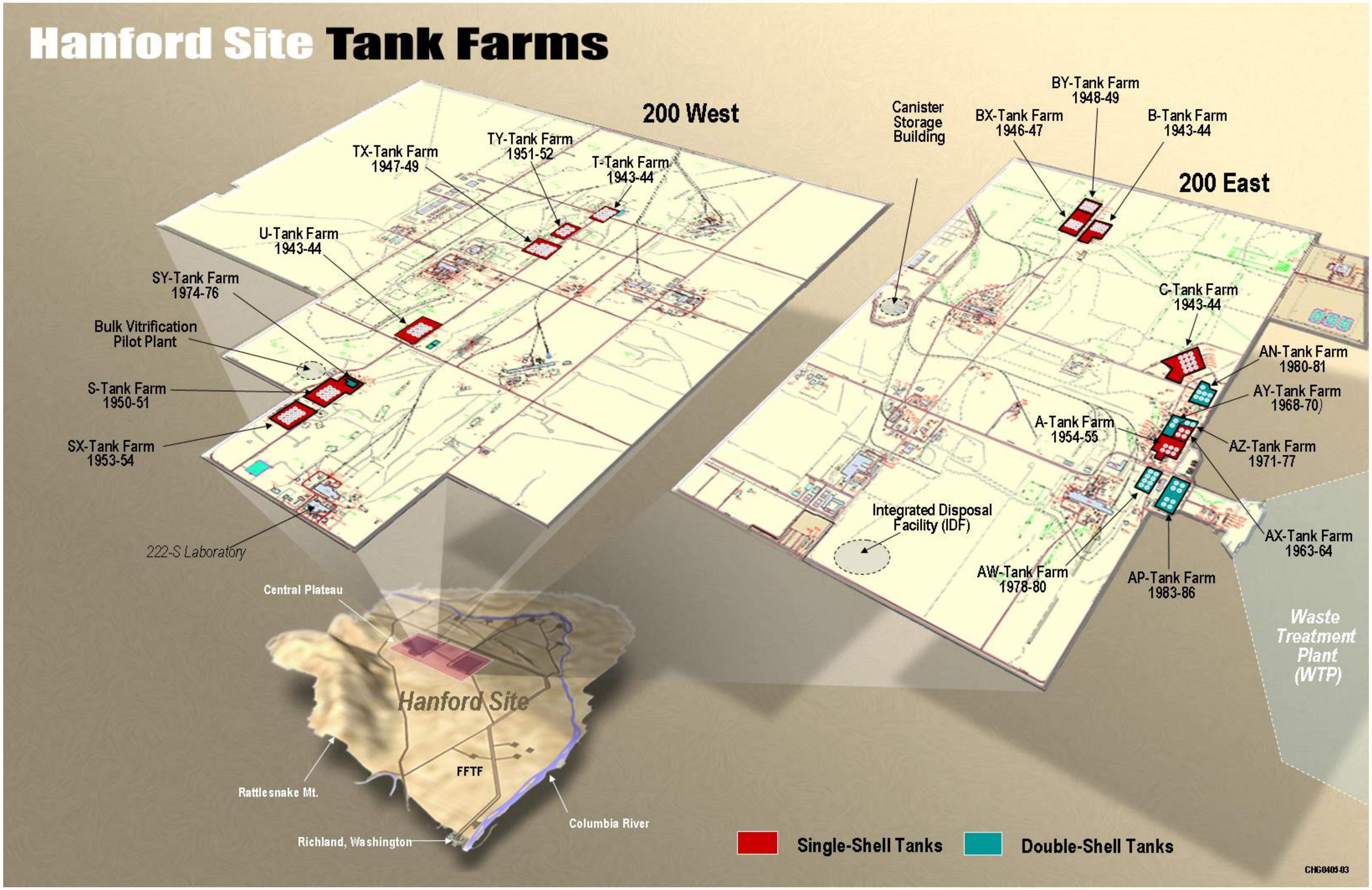

Figure 2-3. Location Map of Waste Management Area A/AX

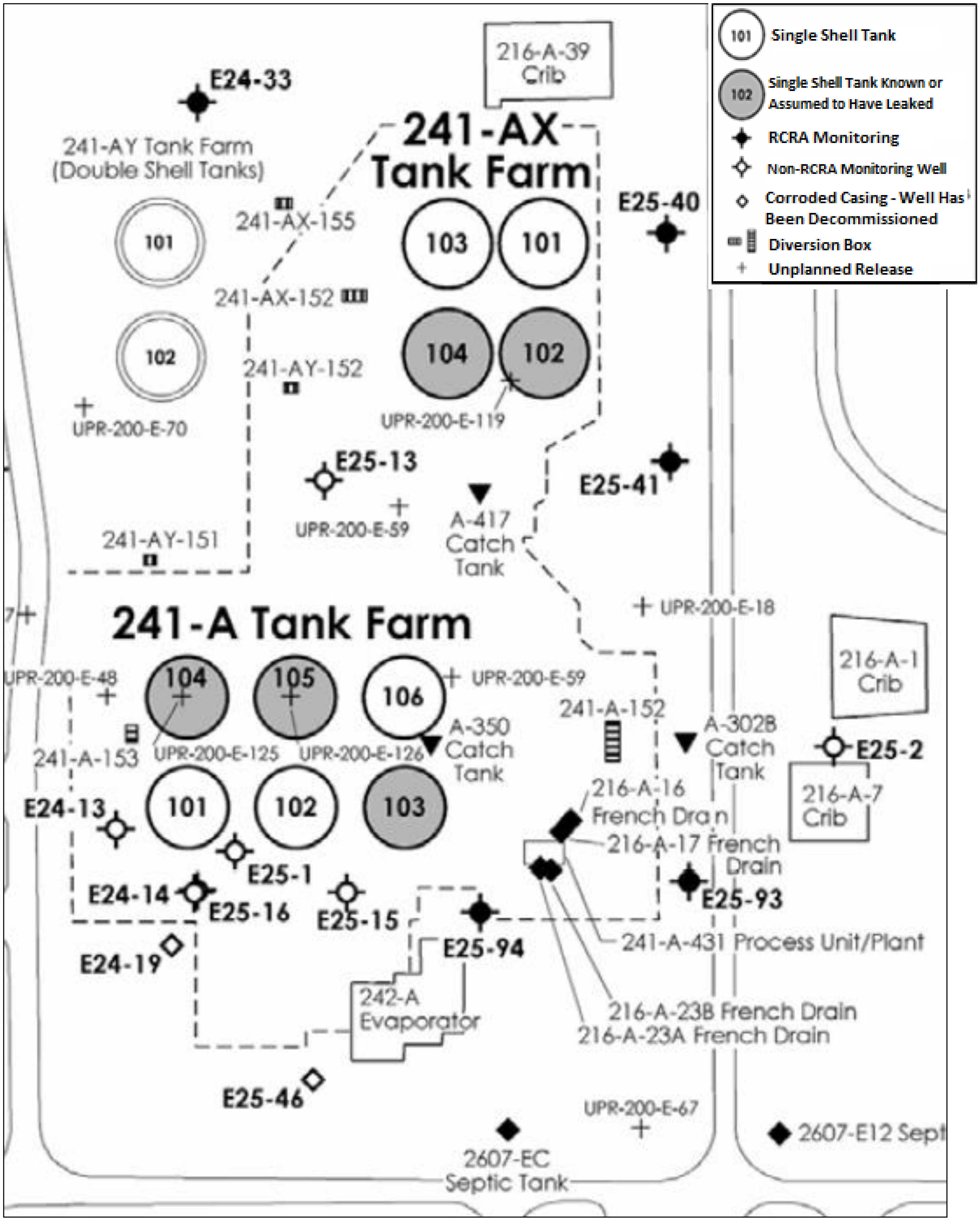

Note: Recent assessments concluded that tanks 241-A-103, 241-AX-102 and 241-AX-104 did not leak (RPP-ASMT-42278, RPP-ASMT-42628, and RPP-ASMT-57574)

3.0 MAJOR FEATURES OF THE NATURAL SYSTEM

This section of the report provides general background information on the regional and local geologic and hydrologic framework that is relevant to the natural system at WMA A/AX. This would include discussions of the:

- Regional geologic framework and history of the Pasco Basin
- Geologic framework, structure, and stratigraphy of the Hanford Site and the Central Plateau
- Local geologic framework in vicinity of WMA A/AX.

Discussions of these topical areas are then followed by general summaries of historical tectonic development, seismic and earthquake activity, and a general assessment of geologic hazards that would be relevant to the Hanford Site. Much of these discussions are taken from information contained in RPP-RPT-46088, *Flow and Transport in the Natural System at Waste Management Area C*, Rev. 1.

3.1 REGIONAL GEOLOGIC FRAMEWORK

The Hanford Site (Figure 3-1) lies within the Columbia Plateau, a broad plain situated between the Cascade Range to the west and the Rocky Mountains to the east, and the Site is underlain by the Miocene Columbia River Basalt Group (CRBG) (Figure 3-2). The northern Oregon and Washington portion of the Columbia Plateau is often called the Columbia Basin because it forms a lowland surrounded on all sides by mountains. The physiographic setting of the Hanford Site is dominated by the low-relief plains of the Central Plains physiographic region and anticlinal ridges of the Yakima Folds region. In the central and western parts of the Columbia Basin and Pasco Basin where the Hanford Site is located, the basalt is underlain predominantly by Tertiary continental sedimentary rocks and overlain by late Tertiary and Quaternary fluvial and glacio-fluvial deposits. All these were folded and faulted during the Cenozoic Era to form the current landscape of the region.

3.2 GEOLOGIC HISTORY OF THE PASCO BASIN

This section describes how the Hanford Site evolved within the context of the Pacific Northwest. It also forms the basis for extrapolating the detailed geology of the tank farms to the surrounding area.

3.2.1 Structural Setting of the Hanford Site with Respect to the Pacific Northwest

The structure of the Pacific Northwest is controlled by a basement rock assemblage of accreted terranes fused onto the structurally complex North American craton by accretion during the early Mesozoic to early Cenozoic. The accreted terranes form the backbone of the Cascade Range, Okanogan Highlands, and the Blue Mountains. The terranes east of the Cascades now are mostly covered by a thick sequence of Cenozoic rocks that were folded and faulted in a north-south oriented compressive regime. North-south compression is continuing today east of the Cascades, and this pattern of Cenozoic deformation is expected to continue into the future.

Figure 3-1. Geographic Elements of the Pasco Basin Portion of the Columbia Basin, Washington

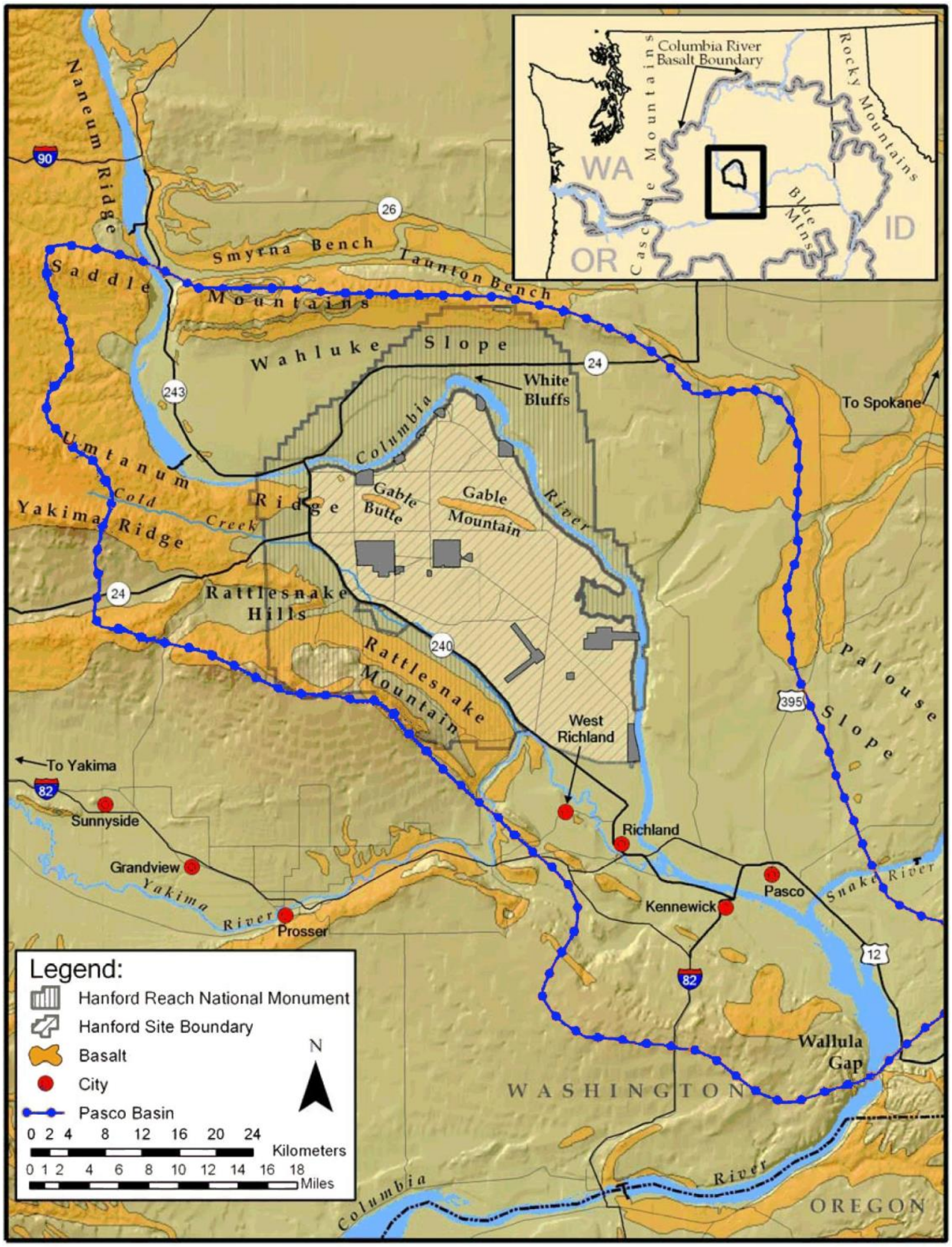

Figure 3-2. Geologic Setting of the Pasco Basin

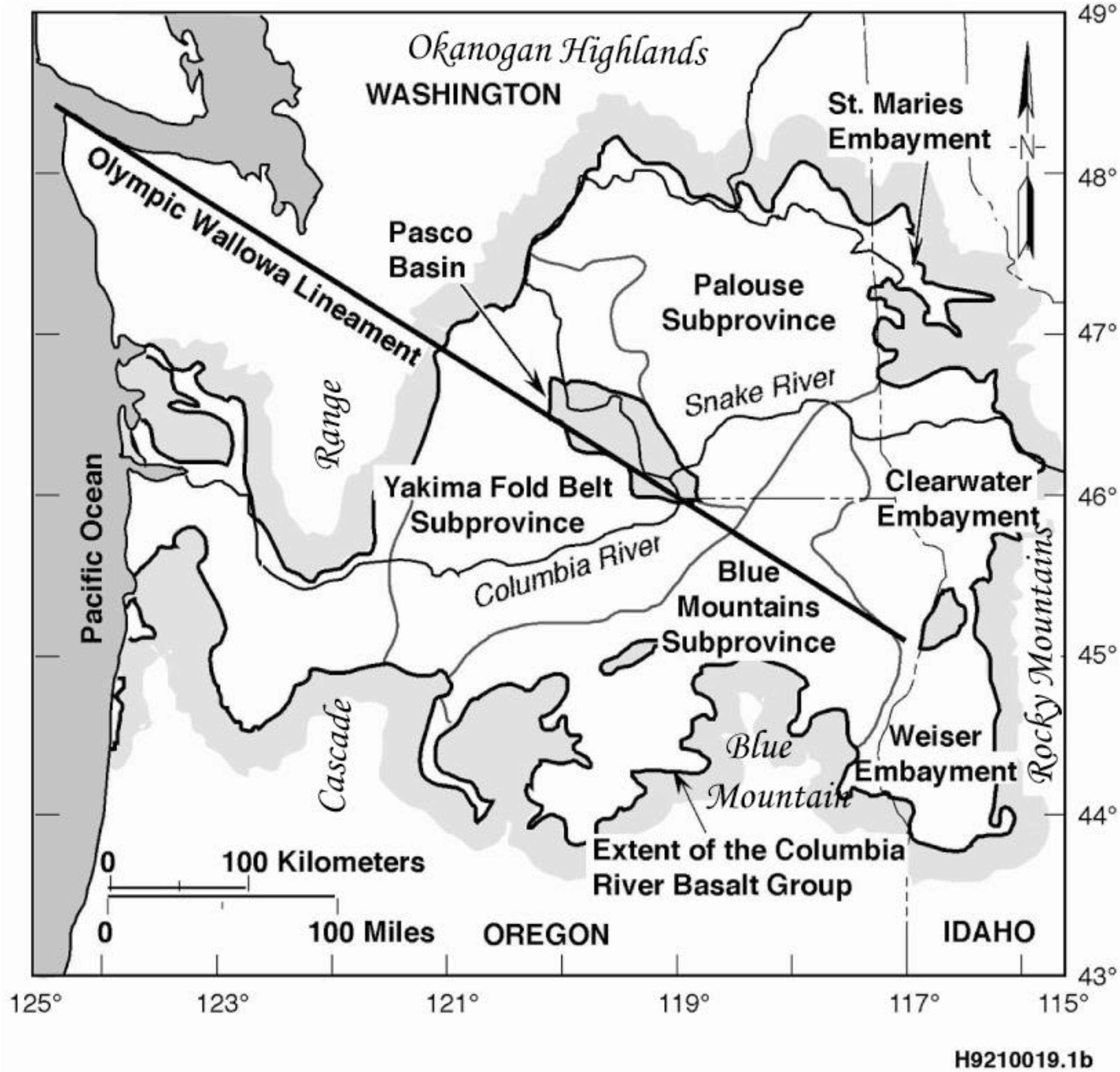

The Columbia Basin is a structurally and topographically low area surrounded by mountains ranging in age from the late Mesozoic to recent (Figure 3-2). The Columbia Basin is composed of two fundamental subprovinces, the Palouse Slope and the Yakima Fold Belt (Figure 3-2). The Palouse Slope is a stable, undeformed area overlying the old continental craton that dips westward toward the Hanford Site. The Yakima Fold Belt is a series of anticlinal ridges and synclinal valleys in the western and central parts of the Columbia Basin. The edge of the old continental craton lies at the junction of these two structural subprovinces and is currently marked by the Ice Harbor dike swarm of the CRBG east of the Hanford Site.

The Blue Mountains subprovince of the Columbia River flood-basalt province is a northeast trending anticlinorium that extends 250 km from the Oregon Cascades to Idaho and forms the southern border of the Columbia Basin and the southern part of the Columbia Plateau.

3.2.2 Geologic History of the Hanford Site in the Context of the Pacific Northwest

The Hanford Site is a small portion of the Columbia Basin, but the geologic record of the Site is representative of the geologic history of the Pacific Northwest. The following discussion is designed to put the Hanford Site geology into perspective with the regional geologic setting.

3.2.2.1 Rocks Older Than the Columbia River Basalt Group. Rocks older than the CRBG are exposed mainly along the margin of the Columbia Basin. However, they are important to understanding the history of the Hanford Site because many extend under the basalt and form the foundation of the area. Stratigraphy along the margin of the CRBG is complex and varies widely in both age and lithology. The principal age, lithologies, and importance to the history of Hanford were taken from “Late Cenozoic Structure and Stratigraphy of South-Central Washington” (Reidel et al. 1994) and are summarized here.

- The oldest rocks in the Pacific Northwest are found along the northeast and east margins of the Columbia Basin near the Idaho border. These are late Precambrian and early Paleozoic metavolcanic and metasedimentary rocks (2.3 billion to 300 million years before present [BP]) interspersed with younger igneous intrusive rocks. These older rocks represent the ancient North American craton and the remnants of the 1-billion-year-old supercontinent Rodinia that broke apart 750 million years ago to form the Pacific Ocean. The boundary of that rifted margin occurs east of the Hanford Site.

- Late Paleozoic, Mesozoic, and early Cenozoic metavolcanics and metasediments are exposed along the south and western margin of the Columbia Basin. These are the rocks that were added onto the North America Plate remnant of Rodinia between 200 and 50 million years ago. Although many are of similar age to rocks along the north and east margins of the Columbia Basin, they formed as ocean islands and microcontinents far away from the Pacific Northwest. Through the process of plate tectonics, these rocks were carried along on the oceanic plate that collided with the North American Plate beginning 200 million years ago. During the collision process, these ocean islands and microcontinents were accreted onto North America and resulted in the westward growth of North America. Similar accreted terrane rocks are thought to occur deep beneath the Hanford Site.

- Along the west and northwest margin, a series of sedimentary basins formed in early Tertiary time (“Structural and Stratigraphic Interpretation of Rocks under the Yakima Fold Belt, Columbia Basin, Based on Recent Surface Mapping and Well Data” [Campbell 1989]). These basins formed in the accreted terranes and are now separated by tectonic “blocks” or uplifts exposing the accreted terranes. The Tertiary rocks extend under the Columbia Basin and Hanford Site. The rocks include the volcanic and sedimentary rocks that are 50 to 20 million years old and were derived from the erosion of highlands in the Pacific Northwest.

3.2.2.2 Columbia River Basalt Group and Ellensburg Formation. The CRBG forms the main bedrock of the Columbia Basin and Hanford Site. This consists of over 200,000 km^3 of tholeitic flood-basalt flows that were erupted between 17 and 6 Ma and now cover approximately 200,000 km^2 of eastern Washington, eastern Oregon, and western Idaho ("An introduction to the stratigraphy, structural geology, and hydrogeology of the Columbia River Flood-Basalt Province: A primer for the GSA Columbia River Basalt Group field trips" [Tolan et al. 2009]). Eruptions had volumes as great as 5,000 km^3 ("The Grande Ronde Basalt, Columbia River Basalt Group; Stratigraphic Descriptions and Correlations in Washington, Oregon, and Idaho" [Reidel et al. 1989]), with the greatest amounts being erupted between 16.5 and 14.5 million years before present. Intercalated with and in some places overlying the CRBG are sedimentary rocks of the Ellensburg Formation (USGS Bulletin 1457-G, *Revisions in stratigraphic nomenclature of the Columbia River Basalt Group*).

3.2.2.3 Post-Columbia River Basalt Geologic History. Most post-CRBG sediments are confined to the synclinal valleys of the Yakima Fold Belt. Although the sedimentary record is incomplete, the sedimentation pattern is what is expected in an area with limited rainfall and significant structural development ("Paleodrainage of the Columbia River System on the Columbia Plateau of Washington State – A Summary" [Fecht et al. 1987]; "Landscape Evolution in a Flood-Basalt Province: an Example from the Pacific Northwest" [Reidel and Tolan 2009]). The dominant source of sediment between the upper Miocene to middle Pliocene (10 to 3 million years ago) is the Columbia River system. The upper Ellensburg Formation and the Ringold Formation are the main sediment packages that contain this history and record the migration of rivers and streams into their present channels (Fecht et al. 1987; Reidel and Tolan 2009). Capping the sedimentary sequence in the synclines and basins are sediments comprising the Pleistocene Hanford formation deposited during cataclysmic floods and recent eolian deposits.

Ridges of the Yakima Fold Belt were growing during the eruption of the CRBG but were usually completely buried by each new basalt eruption. After the last major basalt eruption, the ridges began to develop significant topography. Continued uplift of the Hog Ranch-Naneum Ridge anticline and the ridges of the Yakima Fold Belt forced the Columbia River and its confluence with the Salmon-Clearwater River eastward. By 10.5 million years ago, the Columbia River was flowing along the western boundary of the Hanford Site and then turning southwestward through Sunnyside Gap (Figure 3-1), the water gap through the Rattlesnake Hills to the west, and south past Goldendale, Washington. This is when the Snipes Mountain conglomerate (Figure 3-3), the last Ellensburg Formation unit in the Pasco Basin, was deposited.

Sediment of the Ringold Formation represents evolutionary stages of the ancestral Columbia River as it was forced to change course across the Columbia Basin by the growth of the Yakima Fold Belt. The Ringold Formation time began approximately 8.5 million years ago when the Columbia River abandoned Sunnyside Gap and began to flow across the Hanford Site, leaving the Pasco Basin through the present Yakima River water gap along the southwest end of the Rattlesnake Mountain anticline. The northern margin of the 8.5-million-year-old Ice Harbor basalt controls the Columbia River channel as it exits the Pasco Basin.

The first record of the Columbia River at Hanford is in the extensive gravel and interbedded sand of unit A, Ringold Formation member of Wooded Island (Figure 3-3). The Columbia River was a gravelly braid plain and widespread paleosol system that meandered across the Hanford Site (Fecht et al. 1987; Reidel and Tolan 2009; Reidel et al. 1994; BHI-00184, *Miocene- to Pliocene-Aged Suprabasalt Sediments of the Hanford Site*).

Figure 3-3. Generalized Stratigraphy of the Pasco Basin and Vicinity

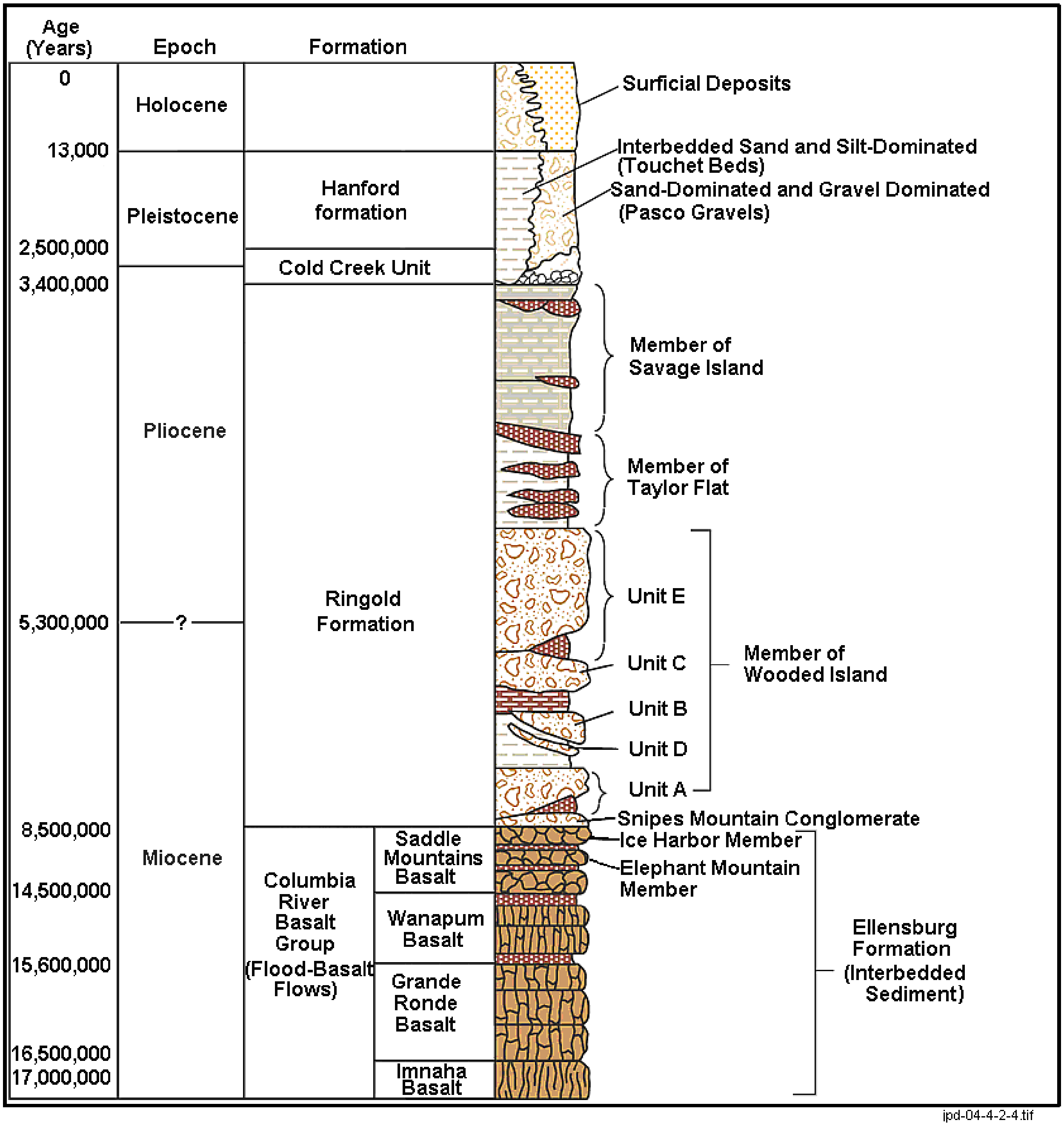

At about 6.7 million years ago, the Columbia River abandoned the Yakima River water gap along the southeast extension of Rattlesnake Mountain and began to exit the Pasco Basin through Wallula Gap (Figure 3-1). The main channel of the Columbia River in the Pasco Basin was still through Hanford and the 200 Areas. At this time, the Columbia River sediments changed to a sandy alluvial system with extensive lacustrine and overbank deposits (Fecht et al. 1987; Reidel and Tolan 2009; Reidel et al. 1994; BHI-00184). A widespread lacustrine-overbank deposit called the lower mud was deposited over some of the Hanford Site at this time and is a nearly continuous feature under the 200 West Area and much of the 200 East Area. The lower mud was then covered by another extensive sequence of fluvial gravels and sands. The most extensive of these is called unit E, Ringold Formation member of Wooded Island, but locally other sequences are recognized (e.g., units C and D). Unit E is one of the most extensive Ringold Formation gravels and appears to be mostly continuous under the 200 Areas. To the north near the 100 Areas, Ringold Formation sediments reflect mostly overbank deposition of fine-grained sediments during this time.

The Columbia River sediments became more sand-dominated about 5 million years ago when over 90 m (295 ft) of interbedded fluvial sand and overbank deposits accumulated at Hanford. These deposits are collectively called the Ringold Formation member of Taylor Flat (BHI-00184). The fluvial sands of the member of Taylor Flat dominate the lower cliffs of the White Bluffs.

Between 4.8 million years ago to the end of Ringold time at 3.4 million years ago, lacustrine deposits dominated Ringold Formation deposition. A series of three successive lakes is recognized along the White Bluffs and elsewhere along the margin of the Pasco Basin (BHI-00184). The lakes probably resulted from damming of the Columbia River farther downstream, possibly near the Columbia Gorge. The lacustrine and related deposits in the Pasco Basin are collectively called the Ringold Formation member of Savage Island.

At the end of Ringold time, western North America underwent regional uplift, resulting in a change in base level for the Columbia River system. Uplift caused a change from sediment deposition to regional incision and sediment removal. Regional incision is especially apparent in the Pasco Basin, where nearly 100 m (328 ft) of Ringold Formation sediment has been removed from the Hanford Area. The regional incision marks the beginning of Cold Creek time and the end of major deposition by the Columbia River.

Regional incision and erosion during Cold Creek time are most apparent in the surface elevation change of the Ringold Formation across the Hanford Site. As incision of the Columbia progressed eastward across Hanford, less erosion occurred on the surface of the Ringold Formation in the 200 West Area, leaving it at a higher elevation than in the 200 East Area. The surface of the Ringold Formation in the 200 West Area is consequently also older than that in the 200 East Area and thus was exposed to weathering processes for a much longer time. Less erosion of the 200 West Area surface accounts for the isolated remnants of the fluvial sands of the Ringold Formation member of Taylor Flat. At the north side of the 200 East Area, the ancestral Columbia River was able to cut completely through the Ringold Formation to the top of the basalt. The channel can be traced from Gable Gap across the eastern part of the 200 East Area and to the southeast. The greatest amount of incision is near the current river channel.

In the Pasco Basin, the Cold Creek unit records most of the geologic events between the incision by the Columbia River and the next major event, the Missoula floods. The older Ringold surface at the 200 West Area was exposed to weathering, resulting in the formation of a soil horizon on its surface. Because the climate was becoming arid, the resulting soil became a pedogenically altered, carbonate-rich, cemented paleosol. The development of this carbonate-rich paleosol is much greater in the 200 West Area than in the 200 East Area due to longer exposure of the surface. This ancient paleosol is referred to as the lower Cold Creek unit (CCU_l) subunit.

Concurrently, eolian sediments and minor fine-grained flood deposits from streams originating from the nearby ridges were deposited on the paleosol, resulting in a wide variety of sediments that are called the upper subunit of the Cold Creek unit (CCU_u). Because of the long time interval (approximately 3.4 to 2 million years ago), several localized paleosols similar to the lower Cold Creek unit were able to develop in the upper Cold Creek unit. Throughout Cold Creek time, streams from the Rattlesnake, Yakima, and Umtanum Ridges were carving channels to the Cold Creek drainage area, depositing basaltic gravels in their stream beds. These form the side stream alluvial facies of the Cold Creek unit.

During Cold Creek time in the central Pasco Basin, the Columbia River flowed through Gable Gap, depositing gravels of mixed lithologies in a sand matrix. These gravels, informally called the "pre-Missoula gravels" (*Skagit/Hanford Nuclear Project, Preliminary Safety Analysis Report*, Vol. 1 [PSPL 1981]), overlie the Ringold Formation and are up to 25 m (82 ft) thick. The 200 East Area lies along the boundary between these two geologic environments, undergoing significantly more erosion than 200 West Area but with some soil development occurring in areas. There may have been other periods of fluvial deposition near the 200 East Area that reworked the existing Ringold gravels. The difficulty and uncertainty in distinguishing between these similar units is reflected in the differing choices for geologic contacts and their differing descriptions between reports.

During the Pleistocene Epoch, cataclysmic floods inundated the Pasco Basin several times when ice dams failed in northern Washington ("Quaternary Geology of the Columbia Plateau" [Baker et al. 1991]). Current interpretations suggest as many as 40 flooding events or more occurred as ice dams holding back glacial Lake Missoula repeatedly formed and broke. In addition to larger major flood episodes, there were probably numerous smaller individual flood events. Deciphering the history of cataclysmic flooding in the Pasco Basin is complicated, not only because of floods from multiple sources but also because the paths of Missoula floodwaters migrated and changed course with the advance and retreat of the Cordilleran Ice Sheet.

Along with sedimentological evidence for cataclysmic flooding in the Pasco Basin, high-water marks and faint strandlines occur along the basin margins. Temporary lakes were created when flood waters were hydraulically dammed, resulting in the formation of the short-lived Lake Lewis behind Wallula Gap. High-water mark elevations for Lake Lewis, inferred from ice-rafted erratics on ridges, range from 370 to 385 m (1,214 to 1,261 ft) above sea level.

The sediment deposited by the cataclysmic flood waters has been informally called the Hanford formation because the best exposures and most complete deposits are found on the Hanford Site. The coarse-grained flood facies (gravel-dominated facies of DOE/RL-2002-39, *Standardized Stratigraphic Nomenclature for Post-Ringold-Formation Sediments Within the Central Pasco Basin*) is generally confined to relatively narrow tracts within or near flood channels. The plane-laminated sand facies (sand-dominated facies of DOE/RL-2002-39), on the other hand, occurs as a broad sheet over most of the central basin. Paleocurrent indicators within beds of plane-laminated sands are unidirectional, generally toward the south and east within the Pasco Basin.

Rhythmite facies (interbedded silt and sand-dominated facies of DOE/RL-2002-39) occur in slackwater areas around the margins of the basin and were deposited by multidirectional currents, including upvalley currents. Individual rhythmites become finer and thinner both laterally and vertically upward.

Recent studies using the magnetic polarity of the Hanford formation sediments have shown that the earliest floods may have occurred as long ago as 2 million years. Four magnetic polarity reversals have been found in sediments from core holes in the 200 East Area ("Magnetostratiphic Evidence from the Cold Creek Bar for Onset of Ice-Age Cataclysmic Floods in Eastern Washington During the Early Pleistocene" [Pluhar et al. 2006]). These polarity reversals have paleosols at the top of each reversed sequence of sediments. The oldest sediments occur in the ancestral Columbia River channels where the pre-Missoula sediments occur. The age of the Hanford formation in the 200 West Area is more difficult to determine because only normal-polarity sediments occur there.

Since the end of the Pleistocene, the main geologic process has been wind. After the last Missoula flood drained from the Pasco Basin, winds moved the loose, unconsolidated material until vegetation was able to stabilize it. Stabilized sand dunes cover much of the Pasco Basin, but there are areas, such as along the Hanford Reach National Monument, where sand dunes remain active.

3.3 GEOLOGIC FRAMEWORK OF THE HANFORD SITE

As discussed in Sections 3.1 and 3.2, the events occurring throughout the Pacific Northwest and Columbia Basin are reflected in the sedimentary record in the Pasco Basin and consequently the Hanford Site. This section provides a description of the large geologic framework for the Hanford Site.

3.4 STRUCTURAL GEOLOGY

The Cold Creek syncline (Figure 3-4) lies between the Umtanum Ridge-Gable Mountain uplift and the Yakima Ridge uplift and is an asymmetric and relatively flat-bottomed structure. The Cold Creek syncline began developing during the eruption of the CRBG and has continued to subside since that time. The 200 Areas lie on the northern flank, and the bedrock dips gently (approximately 5°) to the south. The 300 Area lies at the eastern end of the Cold Creek syncline where it merges with the Pasco syncline. The deepest parts of the Cold Creek syncline, the Wye Barricade depression and the Cold Creek depression, are approximately 12 km (7.5 mi) southeast of the 200 Areas and southwest of the 200 West Area, respectively (Figure 3-4).

Figure 3-4. Geologic and Geomorphic Map of the 200 Areas and Vicinity

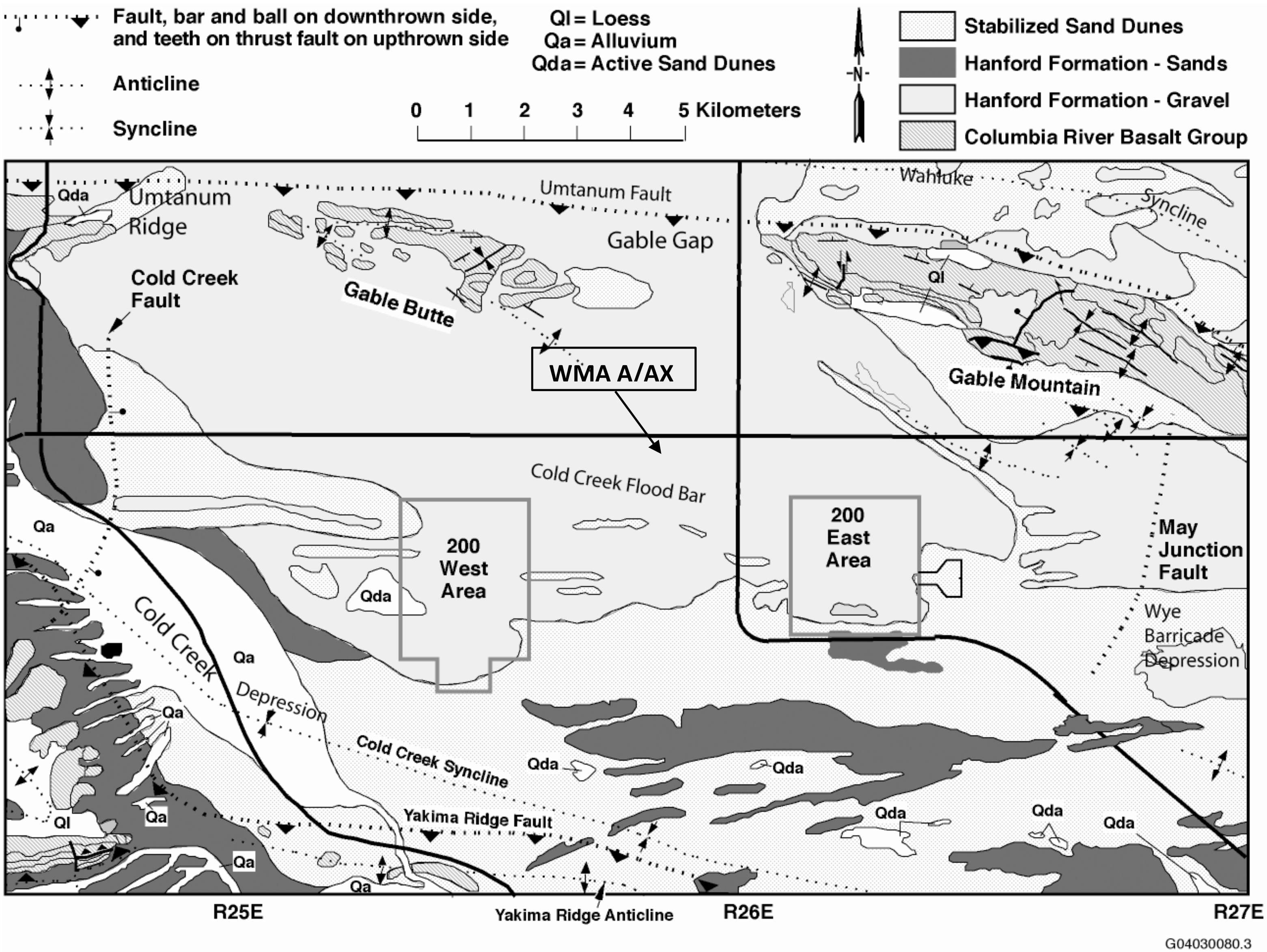

The Wahluke syncline north of Gable Mountain is the principal structural unit that contains the 100 Areas. The Wahluke syncline is an asymmetric and relatively flat-bottomed structure similar to the Cold Creek syncline. The northern limb dips gently (approximately 5°) to the south. The steepest limb is adjacent to the Umtanum Ridge-Gable Mountain structure.

The Umtanum Ridge-Gable Butte-Gable Mountain structural trend (Figure 3-4) is a segmented anticlinal ridge extending for a length of 110 km in an east-west direction and passes north of the 200 and 300 Areas and south of the 100 Areas. The Southeast anticline and Gable Mountain-Gable Butte is the easternmost portion of this ridge.

The Yakima Ridge uplift extends from west of Yakima, Washington, to the center of the Pasco Basin, where it forms the southern boundary of the Cold Creek syncline south of the 200 West Area (Figure 3-4). The easternmost surface expression of the Yakima Ridge uplift is represented by an anticline that plunges eastward into the Pasco Basin (RHO-BWI-ST-4, *Geologic Studies of the Columbia Plateau – A Status Report: October 1979*). The eastern extension of Yakima Ridge is mostly buried beneath late Cenozoic sediments and has much less structural relief than the rest of Yakima Ridge.

The 200 East Area sits on the eastern part of the Cold Creek bar, which is along the northern flank of the Cold Creek syncline (Figure 3-4). Another deep structural low, the Wye Barricade depression, developed along the Cold Creek syncline southeast of the 200 East Area. The May Junction fault is a normal fault that marks the western boundary of the depression.

The 200 East Area sits at the southern end of a series of secondary doubly plunging anticlines and synclines that are associated with the Umtanum Ridge-Gable Mountain anticlinal structure. Waste Management Areas A, AX, B-BX-BY, and C in the 200 East Area lie near the southern flank of the closest secondary anticline. A fault was recently detected during drilling of seismic test boreholes at the Waste Treatment Plant. The fault caused some displacement in the Pomona Basalt that lies beneath the Elephant Mountain Member but is not thought to have caused any displacement in younger basalts or overlying sediments (PNNL-16407, *Geology of the Waste Treatment Plant Seismic Boreholes*).

3.5 STRATIGRAPHY OF THE HANFORD SITE

The generalized stratigraphy of the Pasco Basin and Hanford Site is shown in Figure 3-3. The principal rocks exposed at the surface of the surrounding ridges are the CRBG and intercalated sedimentary rocks of the Ellensburg Formation. In the low-lying basins and valleys, these are overlain by younger sedimentary rocks of the Ringold Formation, Cold Creek unit, and the Pleistocene cataclysmic flood deposits of the Hanford formation.

3.5.1 Columbia River Basalt Group and Ellensburg Formation

The Elephant Mountain Member is the uppermost basalt flow beneath the 200 Areas and much of the Hanford Site. Where folds and faults have formed basalt ridges, other flows from the Saddle Mountains, Wanapum, and Grande Ronde Formations are exposed.

The Ellensburg Formation is intercalated with and overlies the CRBG in the Pasco Basin and includes epiclastic and volcaniclastic sedimentary rocks ("Stratigraphic and Lithologic Variations in the Columbia River Basalt" [Waters 1961]; USGS Bulletin 1457-G). At the Hanford Site, the Ellensburg Formation consists of sediments deposited by the ancestral Clearwater (now the course followed by the Snake River) and Columbia Rivers. Relatively few boreholes in the 200 Areas penetrate the Ellensburg Formation. Those boreholes that do penetrate the Ellensburg Formation generally find tuffaceous siltstones and sandstones, with conglomerates marking ancient main river channels. The Ellensburg stratigraphy of the Hanford Site has been discussed in more detail in Fecht et al. (1987).

3.5.2 Post-Columbia River Basalt Group Sediments

The Hanford Site and tank farms are situated on a sequence of Ringold Formation, Cold Creek unit, and Hanford formation sediments overlying the CRBG. The upper Miocene to middle Pliocene record of the Columbia River system in the Columbia Basin is represented by the upper Ellensburg and Ringold Formations. Except for local deposits (e.g., the Cold Creek unit [CCU]), there is a hiatus (erosion or lack of sedimentation) in the stratigraphic record between the end of the Ringold Formation deposition (3.4 Ma) and the beginning of Pleistocene (1.6 Ma) time (DOE/RW-0164, *Consultation Draft Site Characterization Plan. Reference Repository Location, Hanford Site, Washington*; DOE/RL-2002-39).

Pleistocene to recent sediments overlying the CRBG at the Hanford Site include cataclysmic flood gravels and slackwater sediments of the Hanford formation; terrace gravels of the Columbia, Snake, and Yakima Rivers; and eolian deposits.

3.6 GEOLOGY OF THE CENTRAL PLATEAU

The Central Plateau encompasses the 200 East Area, 200 West Area, and the area between. Because of the need to understand the geologic controls on movement of contaminants in the vadose zone and groundwater, the Central Plateau has become one of the best characterized areas on the Hanford Site. The geology of the Hanford Site has largely been determined using samples from numerous boreholes.

Figure 3-5, a fence diagram of the Central Plateau area, depicts the geology above the CRBG. By necessity, Figure 3-5 is highly generalized, depicting the overall consistency of stratigraphy between the 200 East Area and 200 West Area. The major differences are in the thicknesses of the units in response to the geologic history. For example, the Hanford formation thickens to the east as the Ringold Formation thins. This variation is a response to the downcutting by the Columbia River after Ringold Formation time and then further erosion and filling of the erosional channels by Missoula Flood deposits.

3.6.1 Basalt

The uppermost basalt flow beneath the Central Plateau is the Elephant Mountain Member (RHO-BWI-ST-14, *Subsurface Geology of the Cold Creek Syncline*, Chapter 3 – Wanapum and

Saddle Mountains Basalts of the Cold Creek Syncline Area). The top of basalt surface dips to the southwest beneath the 200 West Area and to the south-southwest beneath the 200 East Area. Low-amplitude secondary folds such as the one to the northeast of the 200 East Area may occur throughout the area and have probably not been fully identified. Between the 200 East Area and Gable Gap to the north, the Elephant Mountain has been eroded to expose underlying basalt flows. There is also a suspected window eroded through the Elephant Mountain near the northeast corner of the 200 East Area.

Figure 3-5. Fence Diagram of Sediment Overlying the Columbia River Basalt Group in the Central Plateau, Hanford Site

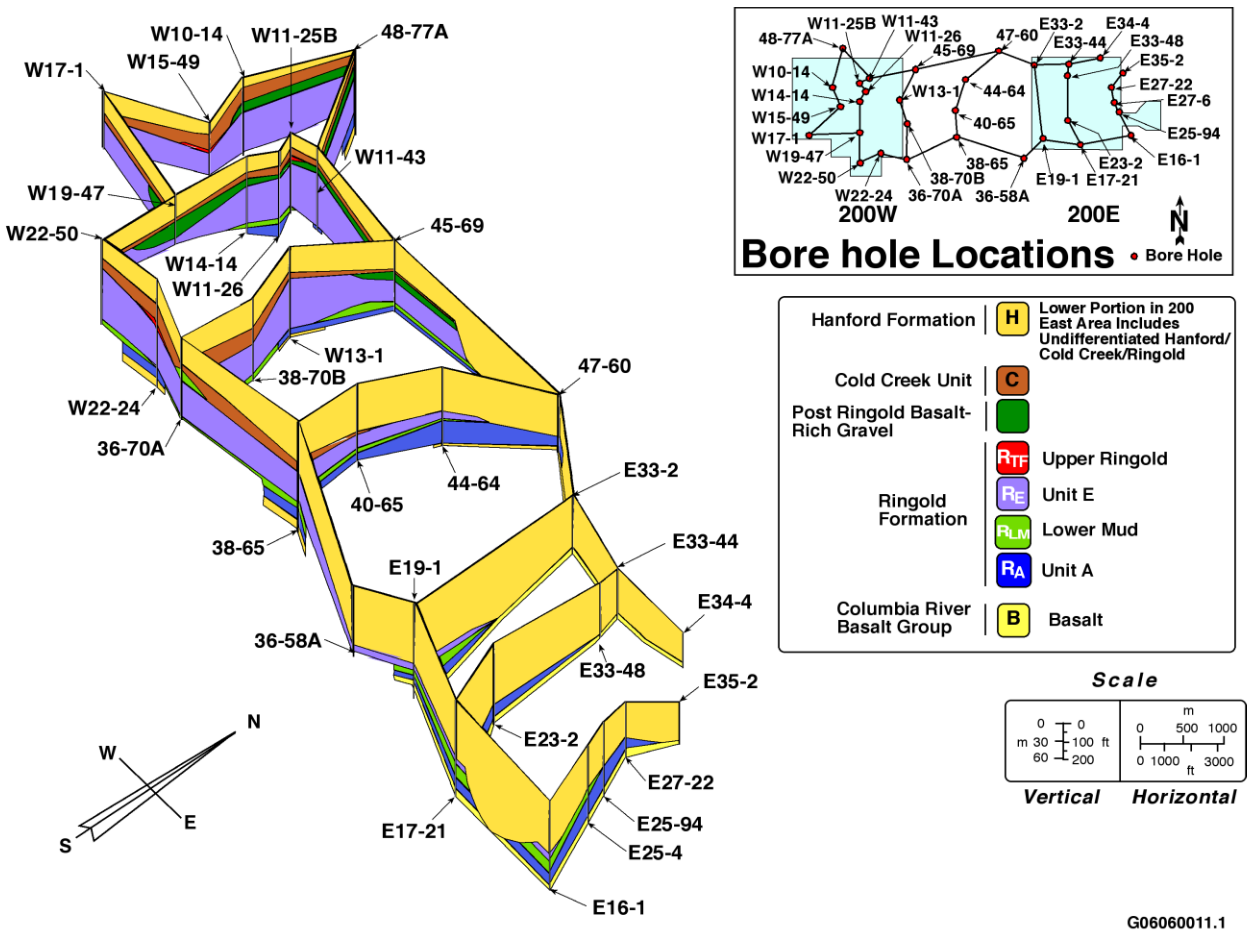

3.6.2 Ringold Formation

The Ringold Formation at the Hanford Site is up to 185 m (607 ft) thick in the deepest part of the Cold Creek syncline south of the 200 West Area and 170 m (55 ft) thick in the western Wahluke syncline near the 100 B Area. The Ringold Formation pinches out against the Gable Mountain, Yakima Ridge, Saddle Mountains, and Rattlesnake Mountain anticlines. It is largely absent in the northern and northeastern parts of the 200 East Area. It consists of semi-indurated clay, silt, pedogenically altered sediment, fine- to coarse-grained sand, and granule to cobble gravel.

Ringold Formation strata typically are below the water table on the Hanford Site, and the textural variations influence groundwater flow.

Studies of the Ringold Formation in the Pasco Basin indicate it contains significant stratigraphic variations (WHC-SD-EN-EE-004, *Revised Stratigraphy for the Ringold Formation, Hanford Site, South-Central Washington*, BHI-00184) that are best described on the basis of sediment facies. Sediment facies in the Ringold Formation are defined on the basis of lithology, stratification, and pedogenic alteration.

In the Pasco Basin, the lower half of the Ringold Formation, the member of Wooded Island, is the main unconfined aquifer under the Hanford Site and contains five separate stratigraphic intervals dominated by the fluvial gravel facies. These gravels, designated units A, B, C, D, and E (Figure 3-3), are separated by intervals containing deposits typical of the overbank and lacustrine facies (WHC-SD-EN-EE-004). In the 200 Areas, only fluvial gravel units A and E occur (Figure 3-5). Between these two gravel units in many places is the lowermost of the fine-grained sequences, designated the lower mud sequence. Fluvial gravel units A and E correspond to the lower basal and middle Ringold Formation units, respectively, as defined by DOE/RW-0164. Gravel units B, C, and D do not correlate to any previously defined units (WHC-SD-EN-EE-004, BHI-00184) and do not occur beneath the tank farms.

The following discussion of the geology of the Central Plateau is based on interpretations of new and old wells for this report as well as geologic contact depths from PNNL-12261, *Revised Hydrogeology for the Suprabasalt Aquifer System, 200-East Area and Vicinity, Hanford Site, Washington*; PNNL-13858, *Revised Hydrogeology for the Suprabasalt Aquifer System, 200-West Area and Vicinity, Hanford, Washington;* and PNL-8971, *Three-Dimensional Conceptual Model for the Hanford Site Unconfined Aquifer System, FY 1993 Status Report*.

Ringold unit A occurs throughout much of the Central Plateau and ranges from 0 to over 30 m (0 to 100 ft) thick. This unit is thickest to the north and south of the 200 West Area. Beneath the 200 West Area, the top of this gravel unit dips to the southwest into the Cold Creek depression, while beneath the 200 East Area, the unit dips to the south into the Cold Creek syncline except in the northern part where it has been eroded. Generally, unit A is a conglomerate with clasts of basalt and other lithologies in a silty sand matrix intercalated with beds of sand and silt. The sediments may be strongly cemented with silica or calcite in places.

The Ringold Formation lower mud unit has had a more complex history in the 200 Areas. The lower mud has been eroded from beneath most of the 200 East Area. There is also a poorly defined channel cut through the lower mud unit in the northeastern corner of the 200 West Area. The lower mud unit ranges in thickness from 0 to 30 m (0 to 103 ft). Thickness of the lower mud increases in the Cold Creek depression, representing subsidence during deposition of the fine-grained sediments. The lower mud is thinnest beneath the 200 East Area and increases to the south. There is a broad zone of decreased thickness that runs southeast from the 200 West Area and may trace an old river channel from early in Ringold Formation unit E time. This unit consists primarily of lacustrine silt and clay, with at least one well-developed paleosol noted in the 200 West Area. It is an aquitard, separating the suprabasalt confined aquifer in unit A from the unconfined aquifer in unit E.

Unit E of the member of Wooded Island is by far the thickest of the Ringold Formation units present in the Central Plateau. It consists of well-rounded gravel in a sand and silt matrix deposited by major rivers. Gravel lithologies are varied with sources outside the Columbia Basin. Cementation varies from well- to poorly-indurated. Unit E ranges from 0 to over 90 m (0 to 300 ft) in thickness. This variation in thickness is due in part to continued subsidence of the Cold Creek syncline and in part to erosion during the Cold Creek unit and Hanford formation times. Increasing thicknesses to the west of the 200 West Area and to the south of the 200 East Area are a combination of both processes. Main channels during both Cold Creek and Hanford floods went through Gable Gap and across the northeastern part of the 200 East Area, removing unit E from most of that area and leaving a complicated surface in the 200 East Area.

In the Pasco Basin, the upper part of the Ringold Formation includes members of Taylor Flat and Savage Island (BHI-00184). The member of Taylor Flat consists of a sequence of fluvial sands and overbank deposits while the member of Savage Island consists of lacustrine sediments. The member of Savage Island is found only along the White Bluffs in the eastern Pasco Basin and corresponds to the upper Ringold Formation unit as originally defined by "Ringold Formation of Pleistocene Age in Type Locality, the White Bluffs, Washington" (Newcomb 1958). In the 200 West Area, erosional remnants of the member of Taylor Flat consists of fine-grained fluvial sand and overbank facies with localized stringers of calcium carbonate. Member of Taylor Flat sediments are found beneath parts of the T, TX, and TY tank farms and in the vicinity of the U tank farm and are discussed in more detail in Section 4.

3.6.3 Pliocene to Pleistocene Transition

Two main alluvial units of the Pliocene to Pleistocene transition are recognized at the Hanford Site—the CCU and the pre-Missoula gravels. Recently, the pre-Missoula gravels have been tentatively incorporated into the CCU (DOE/RL-2002-39); both are discussed together here.

The laterally discontinuous CCU overlies the tilted and truncated Ringold Formation in an unconformable relationship in the western Cold Creek syncline in the vicinity of the 200 West Area (DOE/RL-2002-39). To the east, the pre-Missoula gravels replace the calcrete and silt-dominated subunits of the CCU. The CCU appears to be correlative to other sidestream alluvial, eolian, and pedogenic deposits found near the base of the ridges bounding the Pasco Basin on the north, west, and south. These sedimentary deposits are inferred to have a late Pliocene to early Pleistocene age on the basis of stratigraphic position and magnetic polarity of interfingering loess units (DOE/RW-0164). At a coarse scale, the surfaces of the Ringold Formation and the CCU in the 200 West Area dip to the south. This surface also dips to the east between the 200 West and 200 East Areas.

3.6.3.1 Pre-Missoula Gravels – Central Pasco Basin. The pre-Missoula gravels disconformably overlie the Ringold Formation in much of the central basin and may extend into areas in or near the 200 East Area. The nature of the contact between the pre-Missoula gravels and the overlying Hanford formation is not clear. In addition, it is unclear whether the pre-Missoula gravels overlie or interfinger with the CCU. Previous work at WMA C (RPP-RPT-46088, Rev. 1) included the pre-Missoula gravels in the Cold Creek unit because they overlie the Ringold Formation and underlie the Hanford formation. The gravel lying on basalt beneath much of the northern half of the 200 East Area has been variously interpreted as Ringold Formation unit A, as gravels deposited during Cold Creek time, or as part of the cataclysmic Hanford flood deposits that include some reworked Ringold. The difficulty in distinguishing between these units is reflected in the cross sections for the 200 East waste management areas.

3.6.3.2 Cold Creek Unit – 200 East Area. The CCU as described above is largely absent from the 200 East Area. The exact origin of the sedimentary deposits overlying the CRBG and underlying the Hanford formation is uncertain and still open to interpretation. These deposits beneath the Hanford formation have been called the Hf/CCU (undifferentiated Hanford/Cold Creek) (HNF-5507, *Subsurface Conditions Description of the B-BX-BY Waste Management Area*) and undifferentiated Hanford formation/Cold Creek unit/Ringold Formation unit (Hf/CCU/RF) (RPP-8531, *Vadose Zone Geology of Boreholes 299-W10-27 and 299-W11-39 T-TX-TY Waste Management Area Hanford Site, South-Central Washington*). In this report, they are placed in the CCU or lower Hanford gravel/CCU undifferentiated because they represent sediments deposited between the late Pliocene and early Pleistocene Epochs. This is the age range of the CCU in the 200 West Area. By assigning these deposits to this unit, only the age is implied, not the origin of the deposits.

HNF-5507 recognized two facies of the Hf/CCU beneath the 200 East Area tank farms: a fine-grained eolian/overbank silt (silt facies Cold Creek unit), up to 10 m thick, and a sandy gravel to gravelly sand facies Cold Creek unit. The thick, silt-rich interval is believed to be a pre-Pleistocene fluvial flood deposit because silty layers associated with Ice Age flood deposits of the Hanford formation in this area are generally much thinner (i.e., a few centimeters or less) (HNF-5507). Where the silt unit is absent, the gravel sequence below the silt unit is indistinguishable from similar-appearing facies of the overlying Hanford formation (HNF-5507). If the thick silt layer predates the Hanford formation, however, then the underlying gravels also must predate the Hanford formation. Thus, the gravel sequence beneath the silt layer must belong to either a mainstream alluvial facies of the ancestral Columbia River (pre-Missoula gravels) or the Ringold Formation.

3.6.4 Quaternary Stratigraphy of the Pasco Basin

Quaternary sediments, as much as 100 m thick within the Pasco Basin, overlie the Ringold Formation and/or CCU at the tank farms. The most extensive of these is the Pleistocene-aged Hanford formation (Figure 3-3), but the sediments also include eolian deposits and recent alluvium.

Eolian Deposits. Loess deposits at the Hanford Site contain a detailed Quaternary record; five units are represented within the Pasco Basin (WHC-MR-0391, *Field Trip Guide to the Hanford Site*). These units are informally referred to as L1 through L5 and differentiated on the basis of 1) position relative to other stratigraphic units, 2) color, 3) soil development, and 4) paleomagnetic polarity.

Hanford Formation. The Hanford formation is the main stratigraphic unit at the surface of the tank farms. The Hanford formation consists of pebble to boulder gravel, fine- to coarse-grained sand, and silt. These deposits are divided into three facies: 1) gravel-dominated,

2) sand-dominated, and 3) sand- and silt-dominated. These facies are referred to as coarse-grained deposits, plane-laminated sand facies, and rhythmite facies, respectively, in DOE/RW-0164. The rhythmites also are referred to as the Touchet Beds. The Hanford formation is thickest beneath the Cold Creek bar, particularly in the vicinity of the 200 East Area, where it is over 100 m thick.

The gravel-dominated facies association generally consists of coarse-grained basaltic sand and granule to boulder gravel. These deposits display massive bedding, plane to low-angle bedding, and large-scale planar cross-bedding in outcrop. The gravel facies dominates the Hanford formation in the 100 Areas north of Gable Mountain, the northern part of the 200 East and West Areas, and the eastern part of the Hanford Site including the 300 Area. The gravel-dominated facies was deposited by high-energy flood waters in or immediately adjacent to the main cataclysmic flood channelways.

The sand-dominated facies association consists of fine- to coarse-grained sand and granule gravel displaying plane lamination and bedding and, less commonly, plane bedding and channel-fill sequences in outcrop. These sands may contain small pebbles and rip-up clasts in addition to pebble-gravel interbeds and silty interbeds less than 1 m thick. The silt content of these sands is variable. These sands typically are basaltic, commonly being referred to as black, gray, or salt-and-pepper sands. This facies is most common in the central Cold Creek syncline, in the central to southern parts of the 200 East and 200 West Areas. The laminated sand facies was deposited adjacent to main flood channelways during the waning stages of flooding. The facies is transitional between the gravel-dominated facies and the rhythmite facies.

The interbedded sand- and silt-dominated facies association consists of thinly bedded, plane-laminated and ripple cross-laminated silt and fine- to coarse-grained sand that commonly display normally graded rhythmites a few centimeters to several tens of centimeters thick (RHO-BWI-ST-4; DOE/RW-0164; DOE/RL-2002-39). This facies is found throughout the central, southern, and western Cold Creek syncline within and south of the 200 East and 200 West Areas. These sediments were deposited under slackwater conditions and in back-flooded areas (DOE/RW-0164).

Cataclysmic floods inundated the Pasco Basin several times during the Pleistocene when ice dams failed in northern Washington and Idaho. Net erosion by these floods was minimal and probably associated with only the earliest floods; later floods only partially incised into older flood deposits before backfilling. Recent work on subdividing the Missoula flood deposits at the Hanford Site has shown that paleomagnetic polarity is a useful technique ("Paleomagnetic and Geochemical Applications to Tectonics and Quaternary Geology: Studies at Coso Volcanic Field, CA and the Channeled Scabland, WA" [Pluhar 2003], Pluhar et al. 2006). In a detailed study at the 200 East Area, four magnetic polarity reversals were recognized. These reversals were equated to the Brunhes normal subchron (present to 780,000 years BP) and the Matuyama reversal subchron (780,000 to 1.76 Ma). The Matuyama reversal has a normal excursion at 1 Ma, which Pluhar attributed to the normally magnetized sediments between the upper and lower reversal. The age of the lowest reversal is constrained by the lower limit of 1.76 Ma of the Matuyama subchron.

In the 200 West Area, mainly normally polarized sediments were found with two possible reversed horizons. Pluhar et al. (2006) interpreted the Hanford formation at the 200 West Area as being deposited during the Brunhes normal subchron (present to 780,000 years BP) and the two possible reversals as short magnetic excursions during the Brunhes subchron.

The results of the Pluhar et al. (2006) study suggest that the Hanford formation sediments at the 200 East Area are older than those in the 200 West Area. This further implies that the Hanford subdivisions—upper coarse-dominated (H1), sand-dominated (H2), and lower coarse-dominated (H3) (BHI-00184)—are not the same flooding event in both areas and, thus, cannot be correlated across the Cold Creek bar.

3.6.5 Clastic Dikes

Clastic dikes are vertical to subvertical sedimentary structures that cross-cut normal sedimentary layering and could locally affect the vertical and horizontal movement of water and contaminants. Clastic dikes are a common geologic feature of Pleistocene flood deposits of the Hanford formation, although they also have been found in the underlying Ringold Formation and in CRBG and intercalated sedimentary interbeds. Clastic dikes on the Hanford Site have been described in detail in BHI-01103, *Clastic Injection Dikes of the Pasco Basin and Vicinity: Geologic Atlas Series*.

Clastic dikes typically occur in swarms and as regularly shaped polygonal patterns, irregularly shaped polygonal patterns, pre-existing fissure fillings, and random occurrences. Regular polygonal networks resemble four- to eight-sided polygons. Dikes in irregularly shaped polygon networks generally are cross-cutting in both plane and cross section, resulting in extensive segmentation of the dikes.

Clastic dikes typically show a wide range in width, depth, length, and orientation. They are especially common within the sand- and silt-dominated facies of the Hanford formation (Figure 3-6). The vertical extent of clastic dikes has been observed to range from 30 cm to more than 55 m (~1 to 180 ft), while width ranges from about 1 mm to greater than 2 m (0.04 in. to more than 6.6 ft). Deep exposures of clastic dikes typically show that they have many twists and turns as they are followed deeper. Most do not penetrate through the Hanford formation but typically will turn horizontally into a layer where they end. This horizontal bend has been interpreted as a key to the initial formation of the dikes. These dikes are interpreted as de-watering phenomena and the bend from vertical to horizontal is the point where the original clastic dike formed (the horizontal bed) and then broke upward to the surface as the wet sediment de-watered.

An example of the scale and spacing of clastic dikes is shown in Figure 3-7. In this figure, mapped clastic dikes south of the 200 West Area are projected on the S-SX WMA in 200 West Area. In this area these clastic dikes occur in the slackwater Touche Beds and planar-laminar silts and sands.

The hydrologic properties of a 2-m wide clastic dike near the 200 West Area have been investigated in "Influence of Clastic Dikes on Vertical Migration of Contaminants at the Hanford

Site" (Murray et al 2007). They concluded that "the highly heterogeneous nature of the system led to complex behavior, with the relative flux rates in the matrix and clastic dike being highly dependent on the recharge rates that were imposed on the system." Their study suggested that "the potential role of clastic dikes in vertical transport at the Hanford Site would depend on the leakage rate, and that areas of contaminant deposition formed at high flow rates might become isolated at low flow rates, and vice-versa."

Figure 3-6. Typical Clastic Dike in Touchet Beds of the Hanford Formation. Picture taken in the Walla Walla valley near Touchet, Washington.

3.6.6 Volcanic Ash Deposits

Volcanism in the Cascade Range has been active throughout the Pleistocene Epoch (approximately 2 million years to 10,000 years BP), and throughout the Holocene Epoch (10,000 years BP to present). The eruption history of the Holocene best characterizes the most likely types of activity in the next 100 years. Many volcanoes have been active in the last 10,000 years, including Mount Mazama (Crater Lake) and Mount Hood in Oregon, and Mount

St. Helens, Mount Adams, Mount Baker, and Mount Rainier in Washington. The Quaternary sediments recorded these eruptions in the form of ash deposits that are interlayered with the sediments.

Figure 3-7. Projection of a Hypothetical Network of Clastic Dikes onto Waste Management Area S-SX (from HNF-4936)

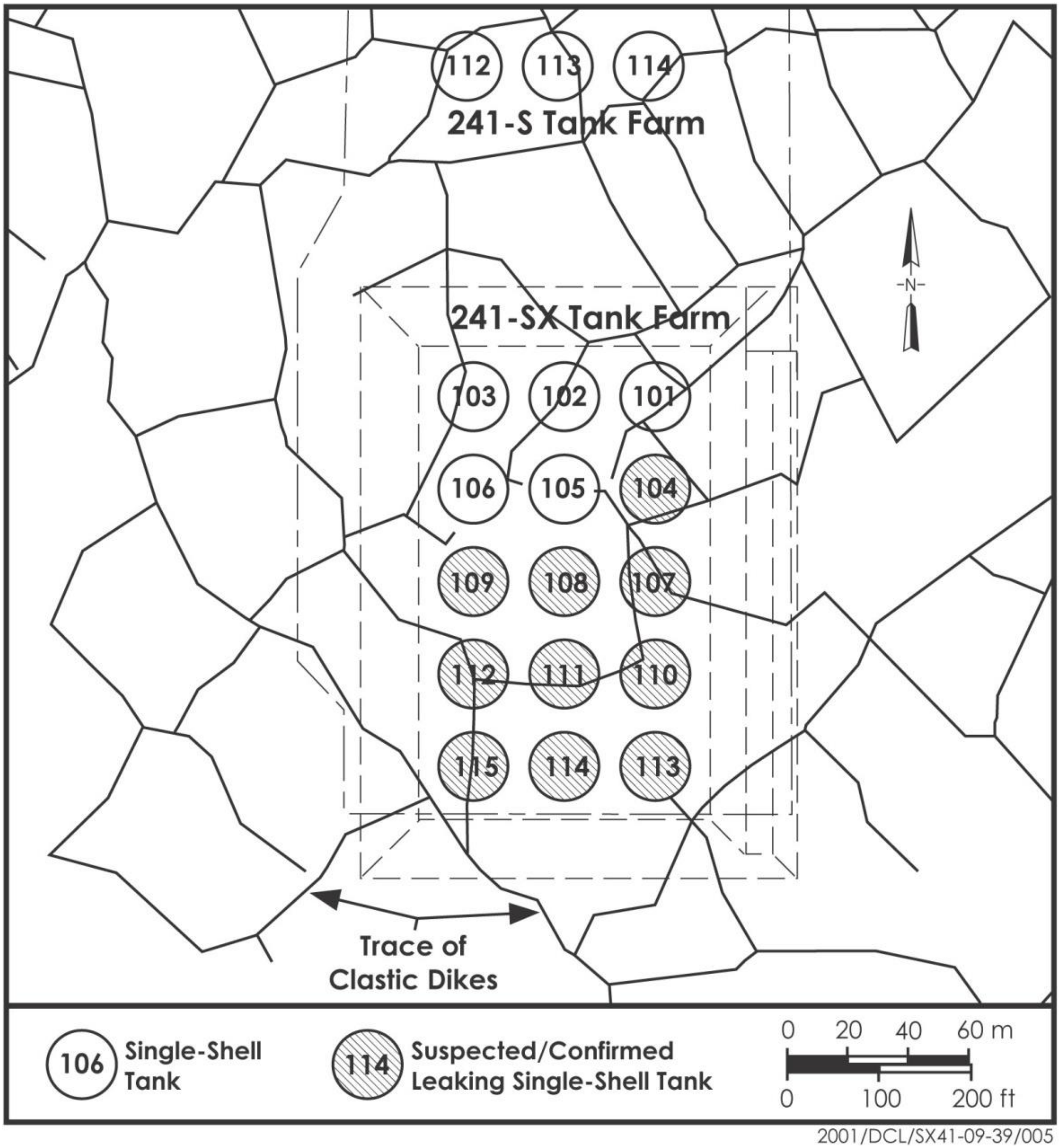

Reference: HNF-4936, *Subsurface Physical Conditions Description of the S-SX Waste Management Area*.

3.6.7 Surface Soil

BNWL-243, *Soil Survey Hanford Project in Benton County Washington* lists and describes 15 different soil types on the Hanford Site, varying from sand to silty and sandy loam. The 200 East Area consists of the Burbank Loamy Sand, the Ephrata Sandy Loam, and the Rupert Sand. The Rupert Sand has now been reclassified as the Quincy Sand (PNL-6415, *Hanford Site National Environmental Policy Act (NEPA) Characterization*). The 200 West Area consists of the Quincy Sand and the Burbank Loamy Sand. The SST WMAs in the 200 East Area are developed in the Burbank Loamy Sand and the Ephrata Sandy Loam. The SST WMAs in the 200 West Area are developed mainly in the Quincy Sand.

The Burbank Loamy Sand is dark-colored, coarse-textured soil underlain by gravel. The surface soil is usually about 40 cm (16 in.) thick but can be 76 cm (30 in.) thick. The gravel content of the subsoil ranges from 20 to 80%. The surface of the Ephrata Sandy Loam is dark-colored, and the subsoil is dark grayish-brown, medium-textured soil underlain by gravelly material, which may continue for many feet. The Quincy Sand (formerly Rupert Sand) is brown to grayish-brown coarse sand grading to dark grayish-brown at about 90 cm (35 in.). Quincy Sand developed under grass, sagebrush, and hopsage in coarse sandy alluvial deposits that were mantled by windblown sand.

Soil horizons have been disturbed or removed over much of the surface within the 200 East and West Area boundaries. It can still be found in undisturbed areas within and between these areas.

3.6.8 Perched Water

Perched water has been encountered locally in the Central Plateau and the 200 Areas. The H1-H2 contact and the Cold Creek unit fine-grained (CCU_u) facies appear to have controlled perched water in localized areas across the 200 West Area, such as east of the T SST WMA, below the U trenches, and under the S-10 Pond. In the 200 East Area, perched water has been encountered at the top of the fine-grained facies of the Cold Creek unit at the B/BY/BX SST WMA. East of the 200 East Area at B Pond, perched water was encountered on top of the Ringold Formation lower mud. At B Pond, the Ringold Formation has been removed above the lower mud so that the Hanford formation directly overlies it.

3.7 LOCAL GEOLOGY IN VICINITY OF WASTE MANAGEMENT AREAS A/AX AND C

This section of the report describes the local geology of the Waste Management Areas A/AX and C.

Data referred to in this section were obtained from published reports, unpublished data on surface geologic studies, and from borehole data. Some graphics are directly from various published reports, leading to a mixture of English and metric units. Where possible, both units are shown.

The information discussed in this document is derived from PNNL-15301, *RCRA Assessment Plan for Single-Shell Tank Waste Management Area T*; RPP-14430, *Subsurface Conditions Description of the C and A-AX Waste Management Areas*; and more recent ground water monitoring reports. The data used here include historic and current water-table elevations; hydraulic properties including hydraulic conductivity, effective porosity, and transmissivity; historic and current groundwater flow directions and flow rates as determined by measured hydraulic properties; and the concentrations and distributions of constituents which are present in the background chemistry of the unconfined aquifer.

Unless otherwise specified, all groundwater chemistry data are from the Hanford Environmental Information System (HEIS) data base and are available from Flour Hanford, Inc. Most groundwater chemistry data collected since the mid-1980s were collected under strict regulatory requirements for the *Resource Conservation and Recovery Act of 1976* (RCRA) or *Comprehensive Environmental Response, Compensation, and Liability Act of 1980* (CERCLA). PNNL-13080, *Hanford Site Groundwater Monitoring: Setting, Sources, and Methods* describes the sampling methods, analytical methods, and quality control and data management practices used to collect and evaluate these data. Groundwater data collected before the mid-1980s are not as well documented and, in a general way, the older the data, the less is known about the data quality. Most of the information presented and discussed in this document is updated from previously published sources by including the latest analytical results from groundwater sampling. Table 3-1 lists the most used sources of groundwater hydrology and geochemistry information.

The detailed description of geologic and stratigraphic relationships are provided for the general area beneath WMA A/AX and some adjoining areas of the 200 East Area, including the C tank farm area (Figure 3-8). The discussion of these relationships is based on a compilation of historical information (HW-61780, *Subsurface Geology of the Hanford Separation Areas*; ARH-LD-127, *Geology of the 241-A Tank Farm*; ARH-LD-128, *Geology of the 241-AX Tank Farm*; ARH-LD-132, *Geology of the 241-C Tank Farm*; RHO-ST-23, *Geology of the Separation Areas, Hanford Site, South-Central Washington*; WHC-SD-EN-TI-012, *Geologic Setting of the 200 East Area: An Update*; HNF-2603, *A Summary and Evaluation of Hanford Site Tank Farm Subsurface Contamination*; PNNL-12261) and some new interpretations allowed by new borehole emplacement and research conducted in calendar year 2003 (PNNL-14538, *Borehole Data Package for RCRA Wells 299-E25-93 and 299-E24-22 at Single-Shell Tank Waste Management Area A-AX, Hanford Site, Washington*; PNNL-14656, *Borehole Data Package for Four CY 2003 RCRA Wells 299-E27-4, 299-E27-21, 299-E27-22, and 299-E27-23 at Single-Shell Tank, Waste Management Area C, Hanford Site, Washington*). The most recent detailed description of the A, AX, and C tank farms is that in RPP-14430, *Subsurface Conditions Description of the C and A-AX Waste Management Areas*, and most of the discussion presented below is built on that report.

Numerous wells have been drilled over the years in the vicinity of these SSTs. Table 3-2 provides geologic contacts for those wells used in the following geologic discussion and cross sections. For some wells, several interpretations of stratigraphic contacts or “picks” have been rendered by various authors over the years. Most of the illustrations presented here reflect picks represented by RPP-14430 with some modification arising from new well logs.

Table 3-1. Stratigraphic Terminology and Unit Thickness for the A/AX and C Tank Farms (3 Pages)

Stratigraphic Symbol	Formation	Facies/ Subunit	Description	A/AX Thickness	C Thickness
Backfill	NA	Backfill – Anthropogenic	Gravel-dominated consisting of poorly to moderately sorted cobbles, pebbles, and coarse to medium sand with some silt derived from coarse-grained Hanford formation (H1 unit) excavated around tanks (ARH-LD-127, ARH-LD-128, ARH-LD-132, RPP-14430); occasional layers of sand to silty sand occur near the base of the backfill sequence.	10 m	10 m
H1	Hanford formation	Unit H1 – (Gravel-dominated facies association). Cataclysmic flood deposits (high-energy)	Gravel-dominated flood sequence; composed of mostly poorly sorted, basaltic, sandy gravel to silty sandy gravel. Equivalent to the upper gravel sequence discussed in PNL-6820, the Q_{fg} documented in Open File Report 94-8, coarse-grained sequence (H1 unit) of RPP-14430 and gravel facies of unit H1 of RPP-8681, and gravel-dominated facies association of DOE/RL-2002-39.	20–30 m	10–30 m
H2	Hanford formation	Unit H2 – (Sand-dominated facies association). Cataclysmic flood deposits (moderate energy)	Sand-dominated flood sequence; composed of mostly horizontal to tabular cross-bedded sand to gravelly sand. Some sand beds capped with thin layers of silty sand to sandy silt. Equivalent to Fine-Grained Sequence (H2 unit) of RPP-14430 and unit H2 of RPP-8681, the sandy sequence of PNL-6820 and WHC-SD-EN-TI-012, to Q_{fs} documented in Open File Report 94-8, and sand-dominated facies association of DOE/RL-2002-39.	30–65 m	45–>70 m
H3	Hanford formation	Unit H3 – (Gravel-dominated facies association). Cataclysmic flood deposits (high-energy)	Gravel-dominated flood sequence; composed of open framework gravel and poorly sorted, basaltic, sandy gravel to silty sandy gravel. Equivalent to the lower coarse-grained unit of the Hanford formation of PNL-6820, to the lower gravel sequence of WHC-SD-EN-TI-012, and to the Hanford formation, H3 sequence of Lindsey et al. (1994).	0–20 m	Not specifically identified as a separate and distinguishable unit in the area of WMA C but may be present and indistinguishable with the lower gravel-dominated sequences belonging to the CCU and Ringold Formation Unit A sediments in the area of WMA C

Table 3-1. Stratigraphic Terminology and Unit Thickness for the A/AX and C Tank Farms (3 Pages)

Stratigraphic Symbol	Formation	Facies/ Subunit	Description	A/AX Thickness	C Thickness
CCU_u/R	Undifferentiated Cold Creek unit and Ringold Formation	Upper subunit	Silty sequence; locally thick layer of silt overlying the gravelly sediments of the lower subunit. Silt facies is light olive-brown to tan colored, massive, well-sorted, fine, calcareous silt to sand with pedogenic traces (i.e., root casts).	0–6 m	Not specifically identified as a separate and distinguishable unit in the area of WMA C
CCU_l/R	Undifferentiated Cold Creek unit and Ringold Formation	Lower subunit	Lower gravel sequence equivalent to pre-Missoula gravels; sandy gravel to gravelly sand beneath the silt-dominated facies and above the top of basalt. Occurs as muddy, sandy gravel to sandy gravel. Moderate to uncemented with some caliche fragments. These sediments may be indistinguishable and may include sediments belonging to the lower H3 gravel-dominated facies associated with the Hanford formation in vicinity of WMA C.	0–>15 m	0 – 25 m
R_{wi}	Ringold	R_{wi} unit – Ancestral Columbia River System braided-stream deposits	Coarse-grained Ringold Formation sequence, consisting of mostly moderately sorted, quartzitic sandy gravel to silty sandy gravel. Equivalent to middle Ringold Formation unit (DOE/RW-0164) and the Ringold Formation unit E gravels (RPP-14430; RPP-8681).	Probably not present	Probably not present

CCU_u/R = upper Cold Creek unit/Ringold Formation.
CCU_l/R = lower Cold Creek unit/Ringold Formation.
H1 = Hanford formation, unit H1; equivalent to upper sand-dominated.
H2 = Hanford formation, unit H2; equivalent to middle sand-dominated.
H3 = Hanford formation, unit H3; equivalent to lower sand-dominated.
NA = not applicable.
Q_{fg} = Quaternary flood gravels.
Q_{fs} = Quaternary flood silt and sand.
R_{wi} = Ringold Formation, member of Wooded Island.

References:
ARH-LD-127, *Geology of the 241-A Tank Farm*
ARH-LD-128, *Geology of the 241-AX Tank Farm*
ARH-LD-132, *Geology of the 241-C Tank Farm*
DOE/RL-2002-39, *Standardized Stratigraphic Nomenclature for Post-Ringold-Formation Sediments Within the Central Pasco Basin*
DOE/RW-0164, *Consultation Draft Site Characterization Plan. Reference Repository Location, Hanford Site, Washington*

Lindsey et al. 1994, “Geohydrologic Setting of the Hanford Site, South-Central Washington”
PNL-6820, *Hydrogeology of the 200 Areas Low-Level Burial Grounds – An Interim Report, Volumes 1 and 2*
Open File Report 94-8, *Geologic Map of the Richland 1:100,000 Quadrangle, Washington*
RPP-8681, *Vadose Zone Geology of Boreholes 299-E33-45 and 299-E33-46 B-BX-BY Waste Management Area Hanford Site, South-Central Washington*
RPP-14430, *Subsurface Conditions Description of the C and A/AX Waste Management Area*
WHC-SD-EN-TI-012, *Geologic Setting of the 200 East Area: An Update*

Figure 3-8. Fence Diagram of the A/AX and C Tank Farms

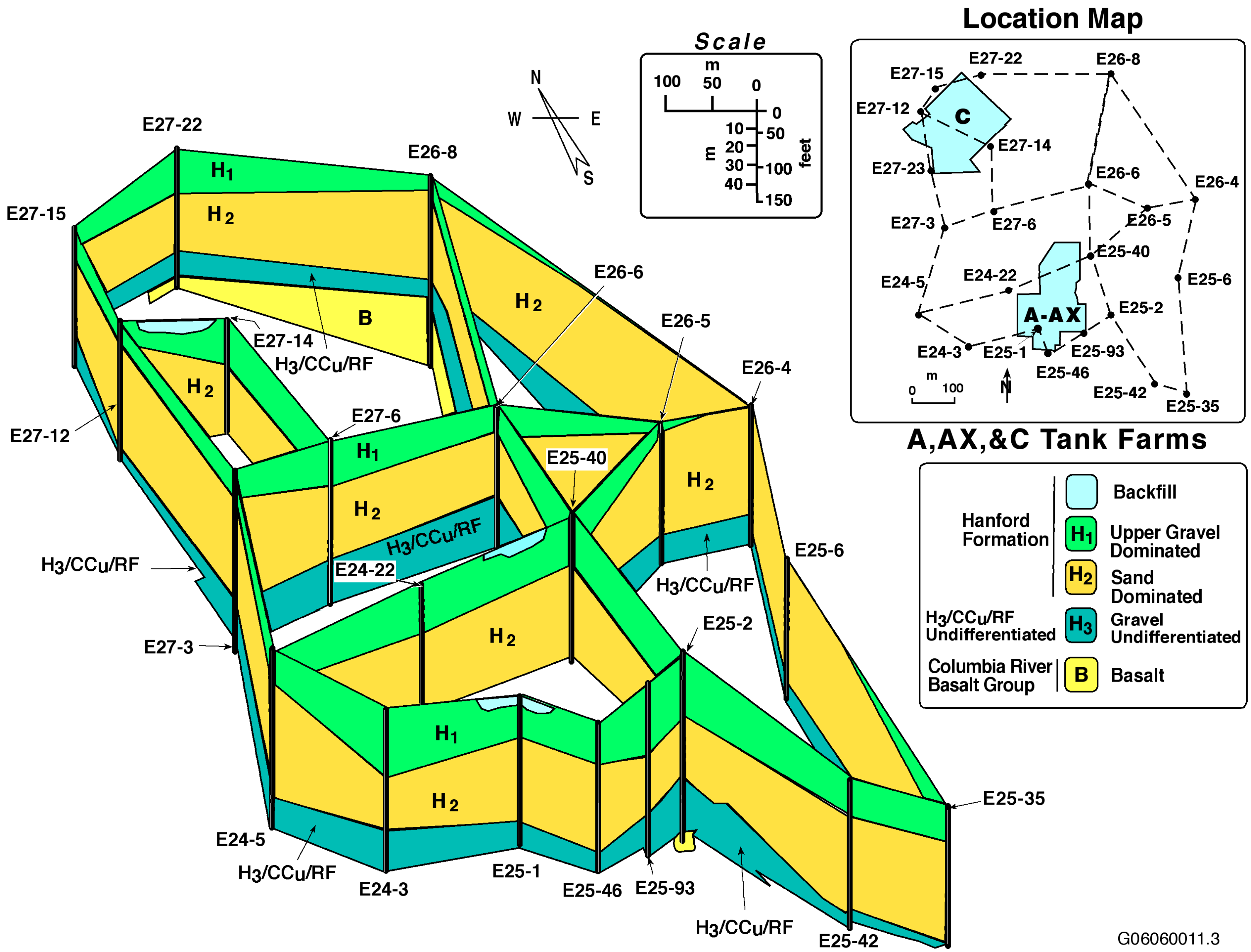

Table 3-2. Stratigraphic Contact Elevations for Boreholes in Waste Management Areas A/AX and C [(a)]

Well No.	Ground Elevation in meters[(b)]	Contact Elevation in meters [(b)]					
		Top H1	Top H2	Top H3	Top CCU_u/R	Top CCU_l/R	Top of Basalt
E24-4	213.4	204.2	187.5	NP	NP	134.1	
E24-5	213.1	213.1	196.3	NP	NP	133.8	
E24-13	210.6	210.6	174.0	NP	128.3	122.2	
E24-20	210.0	210.0	179.5	NP	126.2	124.7	
E25-1	211.5	202.1	185.6	NP	132.3	126.2	
E25-2	206.3	202.1	169.8	143.9	128.6	125.6	98.1
E25-6	201.8	NP	201.8	143.9	121.0	119.5	
E25-7	201.2	NP	201.2	143.3	NP	120.4	
E25-35	205.7	205.7	184.4	141.7	126.5	123.4	
E25-41	204.8	204.8	174.3	143.9	127.1	122.5	
E25-42	209.1	209.1	182.9	140.2	NP	126.5	
E25-46	212.8	212.8	184.4	129.5	126.5		
E25-48	208.2	208.2	180.7	141.1	128.9	122.8	
E25-93	207.3	203.9	170.7	132.6	NP	114.3	
E26-4	197.8	197.8	193.5	157.0	129.5	126.5	
E26-5	198.7	198.7	192.6	154.5	NP	128.6	
E26-6	199.6	199.6	181.4	147.8	125.0	123.7	
E26-8	189.0	189.0	178.3	NP	NP	112.8	
E27-3	208.8	208.8	198.1	124.4	NP	101.5	
E27-4	204.8	196.9	171.3	NP	131.7		
E27-6	205.7	205.4	175.3	128.0	126.2	102.4	
E27-12	201.5	201.5	180.1	NP	132.9		
E27-13	204.2	204.2	167.6				
E27-14	200.9	200.9	172.2	NP	NP	130.8	
E27-15	199.3	199.3	180.7	NP	130.8		
E27-21	205.1	205.1	185.3	NP	132.0		
E27-22	192.6	192.6	168.2	NP	127.1	110.9	
E27-23	205.7	202.4	175.3	NP	137.2		

[(a)] WMP-22817, *Geologic Contacts Database for the 200 Areas of the Hanford Site* and RPP-14430, *Subsurface Conditions Description of the C and A-AX Waste Management Area*.
[(b)] Multiply by 3.281 to convert meters to feet.

NP = unit not present
CCU_u/R = undifferentiated Cold Creek unit/Ringold Formation fine-grained sediments.
CCU_l/R = undifferentiated Cold Creek unit/Ringold Formation coarse-grained sediments.
H1 = Hanford formation, unit H1; equivalent to upper gravel-dominated.
H2 = Hanford formation, unit H2; equivalent to sand-dominated.
H3 = Hanford formation, unit H3; equivalent to lower gravel-dominated.
R_{wia} = Ringold Formation, Member of Wooded Island, unit A.

The A, AX, and C tank farms were built in Hanford formation sediments. Based on RPP-14430, seven stratigraphic units lie beneath WMAs A/AX and C. From oldest to youngest, the primary geologic units are:

- CRBG
- A lower gravel-dominated sequence that has been locally interpreted as including either:
  - An undifferentiated combination of a CCU fine unit and/or Ringold Formation sediments (CCU/R)
  - An undifferentiated combination of Hanford formation gravel and/or CCU gravel and/or Ringold Formation, unit A sediments (H3/CCU/R), or
  - A lower gravel-dominated sequence belonging to the Hanford formation (H3 unit)
- A sand-dominated sequence (H2 unit) belonging to the Hanford formation
- An upper gravel-dominated sequence (H1 unit) belonging to the Hanford formation
- Recent deposits.

The CCU is equivalent to the “Plio-Pleistocene Unit” that was previously used in RPP-14430.

3.7.1 Columbia River Basalt Group

The Elephant Mountain Member is the uppermost basalt flow beneath the A/AX and C tank farms. It lies at an elevation of approximately 100 m (328 ft) above mean sea level and dips gently to the southwest toward the axis of the Cold Creek syncline (ARH-LD-127, ARH-LD-128, ARH-LD-132, DOE/RW-0164). Up to 15 m (50 ft) of topographic relief exists on the basalt surface as a result of tectonic deformation and/or erosion.

3.7.2 Undifferentiated Lower Gravel-Dominated Sediments

Waste Management Areas A/AX and C lie along the edge of a paleochannel that eroded much or all of the Ringold Formation during CCU and/or Hanford time. Because of the difficulty in distinguishing reworked Ringold Formation gravels and pre-Missoula mainstream Columbia River gravels from original Ringold Formation gravels, these units are undifferentiated here (H3/CCU/R). A similar problem arises with fine-grained sediments overlying the basal gravels. In places, these fine-grained layers appear to correlate to Ringold Formation sediments, based in part on color, but in other areas appear to be more closely related to CCU or even Hanford formation sediments. Therefore, the lower fine-grained sediments are also undifferentiated here.

Gravelly facies immediately overlying basalt within most of the study area have been interpreted as belonging to an undifferentiated combination of H3/CCU/R gravel units. An exception is in the northeast of WMA C near borehole 299-E26-8, where the top of basalt has been interpreted as rising above the undifferentiated combination of CCU_l/R sediments, leaving the gravel-dominated Hanford formation sediments lying directly on top of basalt. The CCU_l/R sediments consist of predominantly sandy pebble- to cobble-sized gravel with occasional boulders. Mineralogically, the sand fraction consists of 15 to 60% basalt grains with generally less than 1 wt% calcium carbonate. The total thickness of this unit is less than 27 m (90 ft), based on a limited number of boreholes where the upper and lower boundaries are represented. The top of the undifferentiated combination of H3/CCU/R gravels ranges from about 120 to 130 m (390 to 425 ft) elevation above mean sea level.

The fine-grained unit, H3/CCU/R, is found in most boreholes beneath WMA A/AX. It occurs at a depth of about 79 m (260 ft) and ranges in thickness from 0 to 7 m (0 to 21 ft). Descriptions of this unit vary significantly, which may be due to 1) subjective descriptions and/or interpretations by different drillers and geologists; 2) heterogeneities within the unit, which may include multiple lithologic units (i.e., CCU silts overlying Ringold Formation mud); or 3) a combination of the above. Where present, this fine-grained unit is described in about half of the boreholes as a blue-, gray-, or olive-colored clay or mud; remaining borehole logs describe the unit as a tan to brown sandy silt to “heavy” silt, which may display a laminated to mottled structure. The former description fits that of Ringold Formation paleosol facies (DOE/RW-0164), whereas the latter fits descriptions for the Cold Creek silt facies (HNF-5507), interpreted as eolian-overbank in origin. Unlike most other fine-grained units in the 200 Areas, the undifferentiated Cold Creek silt and/or Ringold Formation mud unit is generally noncalcareous, containing only a few weight percent or less calcium carbonate.

Some gross gamma-ray logs show a moderate increase in activity occasionally accompanied by an increase in moisture. The water table was higher in the past; thus, the increased moisture content may be a remnant of a higher water table.

3.7.3 Hanford Formation Sediments

The Hanford formation makes up the majority of the suprabasalt sedimentary sequence beneath WMA A/AX, ranging in thickness from 61 to 83 m (200 to 275 ft). The Hanford formation has been divided into three informal units (H1, H2, and H3 from top to bottom) in the 200 East Area. These units do not correspond to similarly named units in the 200 West Area.

The H3 unit is the Hanford formation’s lower gravel-dominated sequence in the area and overlies undifferentiated Cold Creek/Ringold Formation deposits. This sequence is equivalent to the lower coarse-grained unit of the Hanford formation of PNL-6820, *Hydrogeology of the 200 Areas Low-Level Burial Grounds—An Interim Report*, to the lower gravel-dominated sequence of WHC-SD-EN-TI-012, and to the Hanford formation H3 sequence of “Geohydrologic Setting of the Hanford Site, South-Central Washington” (Lindsey et al. 1994).

The H3 unit consists of clast-supported, sandy, pebble to boulder gravel to matrix-supported pebbly sand. This unit appears to be missing from beneath most of WMA A/AX. The unit is probably absent from these areas because of lateral facies changes that take place between gravel-dominated facies to the north and sand-dominated facies to the south away from the axis of primary flood channel that exists north and east of the study area. The surface of the H3 unit slopes to the south and west, with the highest elevations occurring in the northeast and east portions of the study area.

The H2 unit is continuous beneath WMAs A/AX and C. It overlies the undifferentiated CCU/R units or the H3 unit where present. The H2 unit is equivalent to the middle sand unit (PNL-6820), the fine sequence of WHC-SD-EN-TI-012, and the Hanford formation H2 sequence of Lindsey et al. (1994).

Dominantly a fine- to coarse-grained sand, the H2 unit also contains lenses of silty sand to slightly gravelly sand. Minor sandy gravel to gravelly sand beds occur sporadically. Consolidation ranges from loose to compact. Cementation is very minor or absent. Silt lenses and thinly interbedded zones of silt and sand are common but are not abundant in the H2 unit. These thin (<0.3 m [1 ft]) fine-grained zones generally cannot be correlated between boreholes and are not reflected in the gross gamma-ray logs or moisture data. Sampling intervals are probably too large to detect such thin zones. The fine structure observed in some older gross gamma-ray logs may reflect changes in the silt content that were not detected during drilling.

The upper portion of H2 may have been scoured by a southeast-trending Ice Age flood channel, associated in part with deposition of the overlying gravelly H1 unit. This is indicated by a south to southeast-trending trough present at the top of the H2 unit. Furthermore, over 40 m (130 ft) of relief exists on top of the H2 unit at right angles to the axis of this trough.

The H1 upper gravel sequence is equivalent to the upper coarse-grained unit of PNL-6820, the upper gravel sequence of WHC-SD-EN-TI-012, and the Hanford formation H1 sequence of Lindsey et al. (1994). This unit consists of predominantly loose, sandy gravel to gravelly sand, with minor beds of sand to silty sand. Coarser beds may contain boulder-sized materials. Occasional thin, discontinuous lenses of fine sand and silt may also be present.

The H1 unit thickens near the center of the study area and beneath WMA A/AX where it reaches approximately 30 m (100 ft) thick.

3.7.4 Clastic Dikes

No clastic dikes have been observed in WMAs A/AX and C. This is probably because sediment at WMAs A/AX and C is reworked Ringold sediment and course-grained sediment of the Hanford Formation. Clastic dikes have been observed, however, in the Waste Treatment Plant (WTP) excavations and in the Integrated Disposal Facility (IDF) excavation. In both localities, they occur within the sand- and silt-dominated facies of the Hanford formation (Figure 3-9) which are absent in WMAs A/AX and C. The vertical extent of clastic dikes in those localities is limited. Excavations at the IDF show that clastic dikes extending from the surface make abrupt bends and become nearly horizontal (see Figures 3-9 and 3-10).

3.7.5 Recent Deposits

Two types of recent deposits are present in WMAs A/AX and C: 1) eolian sand and silt and 2) backfill material. Backfill is found within the tank farms and other disturbed areas. Fine to medium sand to silty sand caps the sedimentary sequence outside the tank farms. These fine-grained eolian deposits are up to 6 m (20 ft) thick and contain up to 10 wt% calcium carbonate associated with recent soil development.

Figure 3-9. Clastic Dikes in the Excavated Wall of the Integrated Disposal Facility. Arrows show the abrupt change from vertical to nearly horizontal.

Source: PNNL-15237, *Geology of the Integrated Disposal Facility Trench*

3.8 TECTONIC DEVELOPMENT OF THE HANFORD SITE

The geologic history of the Pacific Northwest from the Precambrian to the present and the resulting geologic structures that have developed at the Hanford Site significantly affect principally the seismic hazards of the Site (WHC-SD-W236A-TI-002, *Probabilistic Seismic Hazard Analysis, DOE Hanford Site, Washington*). This section summarizes the principal tectonic events in the development of the Hanford Site and their hazards.

The principal tectonic processes in the Hanford area have been north-south compression and subsidence. The present structure of the Columbia Basin and Hanford Site is the product of this compression that began in the early Tertiary prior to the eruption of the CRBG; that compression continues today. This pattern of deformation has produced the Yakima Fold Belt but this area overlies a large, mostly hidden Tertiary basin that began subsiding in the Eocene (approximately 55 Ma) and continues today.

Figure 3-10. Clastic Dikes to Right of Figure 3-9

Source: PNNL-15237, *Geology of the Integrated Disposal Facility Trench*

The rates of deformation (folding, faulting and subsidence) in the Columbia Basin and Hanford Site were greatest during the eruption of the basalt flows in the Miocene (17 Ma). The main form of tectonism has been subsidence of the basin with the Yakima Fold Belt superimposed on this subsidence. The rate of subsidence of the basin and rate of local folding and faulting of the anticlinal ridges have both declined since the Miocene. The present rate of ridge growth is estimated at 0.04 mm/yr and the rate of subsidence in the basin is estimated at $3x10^{-3}$ mm/yr. More recent work using deformation rates determined from the Global Positioning System ("Fault locking, block rotation and crustal deformation in the Pacific Northwest" [McCaffrey et al. 2007]) has determined similar rates of ridge deformation.

Microseismicity, high *in situ* stress conditions, and the geometry of Quaternary-Holocene faulting indicate that the basin is still experiencing N-S compression (Reidel et al. 1994). Although known late Cenozoic faults are found exclusively on the anticlinal ridges, earthquake focal mechanisms and strain measurements suggest that most stress release is occurring in the synclinal areas. The high *in situ* stress in the Cold Creek syncline can explain the microseismicity in the region but the absence of microseismicity associated with the anticlinal ridges may result from a component of aseismic or below detection limit seismic slip, or the fault zones may be locked up.

3.9 SEISMIC ACTIVITY AND EARTHQUAKES ON THE HANFORD SITE

Tectonic studies have concluded that earthquakes can occur in the following six different tectonic environments (earthquake sources) at the Hanford Site (WHC-SD-W236A-TI-002).

- **Major Geologic Structures**. Reverse/thrust faults in the CRBG associated with major anticlinal ridges such as Rattlesnake Mountain, Yakima Ridge, and Umtanum Ridge could produce some of the largest earthquakes (7.0 M_c).

- **Secondary faults**. These faults are typically smaller (1 to 20 km) than the main reverse/thrust faults that occur along the major anticlinal ridges (up to 100 km). Secondary faults can be segment boundaries (tear faults) and small faults of any orientation that formed along with the main structure.

- **Swarm areas (see Figure 3-11)**. Small geographic areas not known to contain any geologic structures produce clusters of events (swarms), usually in the CRBG in synclinal valleys. These clusters consist of a series of small shocks with no outstanding principal event. Swarms occur over a period of days or months and the events may number into the hundreds and then quit, only to start again at a later date. This differs from the sequence of foreshocks, mainshock, and trailing-off aftershocks that have the same epicenter or are associated with the same fault system. In the past, swarms were thought to occur only in the CRBG. Most swarm areas are in the basalt but swarm events also appear to occur in all. There are seven earthquake swarm areas that are recognized in the Hanford Seismic Network area but this list will be updated as new swarm areas develop. The Saddle Mountains swarm area, Wooded Island swarm area, Wahluke swarm area, Coyote Rapids swarm area, and Horse Heaven Hills swarm area are typically active at one time or another during the year (Figure 3-11). The other earthquake swarm areas are active less frequently.

- **The entire Columbia Basin**. The entire basin, including the Hanford Site, could produce a “floating” earthquake. A floating earthquake is one that, for seismic design purposes, can happen anywhere in a tectonic province and is not associated with any known geologic structure. Seismic interpretation classifies it as a random event for purposes of seismic design and vibratory ground motion studies.

- **Basement source structures**. Studies (WHC-SD-W236A-TI-002) suggest that major earthquakes can originate in tectonic structures in the crystalline basement. Because little is known about geologic structures in the crystalline basement beneath the Hanford Site, earthquakes cannot be directly tied to a mapped fault. Earthquakes occurring in the crystalline basement without known sources are treated as random events.

Figure 3-11. Earthquake Swarm Areas in the Vicinity of the Hanford Site

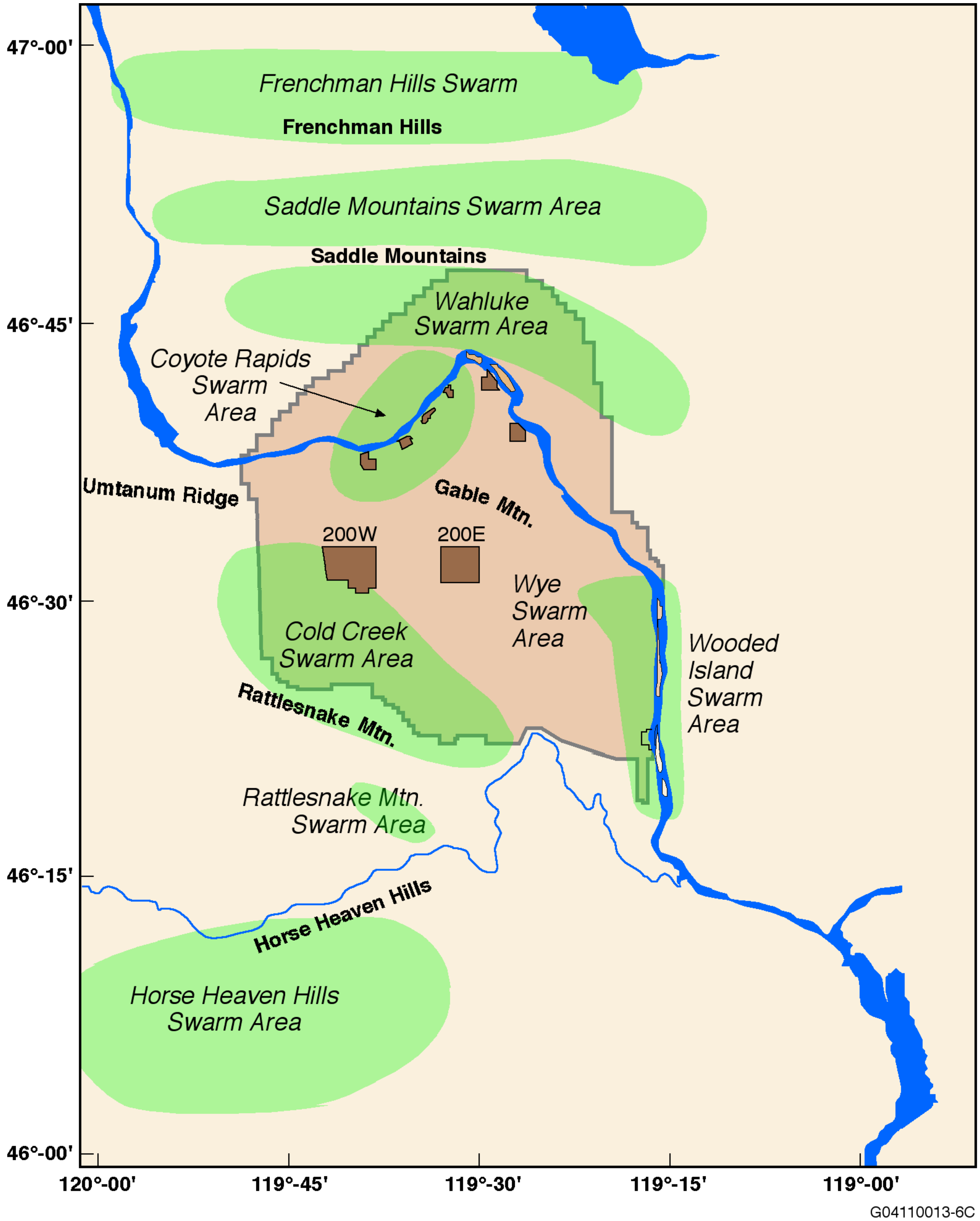

- **The Cascadia Subduction Zone**. This source has been postulated to be capable of producing a magnitude 9 earthquake. Because this source is along the western boundary of Washington State and outside the Hanford Seismic Network, the Cascadia Subduction Zone is not an earthquake source that is monitored at the Hanford Site, so subduction zone earthquakes are not reported here. Because any earthquake along the Cascadia Subduction zone can have a significant impact on the Hanford Site or can be felt like the February 2001 Nisqually earthquake, UW monitors and reports on this earthquake source for the DOE. Ground motion from any moderate or larger Cascadia Subduction Zone earthquake is detected by Hanford seismic monitoring arrays and reported (see Section 5.0).

Since records have been kept, most of the earthquakes at the Hanford Site have originated in the CRBG layer. The crystalline basement has had the next greatest amount of earthquakes followed by the pre-basalt sediments.

Beginning in January 2009, the Pacific Northwest National Laboratory's seismic monitoring array began recording numerous small earthquakes in the Wooded Island earthquake swarm area (Figure 3-11) (PNNL-19071, *Annual Hanford Seismic Report for Fiscal Year 2009*). From January to June, over 1,600 earthquakes were recorded with over 250 events per month. July marked the decline in earthquake activity with only 10 to 15 events per month occurring until activity leveled out in September. The largest earthquake occurred on May 13, 2009 and had a coda Magnitude of 3.0. A few of the larger earthquakes were felt locally.

Most earthquakes were shallow and occurred in the CRBG. The estimated depths were between 1 km and 2.3 km. The U.S. Geological Survey reported that this swarm event resulted in uplift of the Earth's surface of 35 mm ("InSAR measurement of surface deformation at the Hanford Reservation associated with the 2009 Wooded Island earthquake swarm (Invited)" [Wicks et al. 2009]).

3.10 GEOLOGIC HAZARD ASSESSMENT

3.10.1 Volcanic Hazard Assessment

Two types of volcanic hazards have affected the Hanford Site in the past 20 million years:

- continental flood basalt volcanism that produced the CRBG, which underlies the Hanford Site, outcropping in the surrounding ridges, which is no longer a hazard

- volcanism associated with the Cascade Range, which still remains a hazard due to ash fall.

3.10.2 Seismic Hazard Assessment

A seismic hazard analysis was completed for the Hanford Site (WHC-SD-W236A-TI-002). Previous seismic hazard analyses were done for Washington Public Power Supply System WNP 1/4 and WNP/2, which also are located on the Hanford Site.

The following potential seismic sources were determined to be the major contributors to the seismic hazard in and around the Hanford Site.

- Crustal sources:
    - fault sources related to the Yakima Folds
    - shallow basalt sources that account for the observed seismicity within the CRBG and not associated with the Yakima Folds
    - crystalline basement source region.
- Cascadia subduction zone earthquakes.

4.0 VADOSE ZONE SYSTEM AT WASTE MANAGEMENT AREA C

This section provides a detailed discussion of the vadose zone hydrology in vicinity of the WMA A/AX Area. The foundation of the understanding the hydrogeologic system at WMA A/AX is rooted in the geologic framework and history of the Hanford Site and the central Plateau presented in Section 3. Given the proximity of WMA A/AX to WMA C, the majority of information presented in this section is derived from RPP-RPT-46088, Rev. 1.

The vadose zone, the region between the ground surface and the water table, is host to the underground storage tanks and related facilities in WMA A/X and 1) contains the chemical and radionuclide contaminants which have leaked into subsurface from past leaks and unplanned releases from tanks and ancillary facilities and 2) will receive chemical and radiological contaminants that will be released out of wastes remaining in tanks and ancillary facilities in the future. Key features, processes, and events operating within the local-scale vadose zone system of the WMA A/AX area play a key role in controlling contaminant migration from WMA A/AX facilities through the vadose zone to underlying groundwater.

The geology of the vadose zone underlying WMA A/AX forms the media through which the contaminants move and provides the basis with which to interpret and extrapolate the physical and geochemical properties that control the migration and distribution of contaminants. Of particular interest are the interrelationships between the coarser- and finer-grained facies, and the degree of contrast in their physical and geochemical properties. While the exact distribution of these alternating units is not known, their contrast appears to have a strong influence on the distribution of leak and recharge waters and dissolved tank waste constituents.

Important factors (i.e., features and processes affecting moisture and contaminant transport) are presented in this section, including the state of knowledge on vadose zone hydrology, e.g., field variables such as matric potential and moisture content for tank farm soils as well as vadose zone hydraulic properties. Also discussed is state-dependent anisotropy (also referred to as tension-dependent or moisture-dependent anisotropy) – an important field-scale process that enhances fluid flow and therefore contaminant migration in the lateral direction. The section concludes with a discussion of vadose zone flow and transport properties that would affect numerical modeling of local-scale flow and transport at the WMA A/AX.

4.1 KEY FEATURES OF THE VADOSE ZONE

Key features have been identified as potentially important to consider in conceptual models of the vadose zone at WMA A/AX and in the scope of the WMA A/AX PA calculations and related sensitivity analyses. A list of potential key features were identified in the WMA C PA Working Session held on March 30 through April 1, 2010 that was focused on FEPs. The same FEPs from WMA C are deemed to be applicable to WMA A/AX. The FEPs for the vadose zone were identified for two time periods: 1) the time extending from the operational period through the end of the retrieval, remediation, and correction action period and 2) future projected conditions.

The FEPs identified for past to present conditions and for projected future conditions are summarized in Tables A-1 through A-4 in Appendix A of RPP-RPT-46088, Rev. 1. The key general features that were identified for the vadose zone for these time periods include the following general categories: 1) the geometry, physical, hydraulic, and transport properties of the major hydrogeologic units; 2) the occurrence of potential preferential pathways (i.e., river channels, sloping beds, clastic dikes, etc.); 3) the existence of potential made-made preferential pathways (i.e., unsealed dry wells, groundwater wells, and boreholes); 4) the general moisture conditions in the vadose zone; and 5) current soil and water chemistry and contamination in the vadose zone. They are discussed briefly in this section.

Properties of the Major Hydrogeologic Units: The SSTs and related facilities at WMA A/AX were constructed in Hanford formation sediments. Based on recent work by RPP-14430 and PNNL-15955, *Geology Data Package for the Single-Shell Tank Waste Management Areas at the Hanford Site*, seven stratigraphic units, including the underlying CRBG, have been identified beneath WMAs A/AX and C. As indicated in Section 3.7, the primary hydrogeologic geologic units overlying the underlying basalt bedrock in the area of these two WMAs include the following units:

- A lower gravel-dominated sequence that has been locally interpreted as including either :
    - An undifferentiated combination of CCU fine unit and/or Ringold Formation (CCU/R)
    - An undifferentiated combination of Hanford formation gravel and/or CCU gravel and/or Ringold Formation, unit A (H3/CCU/R), or
    - A lower gravel-dominated sequence belonging to the Hanford formation (H3 unit)
- A sand-dominated sequence belonging to the Hanford Formation referred to as the H2 unit
- An upper gravel-dominated sequence belonging to the Hanford formation referred to as the H1 unit, and
- Recent deposits composed of eolian sands and silts and local backfill.

The CCU is equivalent to the "Plio-Pleistocene Unit" in RPP-14430. All interpretations of major units along lines of section in the general area of WMA A/AX and C are shown in Figure B-1 of Appendix B and are provided in Figures B-2 through B-8 of RPP-RPT-46088, Rev. 1.

Descriptions of the general properties of these units relevant to the WMA A/AX and C areas are provided in Section 3.7 and Appendix B of RPP-RPT-46088, Rev. 1. As mentioned in Section 3.7, interpretations in some of the boreholes and wells identify an undifferentiated gravel-dominated unit below the Hanford formation H2 sands that is considered to be made up of combinations of the lower Hanford formation H3 unit, the Cold Creek gravels and the sandy-gravels belonging to the Ringold Formation at some locations due to difficulties in distinguishing the characteristics of the three underlying units. This indistinguishable unit is typically identified using the H3/CCU/RF or CCU/Rf designation.

Potential Natural Preferential Pathways: Previous work in SST WMAs and WMA C has identified a number of potential naturally-occurring preferential pathways for water flow and transport in the vadose zone. These have included the occurrence of broad stratigraphic features and heterogeneities such as river channel deposits, or changes in contrasting soil texture or cross-cutting vertical features such as clastic dikes that could enhance moisture movement and/or contaminant transport. Some of these features are discussed in Section 3.7 and their potential effects are discussed briefly in Section 4.2.3.

Potential Man-Made Preferential Pathways: About 71 dry wells have been drilled at WMA C. The wells are not a direct contributor to vadose zone water contamination; rather they provide a potential preferential pathway for the rapid downward movement of any existing contamination through the vadose zone. The construction of almost all the wells at the SST farms is not in compliance with *Washington Administrative Code* (WAC) 173-160, "Minimum Standards for the Construction and Maintenance of Wells," which came into existence in 1973. Newly constructed wells (C4297) are constructed in accordance with WAC 173-160, which establishes minimum construction standards including sealing requirements to prevent water movement between aquifers.

However, assuming that some waste is left in the ground after closure, an engineered surface barrier will likely be placed above the farm and all drywells within the tank farm are expected to be decommissioned. Assuming that some waste and contamination within the vadose zone is left in place, some post-closure monitoring will be required, but the form that such monitoring will take has yet to be determined. Whether groundwater monitoring wells will be decommissioned as part of closure is yet to be determined because decisions about any cover design including its aerial extent have not been reached. Some of the groundwater monitoring wells could be candidates for such monitoring. If groundwater monitoring wells are used for monitoring they will be properly sealed and decommissioned so that they do not present a preferential pathway in the future.

Moisture Conditions: Direct characterization of moisture conditions has been limited to what can be inferred from neutron logging of dry wells as a part of tank farm monitoring and detailed collection of moisture content data in specific characterization boreholes.

4.2 FACTORS AFFECTING MOISTURE MOVEMENT IN VADOSE ZONE

Figure 4-1 illustrates a vertical cross-section of an outcrop at the Hanford Site. As the figure suggests, the natural subsurface flow systems can be extremely variable. The heterogeneous nature is manifested in the spatial variability in physical and hydraulic properties of Hanford sediments (WHC-EP-0883, *Variability and Scaling of Hydraulic Properties of 200 Area Soils, Hanford Site*). Subsurface heterogeneity is therefore a rule rather than an exception. Of particular importance is the spatial variability in moisture retention and unsaturated hydraulic conductivity relationships within a geologic unit as well as among different units.

Figure 4-1. A Cross-sectional View of Heterogeneous Sediments in 200 Areas

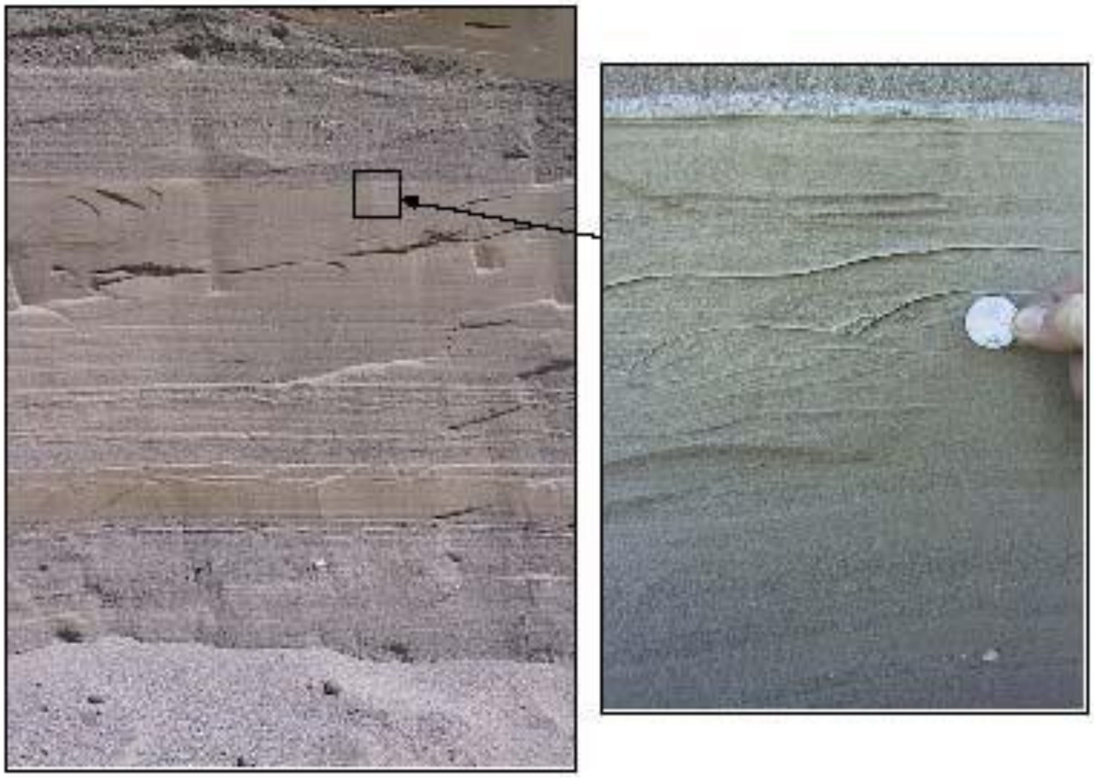

When soil is not saturated, soil moisture moves through interconnected pores that are filled with water and, to a lesser extent, as film flowing around particle surfaces in pores that also contain air. With increasing water content, more pores fill with water, and the rate of downward water movement increases. When considering water infiltration through the unsaturated zone, the total potential in the soil, ϕ, can be expressed mathematically as the sum of both pressure head, *h*, and an elevation head, Z, using the following expression:

$$\phi = h\ (\Theta_v) + Z$$

Where pressure head, *h*, is a function of the volumetric water content, Θ_v. Pressure head is expressed as a negative pressure due to the soil water attraction. Pressure head increases with increasing amounts of soil moisture.

The graphical expression that is typically used to show the non-linear functional relationship between the pressure head, *h* (also referred to as matric potential, ψ), and the corresponding soil volumetric water content, Θ_v, is called the soil moisture retention curve.

Under unsaturated flow conditions, hydraulic conductivity for a particular soil is not a constant property as it would be under fully saturated conditions and is a function of volumetric water content. Unsaturated hydraulic conductivity, K, increases with increasing pressure head and water content. The relationship between unsaturated hydraulic conductivity, K and *h* or the corresponding Θ_v is also a nonlinear function.

4.2.1 Water Retention and Unsaturated Hydraulic Conductivity

Water retention (h versus Θ_v) and the relationships between unsaturated hydraulic conductivity and moisture content (K versus Θ_v) are determined experimentally. As expected, different types of media have different moisture retention characteristics. However, a fundamental porous medium characteristic that influences retention behavior is the sediment particle size distribution, and therefore the pore size distribution for a particular sample. As indicated in Figure 4-2, the moisture content of porous media decreases as the pressure head (or matric potential) becomes more negative. Generally speaking, the rate of reduction in Θ_v as the pressure head h becomes more negative depends on the soil pore size distribution. For instance, sandy sediments tend to have a narrow pore-size distribution (i.e., a relatively large number of large pores and only a few small pores). Therefore, sandy materials tend to have a rapid reduction in Θ_v as h becomes more negative. In contrast, fine-textured materials such as silty sediments have a widespread pore-size distribution and the reduction in moisture content is therefore much gentler (see Figure 4-2).

Figure 4-2. Typical Moisture Retention (volumetric moisture content, Θ_v, versus decreasing pressure head, *h*) Curves for a Fine-textured (e.g., silt) and a Coarse-textured (e.g., coarse sand) Sediment; (the curves represent fit through the experimental data)

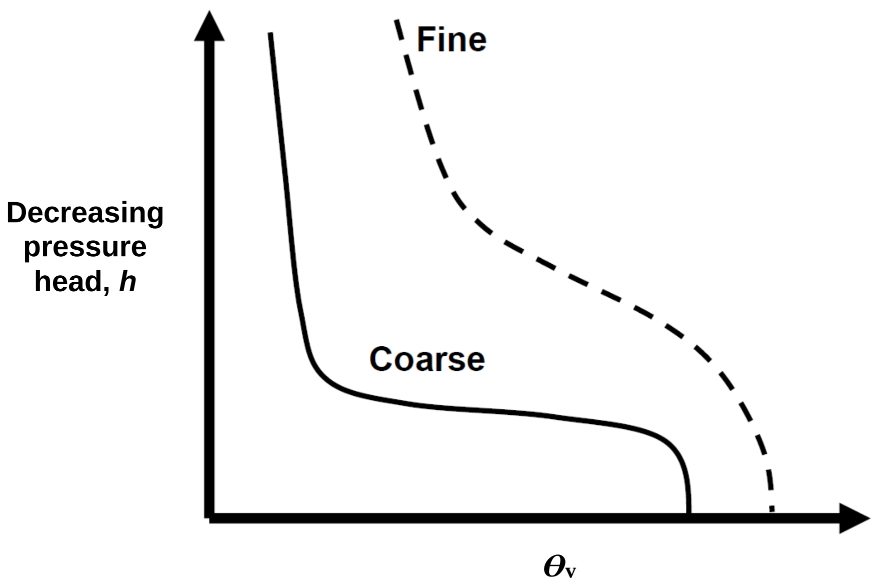

Figure 4-3 illustrates the relationship of unsaturated hydraulic conductivity and pressure head which go with the moisture retention curves for the fine-textured and coarse-textured sediments shown in Figure 4-2. For both fine- and coarse-textured media, the unsaturated hydraulic conductivity (K) decreases with a greater decrease in moisture content (Θ_v); the reduction in K with a reduction in Θ_v is highly nonlinear. The conductivity will asymptotically approach a limiting value after a threshold value of moisture content (i.e., residual water content) is reached. That is, media with moisture content less than the threshold value virtually cannot transmit any significant amount of remaining moisture, because of its being attached to solids or forming films that are isolated from each other.

Figure 4-3. Typical Unsaturated Hydraulic Conductivity, K(*h*) versus Pressure Head, *h* Relation for a Fine-textured (e.g., silt) and a Coarse-textured (e.g., coarse sand) Sediment; (the circles represent the experimental data)

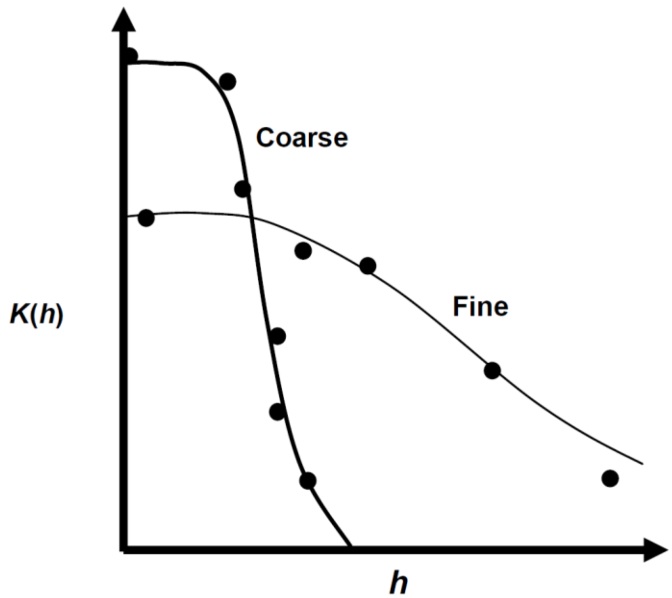

A review of the functional relationships provided in Figures 4-2 and 4-3 indicates the potential impact and enhancement of hydraulic and contaminant transport characteristics of sediments in the vadose zone when a soil profile is wetted, as occurred from intentional and unintentional releases from tanks and pipelines at various tank farm areas during the historical period. The functional relationships also show the potential reduction of the hydraulic and contaminant transport characteristics of the vadose zone sediments with drying of the soil profile in response to emplacement of an engineered surface barrier in the future.

The functional relationships provided in Figures 4-2 and 4-3 are also generally obtained from measurements made as the soil samples are dried. If, at the end of the drying process, the laboratory measurements were continued by rewetting the soil sample, a new retention and unsaturated hydraulic conductivity would be obtained. This phenomenon is known as hysteresis and could be an important process to consider during the historical period when alternate wetting and drying of the soils occurred.

To illustrate the effects of media heterogeneity on unsaturated flow, consider the case where a fine-textured material overlies a coarse-textured material. Suppose the pressure heads (matric potentials) in the two materials are more negative than the cross-over pressure head *h* in their conductivity curves (Figure 4-3). In such a case, moisture in the fine-textured material will not be able to flow into the coarse material below because of its low conductivity (Figure 4-3). In other words, there exists a significant presence of air in the coarse-textured material below, and water from the fine-textured material cannot enter the coarse-textured material unless the pressure head is built up high enough (toward saturation) in the fine-textured material to expel the air in the underlying coarse-textured material. Such a behavior is counter-intuitive, given the fact that the saturated hydraulic conductivity for the coarse-textured material is larger than that of the fine-textured material. Nonetheless, during unsaturated flow conditions (i.e., beyond the cross-over point in Figure 4-3 toward more negative *h*), the unsaturated hydraulic conductivity for the underlying coarse-textured material is much smaller than that of the overlying fine-textured material. This phenomenon is called the capillary barrier effect, and it has been used as a fundamental principle in the design of earth liners for landfills, and “umbrellas” for waste storage facilities to prevent infiltrating moisture migrating below from the surface. As shown in Figure 4-3, up to the cross-over point, the fine-textured material is also a barrier to the flow from any overlying coarse-textured material. This situation also enhances lateral spreading of fluid and solute migration.

In field-scale problems (Sisson and Lu site, T-106 tank leak site) in 200 Areas, we see evidence of such natural capillary breaks during unsaturated flow wherever fine-textured layers are underlain by coarser sediments. The capillary breaks created due to textural discontinuities allow flow to occur laterally until the pressure head, *h* (or matric potential, ψ) in the fine layer is sufficient to overcome the entry pressure head of the underlying coarse layer.

4.2.2 Moisture Dependent Anisotropy

In addition to heterogeneity and textural discontinuities which are ubiquitous with Hanford sediments, an important characteristic is anisotropy (i.e., directional dependence of hydraulic conductivity). Anisotropy in unsaturated hydraulic conductivity and the consequent lateral migration have a strong impact on contaminant fate and transport within the vadose zone. In general, anisotropy in the hydraulic conductivity varies with the observation scale as well as the scale of heterogeneity within the observation scale. In the following paragraphs, we will examine the hydraulic conductivity anisotropy at two observation scales, namely, a pore-scale anisotropy and a field-scale anisotropy.

Pore-scale hydraulic conductivity anisotropy is of interest when we determine the macroscopic hydraulic conductivity over a certain volume of the soil (e.g., a soil core). Within the soil volume, one likely will find that depositional processes cause flat particles (minerals) to orient themselves with the longer dimension parallel to the plane on which they settle. This produces flow channels parallel to the bedding plane, which allow fluid flow with little resistance. Fluid flow in the direction perpendicular to the flat surface of particles, however, must detour and take more tortuous and longer paths than for flow parallel to the bedding plane. Therefore, under the same hydraulic gradient, more flow can occur through a soil core if the gradient is parallel to the bedding plane than if it is perpendicular to the bedding plane. The bulk hydraulic conductivity of the soil core in the direction parallel to the bedding (K_h) is thus greater than in the direction perpendicular to the bedding (K_v). The soil core thus possesses a pore-scale anisotropy in hydraulic conductivity.

In contrast to pore-scale anisotropy, field-scale anisotropy due to hydraulic conductivity arises from the fact that when we determine the hydraulic conductivity in a field situation, we often employ Darcy’s law that assumes homogeneity of the medium over a relatively large flow domain. In essence, we seek to describe effective properties for the media in a large control volume (much larger than the core dimension) that likely includes numerous large-scale structural heterogeneities (such as stratification, cross-bedding, clay lenses, structural discontinuities, etc.). Such anisotropy effects are evident in the experimental work of "Quantifying the Effects of Small-Scale Heterogeneities on Flow and Transport in Undisturbed Cores from the Hanford Formation" (Pace et al. 2003), who found, at lower water contents, a greater conductivity for the Hanford sediment cores parallel to bedding than in sediment cores perpendicular to bedding.

To illustrate impacts of field-scale unsaturated hydraulic conductivity anisotropy on simulated moisture movement, let us assume that Figure 4-4a represents the observed plume due to infiltration into a relatively dry, stratified medium (e.g., Figure 4-1) having heterogeneous and anisotropic properties. In Figure 4-4b, the schematic "classical isotropy" indicates the expected, simulated plume behavior for an equivalent homogeneous medium (i.e., if we assume that the heterogeneous medium is replaced by a homogeneous medium) having isotropic properties ($K_h=K_v$). Note that a constant anisotropy implies that the unsaturated hydraulic conductivity (K) as a function of pressure head (or moisture content) maintains the identical ratio for K parallel to bedding to K perpendicular to bedding. This is illustrated in Figure 4-4d, where the K_h/K_v is constant regardless of variability in pressure head, h or saturation in a partially saturated medium. In case where the media is assumed to be isotropic ($K_h=K_v$), the moisture plume moves predominantly in the vertical than in the lateral direction (Figure 4-4b).

Compared to the observed plume, the vertical extent of the plume is clearly overestimated (Figure 4-4b). In case where a constant anisotropy (K_h/K_v=constant) in unsaturated hydraulic conductivity is assumed (Figure 4-4d), the moisture plume travels more in the lateral than in the vertical direction. Illustrated in Figure 4-4c is the simulated moisture content distribution with a moisture-dependent anisotropy in unsaturated hydraulic conductivity. The moisture content distributions in both Figure 4-4a (observed plume) and Figure 4-4c (simulated plume) show significant lateral movement. The anisotropy in unsaturated hydraulic conductivity retards vertical movement of moisture but enhances lateral spreading (Figures 4-4a and 4-4c). With the moisture-dependent anisotropy, a greater lateral spreading is evident (Figure 4-4c) than in an isotropic profile (Figure 4-4b). As shown in Figure 4-4d, unlike constant anisotropy, for moisture-dependent anisotropy, K_h/K_v is a function of pressure head or moisture content. Also, as shown in Figure 4-4d, as the pressure head, h becomes more negative or as the medium gets drier, for moisture-dependent anisotropy, the K_h/K_v ratio becomes larger. The effects of moisture-dependent anisotropy on moisture plume dynamics are further illustrated for the plume resulting from field injection experiments at the Sisson and Lu site in 200 East Area.

Figure 4-4. Schematics Illustrating Comparison of (a) an Observed Plume with Simulations using (b) an Isotropic, and (c) a Variable Moisture Dependent Anisotropy for Unsaturated Hydraulic Conductivity (K); (d) Constant and Variable Anisotropy; Kh is Horizontal Hydraulic Conductivity Parallel to Bedding and Kv is Vertical Hydraulic Conductivity Perpendicular to Bedding; ψ is Matric Potential or Pressure Head (*h*)

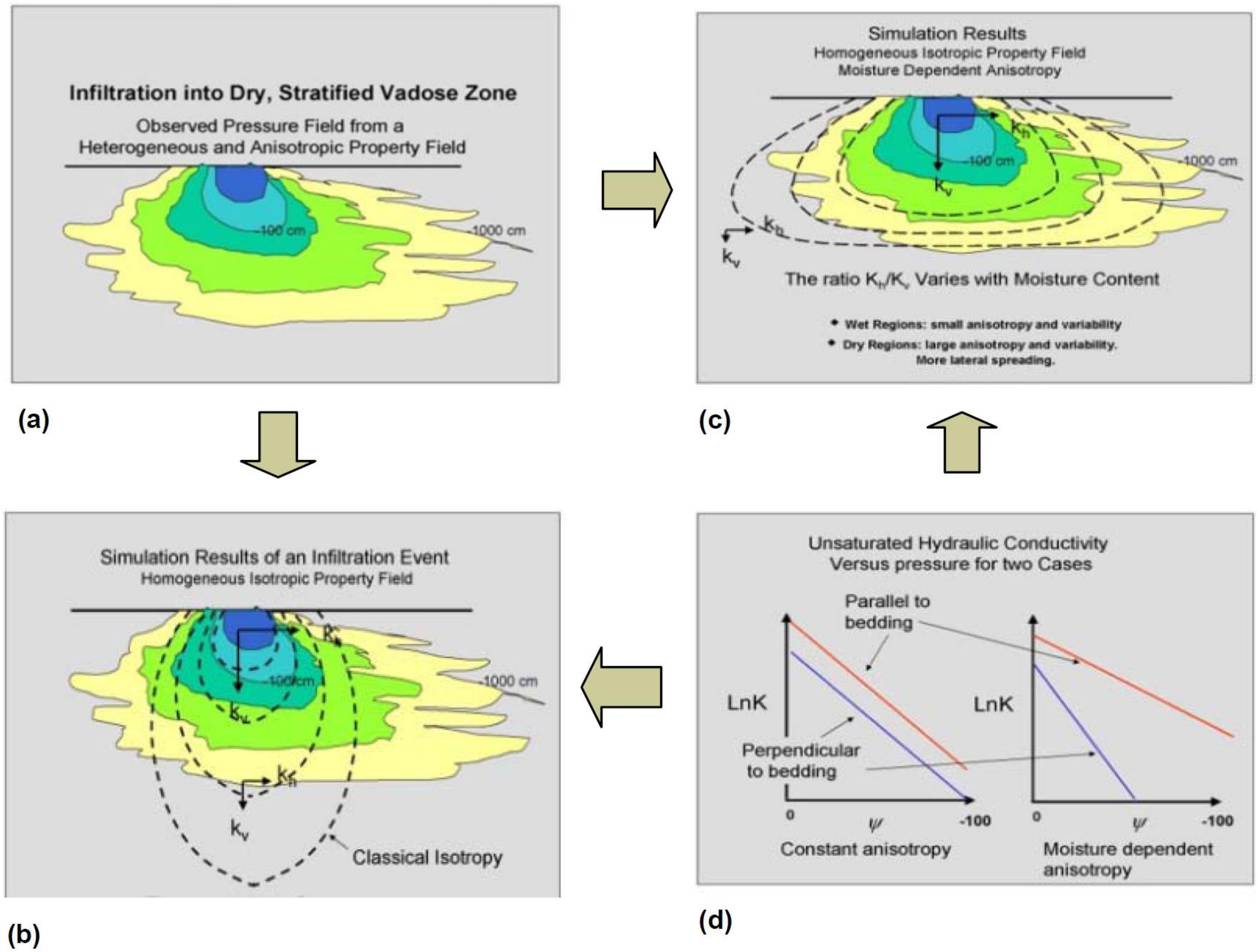

4.2.3 Influence of Preferential Pathways

In addition to the conventional homogeneous approaches to modeling porous medium flow, preferential flow – a process whereby water and contaminants move along preferential pathways, which are not included in the homogeneous medium model – is of interest in analysis of moisture flow through vadose zone soils. Preferential pathways can be natural (e.g., clastic dikes) or manmade (e.g., unsealed monitoring wells). Although preferential flow has been recognized and widely studied under saturated or near saturated flow conditions ("Modeling Tritium and Chloride 36 Transport Through an Aggregated Oxisol" [Nkedi-Kizza et al. 1983], "Solute Transfer through Columns of Glass Beads" [De Smedt and Wierenga 1984]), there is little evidence of it in arid and semiarid climates or under low water fluxes, particularly where soils are coarse-grained such as those under the tank farms. Typically, under natural recharge conditions, meteoric precipitation at arid sites is usually too low to invoke preferential flow; much of the water in the dry soils is simply adsorbed onto the grain surfaces and cannot move along preferred pathways. The flux of natural infiltration from precipitation is generally low, but somewhat higher fluxes developed over the years from inadvertent application of water to wash down contaminants found in surface soils to deeper soils following releases, the use of water to excavate soils around surface facilities (often referred as hydroexcavation), and releases from raw water lines (either deliberate or inadvertent). Potential preferential pathways during release events from tank leaks in the near-field include wetting front instability or 'fingering' flow. Wetting front instability, reported in petroleum related literature, is a special case of interface instability during immiscible fluid displacement in porous media. The phenomenon is triggered by unfavorable differences between the viscosities and densities of two fluids across their interface, which is a condition that can potentially exist during release events, for example, at S-SX tank farm. However, unlike S-SX tank farm conditions where the ionic strength of the plume is extremely high, such conditions are not expected to dominate fluid and contaminant migration during release events at other tank farms.

Among potential preferential pathways, the probability of encountering clastic dikes beneath tank farms is substantial. For example, numerous clastic dikes occur at the US Ecology site southwest of the 200 East Area that may serve as conduits for preferential flow. While a clastic dike can potentially increase flow rate, it is less likely to intersect large segments of leaked wastes, and when it does, the cross-sectional area of the intersection is small (DOE/RL-96-61, *Hanford Site Background: Part 3, Groundwater Background*).

Therefore, the presence of clastic dikes in unsaturated media appears unlikely to contribute much to the transport to groundwater of the bulk quantity of leaked wastes and, based on the results of WMA S-SX FIR simulations (RPP-7884, *Field Investigation Report for Waste Management Area S-SX*), are not expected to contribute significantly to long-term risk in terms of higher peak concentrations for long-lived mobile radionuclides. However, attempts at previous modeling efforts to simulate the effects of clastic dikes have not always adequately represented the geometry and extent of these features. Thus, additional simulations that can better approximate the tabular and three-dimensional characteristics of clastic dikes may be needed to portray the hydraulic and contaminant transport attributes of clastic dikes more realistically. The conceptual models to be used for the PA effort will be developed and documented in a collaborative process involving Ecology. The appropriate modeling of clastic dikes will be evaluated.

Finally, a circumstantial evidence of predominantly porous medium flow is provided by site characterization data for various FIRs. For example, based on the field data (e.g., S-SX 41-09-39 and slant boreholes), and the observation of an apparent ion exchange front for the cations, it can be postulated that the contaminant plume is more likely traveling through the far-field vadose zone sediments via porous media flow as opposed to traveling through preferred pathways. If the latter flow conditions were controlling the plume movement at the SX tank farm, it would be unlikely to encounter the well-developed ion exchange front throughout the borehole profiles.

4.3 ALTERNATIVE CONCEPTUAL MODELS OF VADOSE ZONE FLOW AND TRANSPORT AT WASTE MANAGEMENT AREA C

Alternative conceptual models of vadose zone flow and transport were developed and described as part of the Field Investigation Report for WMA C (RPP-35484, *Field Investigation Report for Waste Management Areas C and A/AX*,) and the data quality objective (DQO) for Phase 2 Characterization Activities (RPP-RPT-38152, *Data Quality Objectives Report Phase 2 Characterization for Waste Management Area C RCRA Field Investigation/Corrective Measures Study*), and include input from the Nez Perce. Five initial alternative models were presented in the WMA C PA Working Session on Assessment Context on September 1 through 3, 2009 and were included in Section 9.3 of RPP-RPT-41918, Rev. 0 as a starting point to facilitate discussion of viable alternative models during this working session.

The alternative models developed for WMA C include:

- a Phase 1 Alternative Model
- a Modified Phase 1 Alternative Model to Account for Additional Recharge
- an Alternative Based on Contaminant Movement Down Stratigraphic Dip (Nez Perce)
- an Alternative Based on Preferential Pathway
- an Alternative Based on Unknown Leak Event.

The order of their presentation in this list is not intended to imply a preference of one over the other. Final alternative model(s) selected for consideration in the integrated WMA A/AX PA may likely reflect elements of one or more of these alternative models and will be developed through the Working Sessions process for WMA A/AX.

A summary of these conceptual models of the vadose zone, that contain many of the FEPs that have been identified to date, were described for conditions prevalent in the past and projected future conditions. These conceptual models will undergo revisions if additional FEPs identified in the screening process are found to be important and should be considered in the WMA A/AX PA. They are provided in Appendix D of RPP-RPT-46088, Rev. 1.

4.4 RECOMMENDED FLOW AND TRANSPORT PROPERTIES

This section provides discussions of the range of flow and transport properties that will be used to evaluate flow and transport through the vadose zone at WMA A/AX. Flow-related parameters considered include fitting parameters associated with models that will be used to evaluate the relationship between capillary pressure and moisture content (i.e., moisture retention characteristics), and the relation of these factors with saturated and unsaturated hydraulic conductivity. An additional flow related parameter will also include estimates of macroscopic anisotropy that will be used to evaluate the effect of tension dependent anisotropy in flow calculations with the vadose zone.

4.4.1 Flow Properties

Discussion of the key features of the sediments within the vadose zone system up to this point has stressed the heterogeneous nature of the sands and gravelly-sands associated with the major hydrogeologic units. The challenge in the PA for WMA A/AX is the development of a suitable approach for treatment of these features given the scale of the flow and transport analysis and limited amount of characterization data and information that is available to define the levels of heterogeneity at the scales of interest.

For purposes of the initial PA for WMA C, the technical approach that has been adopted was to approximate the hydraulic properties of the vadose system with composite properties developed from flow-related parameters acquired from limited sampling of the major hydrogeologic units across the Hanford Site. The composite properties are being used to represent the major units in a proposed base case that provides a basis against which results from other alternative models with other treatments of system heterogeneities could be compared. A similar approach will be followed for WMA A/AX. The effect of system heterogeneities on system performance will eventually be evaluated using a variety of approaches that include:

- Development of alternative conceptual models that consider major features of heterogeneity that can be identified from available characterization data and information

- Evaluation of the range of hydraulic properties in proposed sensitivity cases that could represent the range of hydraulic properties observed during characterization

- One or more sensitivity cases that would attempt to evaluate the effect of system heterogeneities by developing realistic distributions of hydraulic properties based on geostatistical analysis or treatment of available data and information.

Specific flow-related parameters considered include fitting parameters associated with models that will be used to evaluate the relationship between capillary pressure and moisture content (i.e., moisture retention characteristics), and the relation of these factors with saturated and unsaturated hydraulic conductivity. An additional flow related parameter will also include estimates of macroscopic anisotropy that will be used to evaluate the effect of tension dependent anisotropy in flow calculations with the vadose zone.

Specific development of numerical implementation of alternative conceptual models, particularly those that will consider major features of heterogeneity, will be evaluated once the hydrogeologic model and related working version of the numerical model for the WMA A/AX area has been established.

4.4.1.1 Moisture Retention Data. Information on particle-size distributions, moisture retention, and saturated hydraulic conductivity is available for 183 samples in the 200 Areas (RPP-RPT-35222, *Far-Field Hydrology Data Package for the RCRA Facility Investigation (RFI) Report*). These data are corrected for gravel content. Once corrected, hydraulic parameters are determined by fitting the data using a moisture retention model developed in "A Closed-form Equation for Predicting the Hydraulic Conductivity of Unsaturated Soils" (van Genuchten 1980) using the following empirical relationship.

$$\theta(h) = \theta_r + (\theta_s - \theta_r)\left\{1 + [\alpha h]^n\right\}^{-m} \qquad \text{Eq. 4.1}$$

Where:

θ = volumetric moisture content [dimensionless]
h = matric potential or pressure head, which, for notational convenience, is considered as being positive (i.e., tension [cm])
θ_r = residual moisture content [dimensionless]
θ_s = saturated moisture content [dimensionless]
α = a fitting parameter (cm^{-1})
n = a fitting parameter [dimensionless]
m = 1 - 1/n.

Combining the van Genuchten model with "A New Model for Predicting the Hydraulic Conductivity of Unsaturated Porous Media" (Mualem 1976) model for unsaturated conductivity:

$$K(h) = \frac{K_s\left\{1 - (\alpha h)^{mn}\left[1 + (\alpha h)^n\right]^{-m}\right\}^2}{\left[1 + (\alpha h)^n\right]^{m\ell}} \qquad \text{Eq. 4.2}$$

Where:

$K(h)$ = unsaturated hydraulic conductivity [cm/s]
K_s = saturated hydraulic conductivity [cm/s]
ℓ = pore-connectivity parameter [dimensionless], estimated by Mualem to be about 0.5 for many soils.

It is well recognized that the estimated unsaturated conductivities, based on saturated conductivity and the van Genuchten retention model, can differ by up to several orders of magnitude with measured conductivities at the dry end (e.g., "Evaluation of van Genuchten-Mualem Relationships to Estimate Hydraulic Conductivity at Low Water Contents" [Khaleel et al. 1995]).

A simultaneous fit of laboratory-measured moisture retention and unsaturated conductivity data was used in this work, and all five unknown parameters θ_r, θ_s, α, n, and K_s, with m=1-1/n (van Genuchten 1980) were fitted to the data via a code named RETention Curve (RETC) (EPA/600/2-91/065, *The RETC Code for Quantifying the Hydraulic Functions of Unsaturated Soils*). Thus, in order to obtain a better agreement with experimental data for the region of interest (i.e., relatively dry moisture regime), K_s is treated as a fitted parameter during the curve fitting process. The pore size distribution factor, ℓ, (Mualem 1976) was kept fixed at 0.5 during the simultaneous fitting.

Specific values for composite van Genuchten-Mualem parameters for the major hydrogeologic units identified at WMA A/AX for use in the SST PA (DOE/ORP-2005-01, *Initial Single-Shell Tank System Performance Assessment for the Hanford Site*) were made in RPP-RPT-35222. These recommended values, which were used as an initial estimates in the WMA C PA, were summarized in RPP-RPT-46088, Rev. 1, and provided the basis for a denominator case in the WMA C PA. The WMA C PA is currently evaluating revised estimates of these parameter based on comparison of model generated moisture contents with field measured values at WMA C as a part of establishing a base case for use in the PA effort. These revised estimates of hydraulic properties and related documentation will likely form the basis for initial estimates of hydraulic properties used in the WMA A/AX PA.

4.4.1.2 Macroscopic Anisotropy. RPP-RPT-35222 proposed a stochastic model approach to evaluate tension-dependent anisotropy for major sediment units. Variable, tension-dependent anisotropy provides a framework for up-scaling small-scale measurements to the effective (up-scaled) properties for the equivalent, large scale vadose zone. The specific details and equations associated with the proposed methods are described in section 6.7.2 in RPP-RPT-35222. Results of application of the approach in RPP-RPT-35222 for major sediment units are summarized in RPP-RPT-46088, Rev. 1. Based on initial modeling efforts for WMA C, revised estimates of these parameter are being evaluated for purposes of establishing a base case for use in the PA effort. These revised estimates of macroscopic anisotropy and related documentation will likely form the basis for the initial estimates of these parameters in the WMA A/AX PA.

4.4.2 Transport-Related Properties

Specific transport parameters considered include estimate of bulk density, diffusivity and macro-dispersivity, which are used to estimate the effect of concentration gradients and hydraulic gradients on the process of diffusion and dispersion in contaminant transport calculations. Other transport parameters considered include recommended estimates of constituent–specific distribution coefficients (K_d's) which will be used to approximate the effect of chemical factors affecting contaminant-specific mobility or retardation in the transport process.

4.4.2.1 Bulk Density. In the WMA A/AX PA, bulk density estimates, when combined with contaminant-specific distribution coefficients, are required to estimate retardation factors for different specific species. Recommendations, taken from RPP-RPT-35222 for composite bulk density estimates for sediments found within WMA C were provided in RPP-RPT-46088, Rev. 1. These estimates of bulk density for the WMA C PA were revised based on data used to update hydraulic properties discussed in sections 4.4.1.1 and 4.4.1.2. The revised estimates of bulk density and related documentation will likely form the basis for the initial estimates of bulk density in the WMA A/AX PA.

4.4.2.2 Diffusivity. For purposes of the WMA A/AX PA, we will assume that the effective, large-scale diffusion coefficients for all strata at a WMA are a function of volumetric moisture content, θ, and can be expressed using the "Permeability of Porous Solids" (Millington and Quirk 1961) empirical relation:

$$D_e(\theta) = D_0 \frac{\theta^{10/3}}{\theta_s^2} \qquad \text{Eq. 4.3}$$

Where:

$D_e(\theta)$ = effective diffusion coefficient of an ionic species as a function of moisture content
D_0 = molecular diffusion coefficient for the same species in free water.

The molecular diffusion coefficient for all species in free water was assumed to be 2.5×10^{-5} cm^2/sec (WHC-SD-WM-EE-004, *Performance Assessment of Grouted Double-Shell Tank Waste Disposal at Hanford*).

4.4.2.3 Dispersivity

4.4.2.3.1 Macro-dispersivity Estimates for Nonreactive Species. The Gelhar and Axness equation (*Stochastic Subsurface Hydrology* [Gelhar 1993]) is used to estimate asymptotic values of macro-dispersivity. To account for the effects of unsaturated flow, a modified version is used:

$$A_L(< h >) = \sigma_{LnK}^2 \lambda \qquad \text{Eq. 4.4}$$

Where the longitudinal macro-dispersivity depends on the mean tension $< h >$.
To apply Equation 4.4, an estimate of the vertical correlation scale for unsaturated conductivity is needed. A correlation length of the order of about 50 cm was obtained for saturated hydraulic conductivity for sediments near the C tank farm (RPP-13310, *Modeling Data Package for an Initial Assessment of Closure of the C Tank Farm*). For unsaturated conditions, an increase in the variance of log unsaturated conductivity is expected to be compensated in part by a decrease in the correlation scale of log unsaturated conductivity. A correlation length of 30 cm is assumed for log unsaturated conductivity for all strata. RPP-RPT-46088, Rev. 1 provides the log unsaturated conductivity variances and the estimated longitudinal (A_L) and transverse (A_T) macro-dispersivities for various strata. The transverse dispersivities are estimated as one tenth of the longitudinal values ("A Critical Review of Data on Field Scale Dispersion in Aquifers" [Gelhar et al. 1992]). The same estimations of macro-dispersivity can be applied to the WMA A/AX PA.

4.4.2.3.2 Heterogeneous Sorption Enhanced Macro-dispersivities for the Reactive Species. The net effect of sorption is to retard the velocity at which the contaminant migrates through the porous media. Because sorption for specific contaminants may be a function of soil properties, as the soil properties experience spatial variability, the sorption also varies (Gelhar 1993; NUREG/CR-6114, *Auxiliary Analyses in Support of Performance Assessment of a Hypothetical Low-Level Waste Facility: Groundwater Flow and Transport Simulation*, Vol. 3). Stochastic analysis developed by Gelhar (1993) was recommended for evaluating macro-dispersivity enhancement that considers the effect of sorption for various strata in WMA A/AX in the modeling data package reports (RPP-13310, RPP-17209, *Modeling Data Package for an Initial Assessment of Closure of the S and SX Tank Farms*, and RPP-RPT-35222).

In RPP-RPT-35222, this macro-dispersivity enhancement was only developed for consideration for uranium. This theoretical basis for this treatment is described more fully in Section 6.8.8 of RPP-RPT-46088, Rev. 1. The resulting estimates of macro-dispersivity for uranium for key sediment units will likely form the basis for the initial estimates in the WMA A/AX PA.

4.4.3 Contaminant-Specific Distribution Coefficients

Contaminant migration rates are element-specific because of the varying degrees of their chemical reactivity with soils (PNNL-13037, *Geochemical Data Package for the 2005 Hanford Integrated Disposal Facility Performance Assessment*). Some contaminants are largely non-sorbing (i.e., technetium) and migrate with recharge water. Others are highly reactive and migrate very slowly (i.e., cesium).

Chemical reactions that occur when contaminants interact with soil solid phases and retard contaminant migration relative to water flow through the vadose zone are often represented in risk and performance assessments by an adsorption isotherm that makes use of a distribution coefficient (K_d). The K_d value is a lumped parameter and, as a result, neglects many of the chemical complexities of the adsorption processes such as saturation of adsorption sites and aqueous complexation.

The simplest type of adsorption isotherm is a linear adsorption isotherm that is defined using the distribution coefficient, K_d (in ml/g or m^3/kg) as seen in Equation 4.5:

$$S = K_d * C \qquad \text{Eq. 4.5}$$

Where:

S (g/g) = concentration of solute adsorbed onto the solid phase
C (g/ml) = concentration of the solute in solution.

A linear isotherm (or K_d) approach is generally applied as a constant property of the vadose zone and groundwater system, and forms the basis of the general retardation factor (Rf) through the relationship in Equation 4.6 (*Groundwater* [Freeze and Cherry 1979]):

$$Rf = 1 + (\rho/\theta)K_d = Vw/Vc \qquad \text{Eq. 4.6}$$

Where:

ρ = bulk density of the media
θ = effective porosity of the media
Vw = water velocity in the media
Vc = contaminant velocity in the media.

The lower the value of K_d, the lower the retardation factor, and the faster a species migrates through the subsurface. For a non-adsorbing species, $K_d = 0$, Rf reduces to 1, and the species migrates at the water flow velocity.

The K_d value is the ratio of contaminant mass attached to soil solids versus mass dissolved in solution. The advantage of this approach is that K_d values can be easily incorporated in modeling transport. The disadvantage is that K_d values are entirely empirical and are used to represent many different kinds of chemical reactions that are dependent on the contaminant of interest, the soil solid phases present in the vadose zone, and the soil water chemistry. The effects of physical variables (moisture content and gravel fraction) and reactions (colloid formation and migration) can be also incorporated in the K_d approach.

It is recognized that, at WMA A/AX, the sorption characteristics of any one constituent are potentially variable as a function of the heterogeneous nature of physical, textural and chemical properties of the sediments encountered during the transport process. It is likewise acknowledged that the use of a constant K_d model may not provide an adequate approximation for predicting the effects of the adsorption process in situations where spatial mineralogical and hydrochemical characteristics within the vadose zone are variable. This could be particularly true in close proximity to source release areas where unique chemistry associated with tank waste release could have a significant effect on sorption and reactive process for selected constituents. However, the use of spatial and temporal variation in K_ds to account for specific mineralogical and chemical heterogeneity is limited because of general lack of characterization data and information that could support such an approach.

The potential presence of ligands and chelating agents in tank wastes can have some influence and enhance the mobility of some metal constituents. PNNL-13895, *Hanford Contaminant Distribution Coefficient Database and Users Guide*, notes specific examples of such agents enhancing the potential mobility of two normally immobile constituents such as americium and cobalt. Discussion of the effect on mobility of these two constituents in the presence of ligands and chelating agents such as ethylenediaminetetraacetic acid are discussed in detail in PNNL-13895.

The attachment (by adsorption or precipitation) of strongly sorbing radionuclides to colloidal-size materials (1 nm to 1 μm) that may be transported by mobile pore fluids is also potentially an important transport mechanism (*Cation and Anion Adsorption at the Oxide/Solution Interface in Systems Containing Binary Mixtures of Adsorbents: An Investigation of the Concept of Adsorptive Additivity* [Honeyman 1984]; "Migration of Plutonium in Ground Water at the Nevada Test Site" [Kersting et al. 1999]; "Subsurface Transport of Contaminants" [McCarthy and Zachara 1989]; "Review on Subsurface Colloids and Colloid-Associated Contaminant Transport in Saturated Porous Media" [Sen and Khilar 2006]). While little evidence exists at Hanford to support this type of transport mechanism at the field scale, the potential impacts from colloid development to enhance mobility of certain constituents may need to be considered. Susceptible contaminants include those of very low solubility (e.g., americium, plutonium, and thorium) or those that strongly adsorb to mineral phases of clay-size (e.g., <2.0 μm) particles (e.g., $^{137}Cs+$). Mobile colloids are generated when subsurface water systems experience chemical perturbations that cause (1) relatively rapid, in-situ precipitation events; or (2) ionic strength induced particle disaggregation (McCarthy and Zachara 1989, "Chemical Factors Influencing Colloid-Facilitated Transport of Contaminants in Porous Media" [Roy and Dzombak 1997]). These conditions have occurred at Hanford as caustic, saline tank wastes have been neutralized by dissolution and precipitation reactions with surface sediments, and as low ionic strength recharge waters resulting from meteoric water infiltration and infrastructure water losses have migrated behind relatively small volumetric releases of tank wastes causing salinity fronts.

Laboratory studies also show that colloid formation can be significant at tank waste plume fronts as high waste Na^{+} displaces Ca^{2+}, Mg^{2+}, and Sr^{2+} from the exchanger phase and induces the supersaturation of calcite and other phases ("Colloid Formation at Waste Plume Fronts" [Wan et al. 2004a], "Geochemical Evolution of Highly Alkaline and Saline Tank Waste Plumes during Seepage through Vadose Zone Sediments" [Wan et al. 2004b]). The colloid load also produced accumulates in the aqueous phase and significantly exceeds the concentrations produced by salinity gradients ("In Situ Mobilization of Colloids and Transport of Cesium in Hanford Sediments" [Flury et al. 2002]; Wan et al. 2004b). The precipitation reactions neutralize and lower pH at the plume front allowing for supersaturation and precipitation of other phases including uranyl solids ("Geochemical Processes Controlling Migration of Tank Wastes in Hanford's Vadose Zone" [Zachara et al. 2007]) that may also migrate for unknown distances as colloidal material.

Away from the near-field source zones along the total thickness of the vadose zone and the length of the groundwater flow path, field characterization has shown that the unique chemistry and pH conditions from the source zone are buffered as it equilibrates with the background chemical and mineralogical characteristics of natural sediments and concentrations of constituents of concern generally become low relative to the adsorption capacity of the sediments. For these far-field conditions, a constant K_d model can provide a reasonable approximation of the sorption process.

Use of variable or compartmentalized K_d values is one way to deal with spatially variable mineralogy and hydrochemistry that result in significant variability in K_d values along different components with the combined vadose zone-groundwater flow path. In this approach, different K_d values are used for different spatial compartments. Each compartment is assumed to have an average representative mineralogy, hydrochemistry, and associated K_d value. In principal, this approach could be used to deal with adsorption due to unique chemical characteristics in close proximity to the source release zones.

The specific details of K_d implementation in models used in the initial WMA A/AX PA will be developed and will be presented in a data package and presentation for an upcoming Working Session.

RPP-RPT-46088, Rev. 1 listed the contaminant distribution coefficient (K_d) bins that were used as initial estimates in the WMA C PA for various contaminants. Contaminant K_d values were adapted from:

- guidance provided in Washington State Department of Ecology Toxics Clean-up Program Publication No. 94-145, *Model Toxics Control Act Cleanup Levels & Risk Calculations (CLARC) Version 3.1*
- EPA/540/R-95/128, *Soil Screening Guidance: Technical Background Document*
- Letter EM-ER-01-115, "K_d Values for INTEC Groundwater Modeling"
- EDF-ER-275, *Engineering Design File – Fate and Transport Modeling Results and Summary Report*
- *A Practical Guide to Groundwater and Solute Transport Modeling* (Spitz and Moreno 1996)
- *Risk Assessment Information System*, http://rais.ornl.gov/
- Section 4.3 of PNNL-14702, *Vadose Zone Hydrogeology Data Package for Hanford Assessments*
- PNNL-13895.

These estimates of K_d will likely undergo revisions based on more recent available information developed at Hanford by PNNL (PNNL-16663, *Geochemical Processes Data Package for the Vadose Zone in the Single-Shell Tank Waste Management Areas at the Hanford Site* and PNNL-17154, *Geochemical Characterization Data Package for the Vadose Zone in the Single-Shell Tank Waste Management Areas at the Hanford Site*). These revised estimates and associated documentation will be used as the initial estimates in WMA A/AX.

Distribution coefficients are only provided for those constituents with known toxicological effects. Should new information on toxicology require that new constituent be considered, K_d estimates for these contaminants can be added at some later time.

Many of the bulk distribution coefficient (K_d) for non-radiological constituents used in initial efforts at WMA C were taken directly from tables in the "Chemical-Specific Parameter Values - Physical and Chemical Properties" Section of Ecology Publication No. 94-145. The publication has been superseded by the establishment of CLARC Database located at https://fortress.wa.gov/ecy/clarc/Reporting/CLARCReporting.aspx

Contaminant K_d values for many of the organic chemicals were estimated using the organic carbon partition coefficients (K_{oc}) method described in EPA 402-R-99-004A, *Understanding Variation in Partition Coefficient, K_d, Values*, and an estimated fractional organic carbon content for Hanford Site sediments of 0.03% (PNNL-14702).

Contaminants for which inventory estimates exist and that do not have an assigned K_d value are assumed to have a $K_d = 0$. A soil material description of low organic, low salt, with a near-neutral pH is assumed.

No WMA A/AX specific measurements for K_d exist. For uranium, however, PNNL-15503 and PNNL-15617, *Characterization of Vadose Zone Sediments from C Waste Management Area: Investigation of the C-152 Transfer Line Leak* present estimated uranium K_ds from 83 samples taken within WMA C from uranium concentrations on the sediments and in the pore water. For uranium, it was found that the natural background concentrations must be separated from Hanford added material in discussing risk potential. Natural uranium is almost entirely resistant to water leaching and becoming mobile, whereas the material added by Hanford activities appears to have some mobility. The range for uranium K_ds related to Hanford activities based on samples taken at WMA C ranged from 1.09 to 8.32 and these reports recommended a value of 1.0 for WMA C. However, to be consistent with *Technical Guidance Document for Tank Closure Environmental Impact Statement Vadose Zone and Groundwater Revised Analyses* (http://www.hanford.gov/orp/uploadfiles/TCEIS-Vadose.pdf), the WMA C PA used an initial value 0.6 mL/g with sensitivities of 0.2 mL/g and 2.0 mL/g because of the greater range of uranium K_d observed in the 200 Areas of Hanford (PNNL-13895 Rev. 1).

Based on input received during the review of the WMA C data package during the Natural System working session held May 25 to 27, 2010, and in subsequent review of the modeling cases focused on the Natural System during the Engineered System working session held in January 25 to 27, 2010, alternative models are proposed that would examine the effect of using non-linear adsorption isotherms. Commonly used non-linear adsorption isotherms include those based on the Freundlich and Langmuir approaches. These cases would be used to evaluate uranium mobility based on data and analysis performed in the B-Complex area that does not appear to follow a linear isotherm. The results from sensitivity cases examining these approaches at WMA C will be evaluated to determine if these alternative adsorption isotherms should be considered for the WMA A/AX PA effort.

Freundlich sorption isotherm is a more general equilibrium isotherm. It is shown graphically in Figure 4-5 and mathematically given by

$$S = K_f C^N$$

Where K_f is the Freundlich adsorption constant, N is the Freundlich exponent, C is the solution concentration (mg/l), and S is the adsorbed concentration in mg/kg (*Ground Water Contamination – Transport and Remediation* [Bedient et al. 1994]).

The Langmuir Isotherm is based on the concept that a solid surface possesses a finite number of sorption sites. When all the sorption sites are filled, the surface will no longer sorb solute from solution. The Langmuir isotherm is given by

$$S = \frac{\alpha\beta C}{1 + \alpha C}$$

Where α is an absorption constant related to the binding energy (L/mg), and β is a maximum amount of solute that can be sorbed by the solid (mg/kg) (see Figure 4-6). C is the solution concentration (mg/l) and S is the adsorbed concentration in mg/kg (Bedient et al. 1994).

Figure 4-5. Example Plots of Freundlich isotherm in terms of S versus C using Freundlich Adsorption Constant (K_f) ranging from 1 to 10 and Freundlich exponent (N) of 0.6

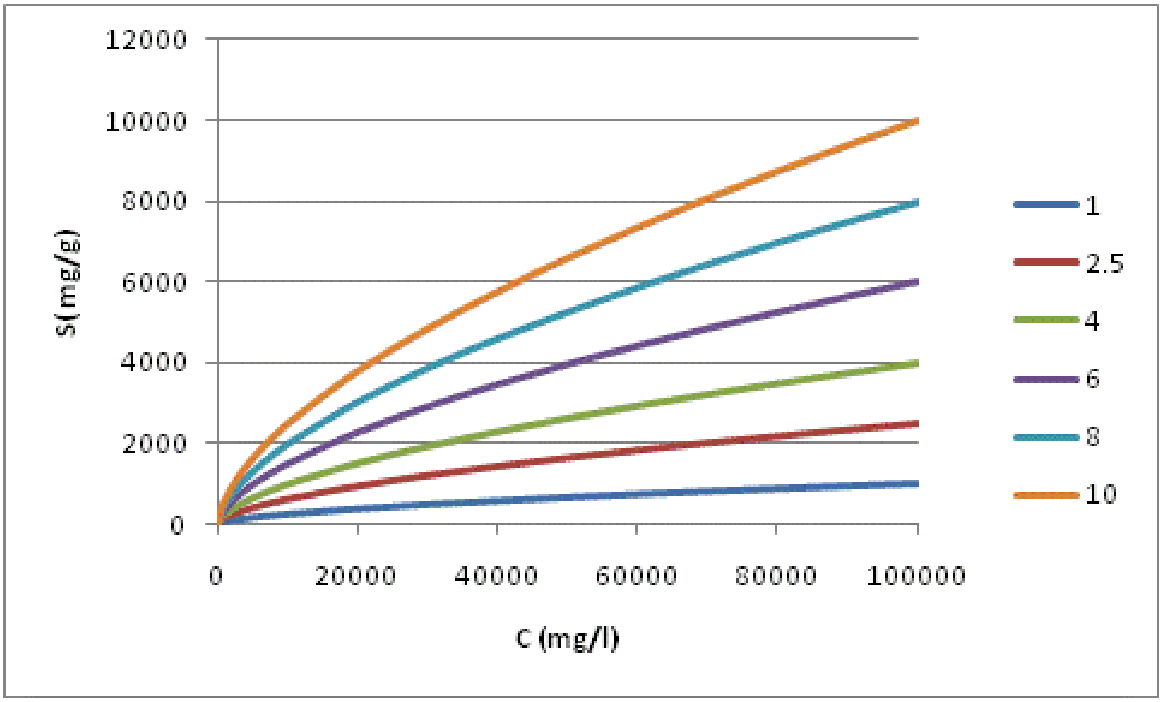

Figure 4-6. Example Plots of Langmuir Adsorption Isotherm in terms of S versus C using a binding energy constant (α) ranging from 0.001 to 1 l/mg and maximum amount of solute sorbed onto solid (β) of 100 mg/kg

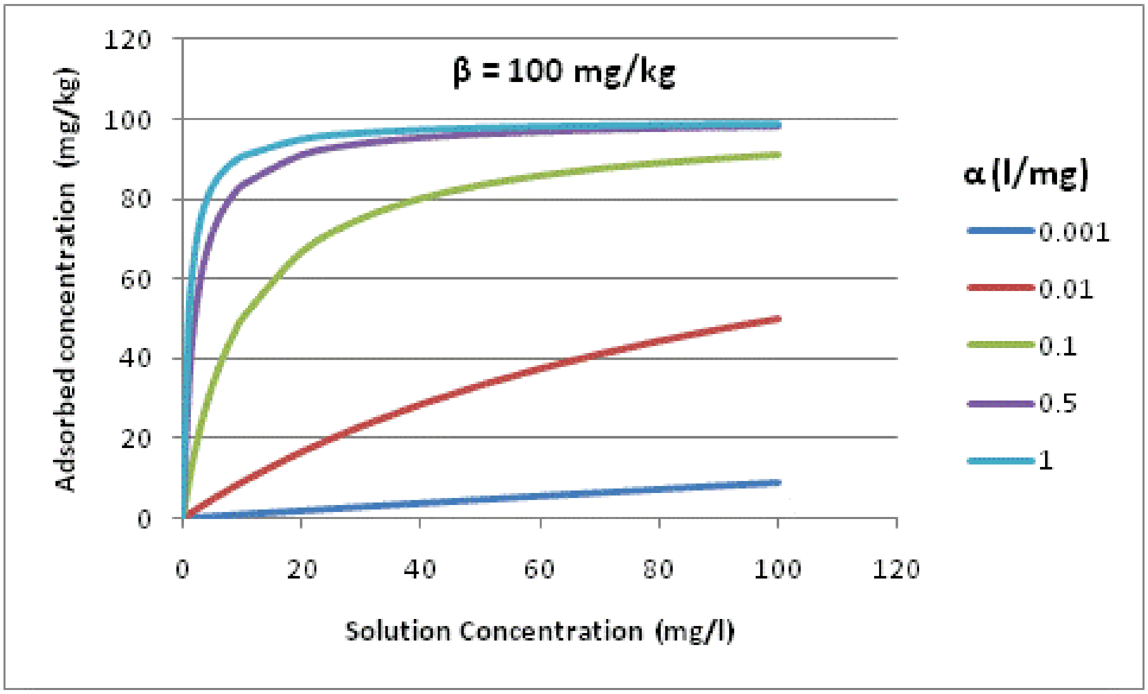

5.0 GROUNDWATER SYSTEM AT WASTE MANAGEMENT AREA A/AX

This section provides a summary of the groundwater system at WMA A/AX which includes a brief description of the uppermost unconfined aquifer system including a discussion of the historic and recent groundwater data collected beneath the 200 East Area with emphasis on the A/AX Tank Farm. Most of the information in this section is derived from RPP-23748, *Geology, Hydrogeology, Geochemistry, and Mineralogy Data Package for the Single-Shell Tank Waste Management Areas at the Hanford Site*, PNNL-15301, and RPP-RPT-46088, Rev. 1. This section also provides a summary of potential key FEPs operating within the unconfined aquifer and the associated conceptual models of groundwater flow and transport that may need to be considered in the WMA A/AX PA. Finally, this section provides recommendations for groundwater flow and transport properties that would be appropriate to use in numerical modeling of local-scale flow and transport at WMA A/AX.

Key features have been identified as potentially important to consider in conceptual models of the vadose zone at WMA A/AX and in the scope of the WMA A/AX PA calculations and related sensitivity analyses. A summary of FEPs related to the groundwater system at WMA C are presented for consideration in Appendix E of RPP-RPT-46088, Rev. 1. The FEPs are identified for two time periods: 1) the time extending from the operational period through the end of the retrieval, remediation, and correction action period and 2) future projected conditions. Due to the proximity of WMA A/AX to WMA C, these same FEPs are deemed to be applicable to WMA A/AX. The FEPs identified for past to present conditions and for projected future conditions are summarized in Tables E-1 through E-3 in Appendix E of RPP-RPT-46088, Rev 1. The key general features that were identified for the groundwater for these time periods include the following general categories.

<u>Properties of the Major Hydrogeologic Units</u>: The SSTs and related facilities at WMA A/AX are constructed in Hanford formation sediments, and below the water table at depth of about 80 m, these facilities are underlain by an undifferentiated unit composed of Hanford formation gravel and/or CCU (l) gravel and/or Ringold Formation, unit A referred to as the H3/CCU/R unit.

Descriptions of the general properties of the units within the unconfined aquifer beneath WMA A/AX are provided in Section 3.7 of this report and Appendix B of RPP-RPT-46088, Rev 1. All interpretations of major units along lines of section in the general area of WMA A/AX are shown in Figure B-1 of Appendix B and are provided in Figures B-1 through B-7 of RPP-RPT-46088, Rev 1.

<u>General Flow Conditions in the Groundwater</u>: Since the start of Hanford Site operations in the mid-1940s, artificial recharge from wastewater disposal facilities has been several times greater than the estimated recharge from natural sources. This caused an increase in the water-table elevation over most of the Hanford Site and the formation of groundwater mounds beneath major wastewater disposal facilities. In vicinity of WMA A/AX, long-term hydrographs of water-level measurements suggests that unconfined aquifer has risen as much as 5 m in response to the artificial recharge from nearby wastewater disposal facilities. More detailed discussions of regional flow in the unconfined aquifer and hydraulic impacts from past operations are provided in Sections 5.1 and 5.3.

5.1 UPPERMOST AQUIFER SYSTEM

Aquifers at the Hanford Site are divided into 1) confined, and 2) suprabasalt or unconfined, aquifer systems. The regional, confined aquifer system occurs within the CRBG and extends from western Idaho through eastern Washington and northeastern Oregon (RHO-BWI-ST-4). Basalt-confined aquifers beneath the Hanford Site are grouped into three separate hydrogeologic units corresponding to the three basalt formations discussed above: from deepest to shallowest, the Grande Ronde, Wanapum, and Saddle Mountains (DOE/RW-0164). The basalt-confined aquifers are composed of intraflow zones (mainly flow tops) between the relatively impermeable interiors of basalt flows. The unconfined aquifer system occurs within fluvial, lacustrine, and glacio-fluvial sediments deposited on top of the Columbia River Basalts.

The sediment above the basalt in which groundwater occurs is subdivided into the glacio-fluvial sands and gravels of the Hanford formation, the fluvial-lacustrine sediments of the Ringold Formation, and the Cold Creek unit which is primarily reworked sediment of the Ringold Formation. The suprabasalt aquifer system is approximately 180 m thick near the center of the Cold Creek syncline but thins laterally, anticlinal basalt ridges that extend above the water table. It is thickest in the Wye Barricade depression and the Cold Creek Depression (see Figure 3-4). A generalized east to west geologic cross section showing the position of the water table and major stratigraphic units beneath the Hanford Site is shown in Figure 5-1.

The base of the suprabasalt aquifer in the vicinity of WMA A/AX is the basalt surface. Sediment below SST WMA A/AX consists primarily of the undifferentiated lower sands and gravels associated with the Hanford formation, Cold Creek unit, and the Ringold Formation (Unit A) which lie in an eroded channel caused by the cataclysmic floods of the Pleistocene. Where the Ringold Formation is present in the suprabasalt aquifer, the silt and clay horizon of the formation's hydrogeologic unit 8 (lower mud unit) forms a confining layer that separates the suprabasalt aquifer into the uppermost and unconfined aquifer and an underlying confined or semi-confined aquifer in the Ringold Formation. The hydrogeologic unit 8 occurs at or above the water table east of the 200 East Area and in an area between the 200 East and 200 West Areas. The lower mud unit thus creates a thinning of the unconfined aquifer and a barrier to eastward groundwater flow in very localized areas.

The general direction of groundwater flow is primarily from natural recharge areas on the basalt ridges west of the Hanford Site to discharge along the Columbia River (see Figure 5-2). The general west to east flow was interrupted locally by artificial groundwater mounds that developed in the unconfined aquifer in the 200 Areas due to artificial recharge from liquid waste disposal operations that began in the 1940s. Artificial recharge, estimated to be 10 times natural recharge, created large water-table mounds primarily below the 200 East and 200 West Areas. Since cessation of these discharges, the water table has declined about 6 m in the 200 East Area from the highest, historic water levels and flow directions of the unconfined aquifer are returning to pre-Hanford Site directions toward the east. A component of groundwater flow and contaminant transport also exists to the north, between Gable Mountain and Gable Butte.

Figure 5-1. Generalized Geologic Cross-Section through the Hanford Site. (Location of cross-section A-A' is shown as west-east line on outline of Hanford Site in upper right.)

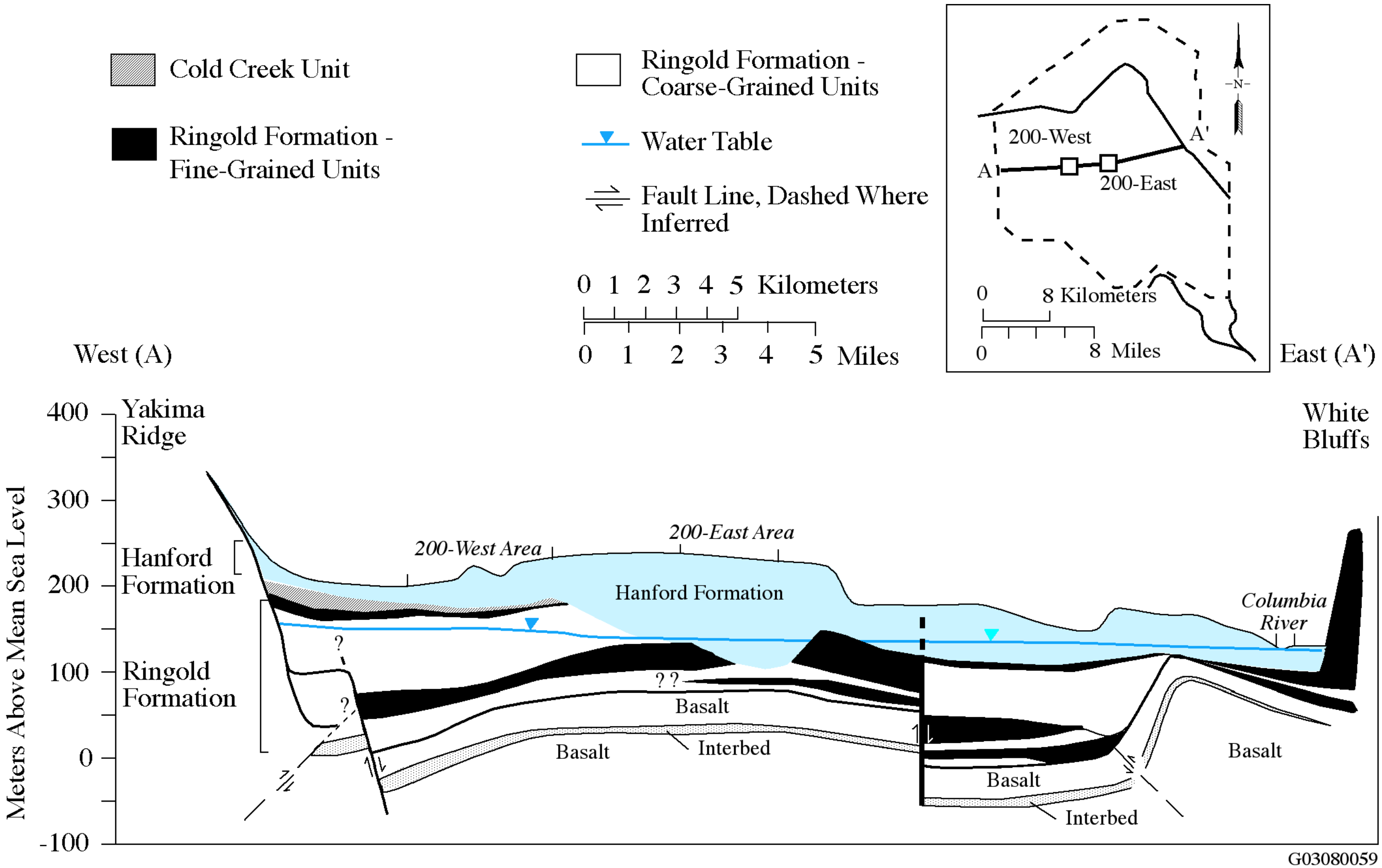

Figure 5-2. Hanford Site and Outlying Areas Water Table Map, March 2013

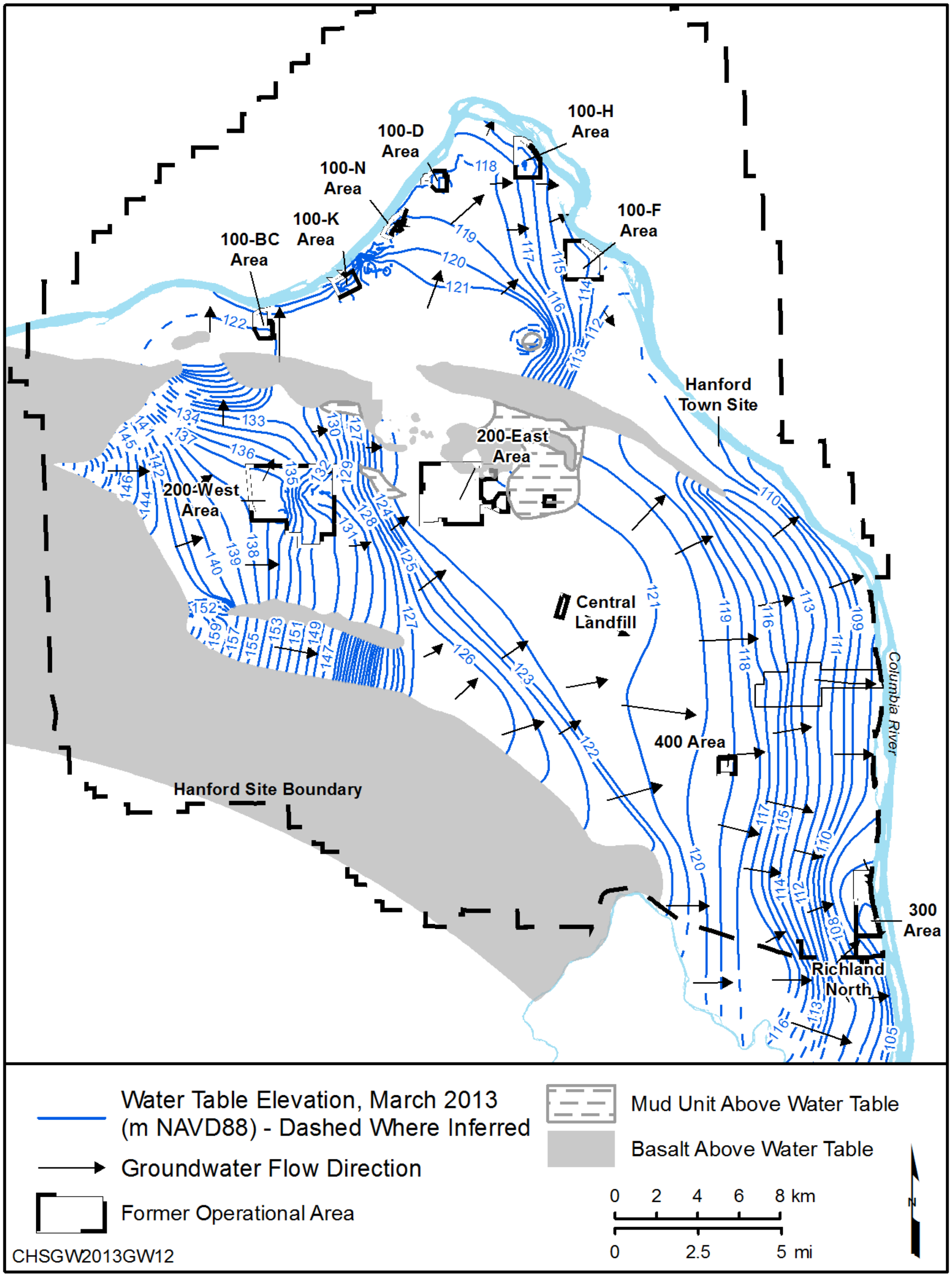

Reference: DOE/RL-2014-32, *Hanford Site Groundwater Monitoring for 2013*

Recharge from agricultural activities offsite and west of the Hanford Site also has affected the groundwater. The continued use of irrigation up gradient of the Hanford Site is expected to sustain recharge to the unconfined aquifer.

The regional-scale interpretation of the water-table elevation in Figure 5-2 from DOE/RL-2014-32, *Hanford Site Groundwater Monitoring Report for 2013* infers a southeast flow in the southern part of this area (Figure 5-2). However, small differences in water elevations make it difficult to define the exact direction and magnitude of groundwater flow in the 200 East Area (see Figures 5-2 and 5-3).

In the Northwest quadrant of 200 East Area near the WMA B-BX-BY and LLWMA 1, the average flow direction has been interpreted in DOE/RL-2014-32 to have changed from northwest through Gable Gap to a primarily southeast direction.

The local-scale flow directions along the southern boundary of the 200-BP-5 Operable Unit and central part of 200 East Area are uncertain (Figure 5-3). The range in water table elevations is only a few centimeters across the 200 East Area and the water level measurements in wells exhibit spatial variability. In the vicinity of the WMA A/AX, the average flow direction is currently inferred – based in part on water-level measurements and in evaluation and interpretation of local-scale plume migration – to be to the southeast. Methods being used to reduce uncertainty in these measurements include higher resolution well elevation surveys and gyroscopic surveys to determine borehole deviation from vertical.

5.2 AQUIFER PROPERTIES

This section describes the aquifer properties beneath the 200 East Area and specifically SST WMA A/AX. This discussion includes a summary of data and information collected on hydraulic properties, aquifer thickness, and groundwater flow directions and flow rates in these areas. This section also describes historic changes in the aquifer conditions due to past fuel processing operations and associated waste disposal to cribs and ponds. Changes in the aquifer properties during the past 60 years have large implications for direction and rate of contaminant movement in the aquifer and for residual vadose zone contamination where the water table has decreased in elevation.

The base of the unconfined aquifer in most of the 200 East Area is generally regarded as the basalt surface, and the supra-basalt aquifer system consists entirely of the unconfined aquifer. The unconfined aquifer consists primarily of hydrogeologic unit 1 (undifferentiated Hanford formation and coarse-grained Cold Creek unit deposits [CCU]) and hydrogeologic unit 9 (Ringold Formation unit A) beneath the SST WMAs in the 200 East Area (see Figure 5-4). Hydrogeologic unit 8, the lower mud unit, has been removed from beneath almost all of the 200 East Area and is not present beneath any of the SST farms in the area.

Figure 5-3. Groundwater Flow Direction in the 200 East Area, March 2013

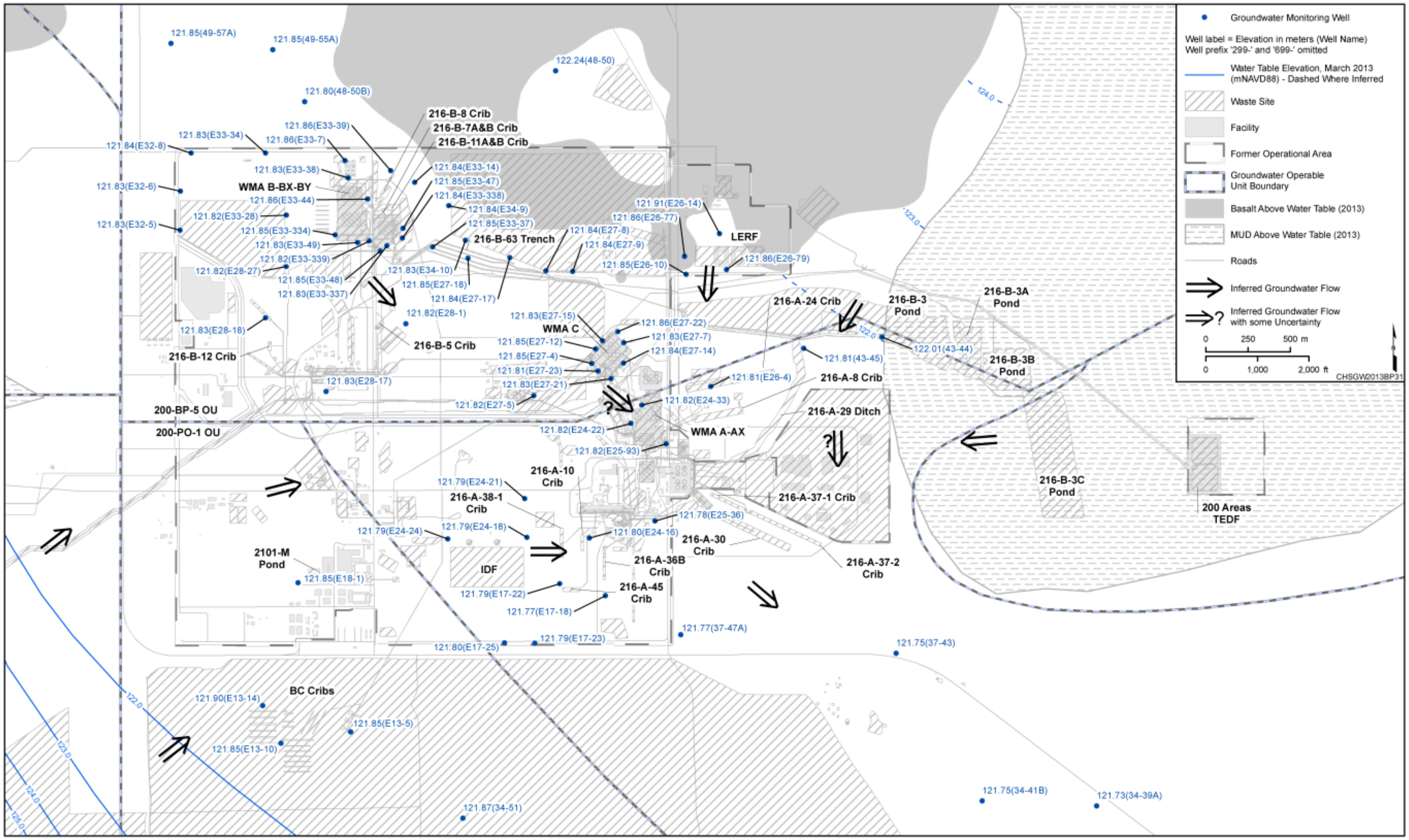

Reference: DOE/RL-2014-32, *Hanford Site Groundwater Monitoring for 2013*

Figure 5-4. Comparison of Major Hydrologic Units and Geologic Stratigraphy at Hanford (adapted from PNNL-13080)

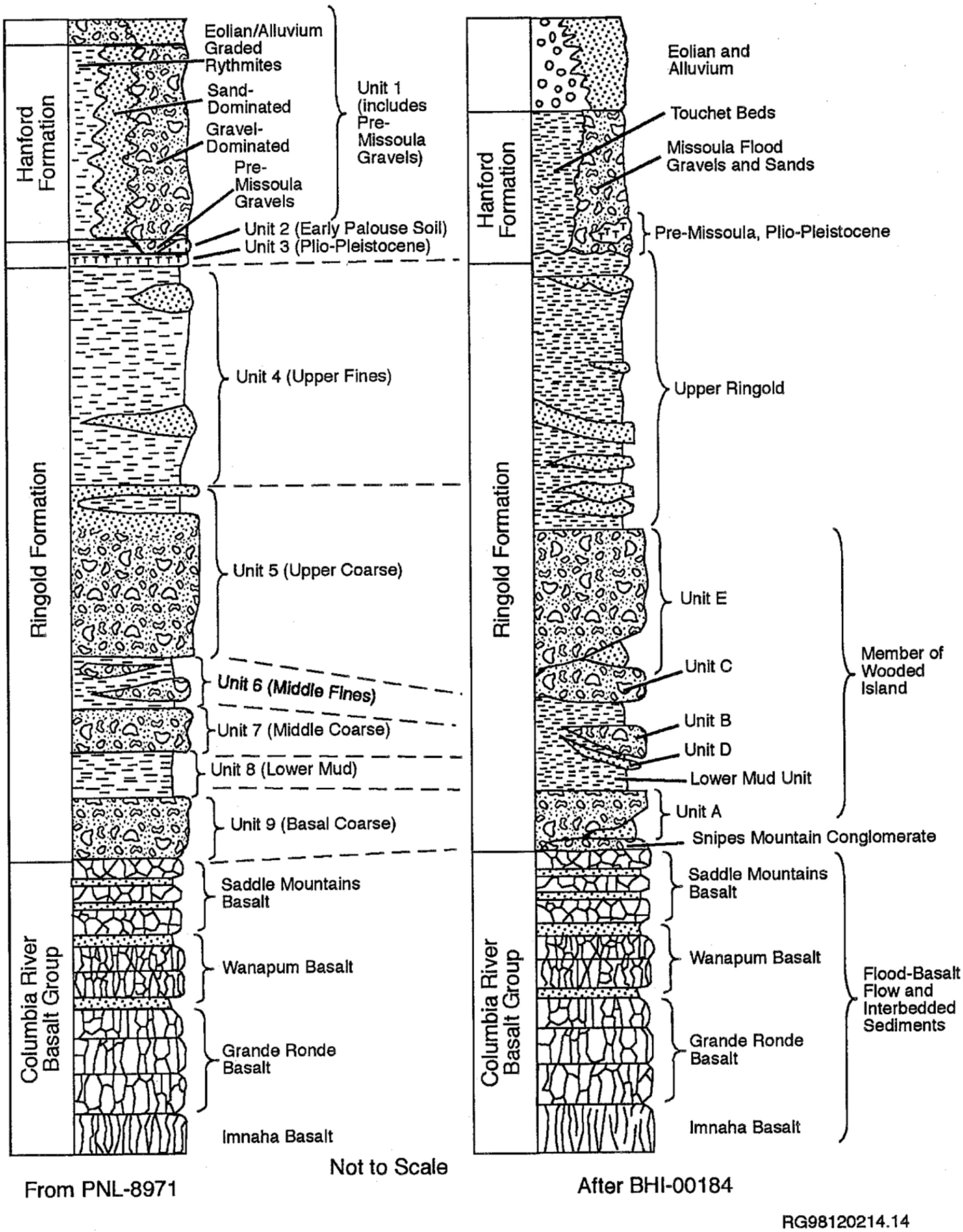

Reference: PNNL-13080, *Hanford Site Groundwater Monitoring: Setting, Sources, and Methods*.

Table 5-1 contains a list of wells near SST WMA A/AX in 200 East Area that penetrate through the entire unconfined aquifer and have 2013 water level measurements. The location of these wells is provided in Figure 5-5. Also in Table 5-1 are calculated thicknesses for the unconfined aquifer. There are very little data for WMA A/AX. The thickness of the uppermost aquifer generally increases from north to south as the top of basalt dips into the Cold Creek syncline. The unconfined aquifer beneath the SST WMAs in the 200 East Area ranges from between 0 and 7 m beneath WMA B-BX-BY which lies to the west of SST WMA C, to about 9 to 10 m beneath WMA C, to about 27 m beneath WMA A/AX.

Table 5-1. Thickness of the Unconfined Aquifer Beneath the A/AX and C Single-Shell Tanks in 200 East Area

Well Name	Well Location	Elevation of Top of Basalt[(a)] (m amsl)	Elevation of Water Table[(b)] (m amsl)	Aquifer Thickness (m)
Waste Management Area A/AX				
299-E25-2	East side of WMA A/AX	94.49	120.70	26.21
299-E24-8	~ 550 m southwest of WMA C	95.71	120.72	25.01
Waste Management Area C				
299-E26-8	~ 300 m east of WMA C	113.02	120.57	7.55
299-E27-22	North corner of WMA C	112.38	120.73	8.35

(a) Top of basalt elevation from PNNL-13024, *RCRA Groundwater Monitoring Plan for Single-Shell Tank Waste Management Area C at the Hanford Site*; PNNL-13023, *RCRA Groundwater Monitoring Plan for Single-Shell Tank Waste Management Area A/AX at the Hanford Site*; PNNL-12261, *Revised Hydrogeology for the Suprabasalt Aquifer System, 200-East Area and Vicinity, Hanford Site, Washington*; RPP-14430, *Subsurface Conditions Description of the C and A/AX Waste Management Area*; Hanford Well Information System.

(b) July 2013 data except where noted.

amsl = above mean sea level WMA = waste management area

General groundwater flow directions and general flow rates are difficult to determine for the SST WMA A/AX due to the relatively flat water table beneath the 200 East Area (DOE/RL-2014-32). The principal vector of groundwater flow has historically been to the southeast. As the water table returns to its natural equilibrium, changes in the magnitude and direction of the hydraulic gradient are occurring. Information on the direction of flow is generally based from the examination of changes in contaminant plume movement over several years. Information on the variability/uncertainty is very limited based on the flat gradient and the small number of samples taken in any given year on contaminants of interest. Generally, the magnitude of the gradient in the area surrounding WMA A/AX is on the order of magnitude of 1E-5.

Several slug tests were done prior to 1997 in wells near 200 East Area SST farms. Table 5-2 gives the resulting hydraulic conductivity and transmissivity data from those tests. In most cases, the analyses of the data from these tests are less well documented than are more recent analyses. The original source for the data should be consulted for details of testing and analysis. The hydraulic conductivities obtained from the earlier slug test (Table 5-2) are generally lower than those measured in the more recent tests.

Figure 5-5. Well Location Map at WMA A/AX

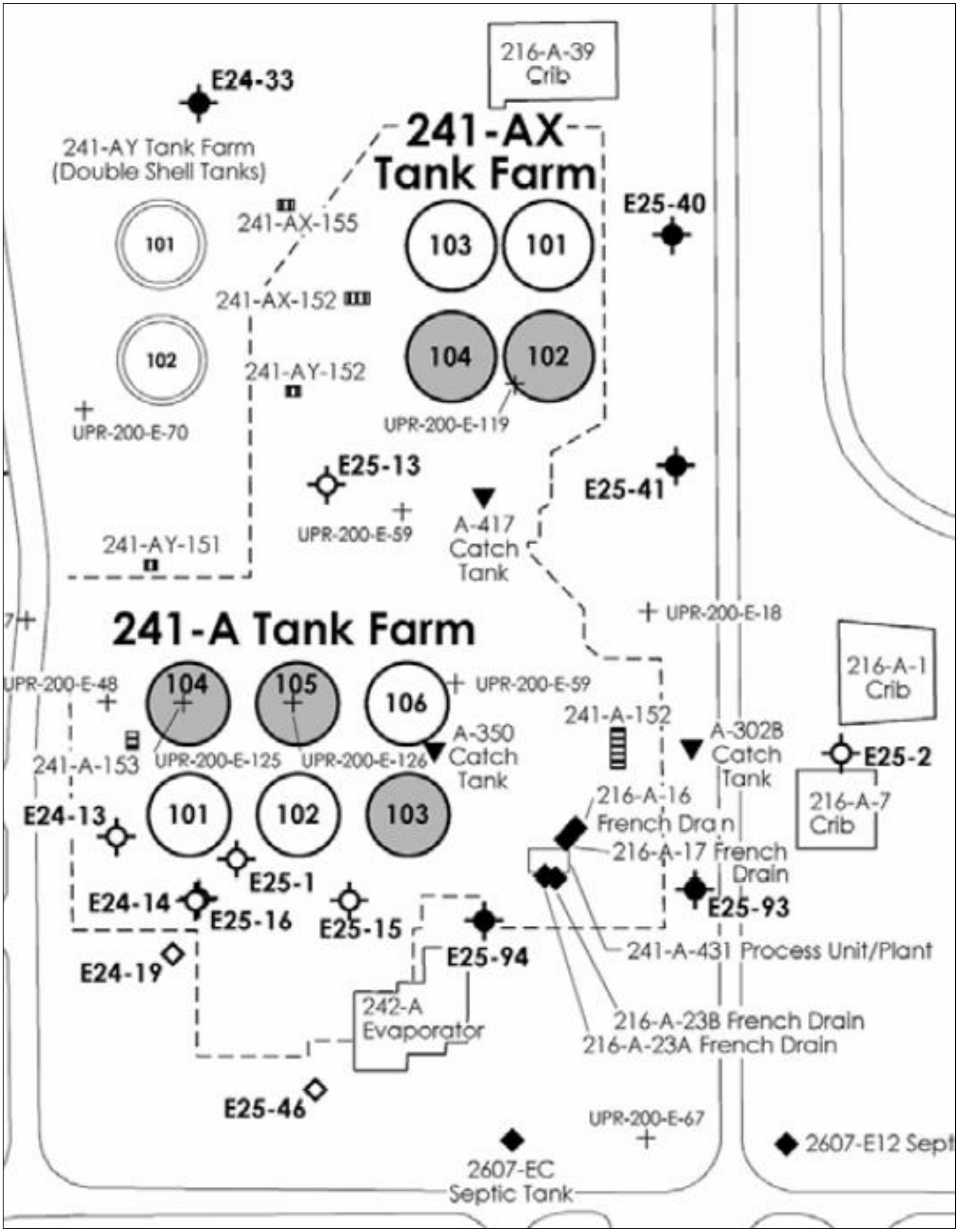

Reference: DOE/RL-2008-66, *Hanford Site Groundwater Monitoring for Fiscal Year 2008.*

Table 5-2. Results of Pre-1997 Slug Testing at A/AX Single-Shell Tank Waste Management Area in the 200 East Area

Well Name	Hydraulic Conductivity (m/day)	Transmissivity[a] (m^2/day)
299-E24-19	33.5	158
299-E27-14 (Between WMAs A/AX and C)	48.8	242
299-E27-15 (Upgradient of WMA C)	118.9	520

[a] Transmissivity calculated by multiplying hydraulic conductivity by thickness of test interval.
Source: WHC-SD-EN-TI-147, *Hydrologic Testing at the Single-Shell Tanks, 1989*.

The differences in hydraulic properties among wells and within single wells illustrate the difficulty in assigning accurate values to specific hydrogeologic units. The differences are due to different testing and analysis methods used through time, different assumed values for certain parameters such as effective porosity, and natural variation in lithologic properties that affect the hydraulic properties. As more hydrologic data become available, perhaps the relatively large ranges of some hydraulic properties will decrease. Until then, the existing data set must be considered plausible within the uncertainties in the analyses.

5.3 CHANGES IN GROUNDWATER FLOW DIRECTION

Water levels beneath 200 East Area rose as much as 9 m (well 699-45-42, located near 216-B pond [B Pond]) because of artificial recharge from liquid waste disposal operations at the B Pond area. The largest volumes of discharge were to the B Pond system east of the 200 East Area, the 216-A-25 (Gable Mountain) pond system north of the 200 East Area, and several of the Plutonium Uranium Extraction (PUREX) Plant cribs east and south of WMA A/AX. Figure 5-6 shows the liquid discharge history for the two pond systems. The Gable Mountain pond system is estimated to have received approximately 307 billion L of effluent and B Pond to have received about 240 billion L of effluent (DOE/RL-92-05, *B Plant Source Aggregate Area Management Study Report*). These large volumes disposed to the ponds (and, lesser volumes to cribs and ditches) artificially recharged the unconfined aquifer creating large water-table mounds. The increase in water-table elevation was most rapid from 1954 to 1963, increasing as much as 0.6 m/year at times. The water table declined somewhat in the late 1960s and early 1970s, then increased again in the early 1980s before a final decline beginning in 1988 and continuing throughout the 1990s when wastewater discharges in the 200 East Area were reduced.

Figure 5-6. Discharge History for and Location of the B Pond and the Gable Mountain Pond Systems. Location map of the pond is adapted from PNNL-15837.

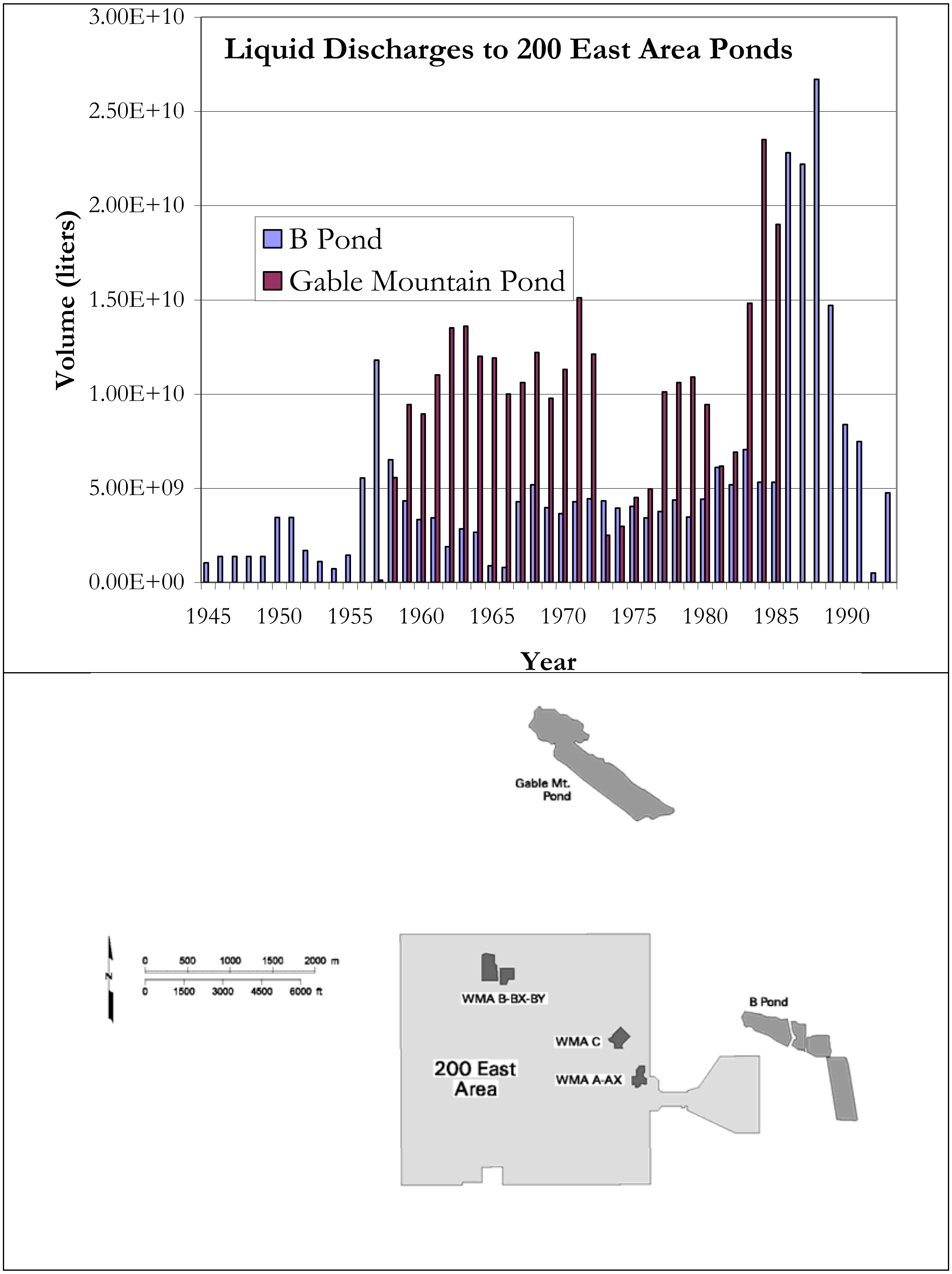

Reference: PNNL-15837, *Data Package for Past and Current Groundwater Flow and Contamination Beneath Single-Shell Tank Waste Management Areas*.

Past discharges to B Pond and 216-A-25 (Gable Mountain Pond, Figure 5-6) systems exerted significant effects on groundwater, not only in changes in head and flow direction, but also gradients and groundwater fluxes and the direction of contaminant transport from past water quality impacts near wastewater discharge facilities. Contaminant concentration in discharges to these large volume discharge facilities were generally dilute in comparison to contaminant concentration levels in wastewater discharges to cribs and trenches. The volume of relatively dilute water arising from pond discharges and associated water table mounds affected water quality as well, with some dilution of lower volume but higher contaminant content from local sources. Historical interpretation of water quality impacts from past operations needs to give careful consideration to the completion of local-scale groundwater wells in the uppermost part of the unconfined aquifer.

Figure 5-7 shows hydrographs for the area around SST WMA A/AX. The hydrograph illustrates the changes in water-table elevation that have occurred since at least the mid-1950s. All data used to make the hydrographs were obtained from the HydroDat database (see data files on CD included in PNNL-15670, *Hanford Site Groundwater Monitoring for Fiscal Year 2005*).

The hydrographs in this figure show a maximum in water-table elevation in about 1968 that corresponds to a time of high discharge to Gable Mountain pond (Figure 5-6). This maximum is followed by a minimum, centered around 1978, that corresponds to a minimum in the discharges to both pond systems. Finally, a second maximum is seen in 1986 to 1987 corresponding to peak discharge to the B Pond system. Hydrographs from C and B-BY-BX SST WMAs show similar patterns (PNNL-15301).

The pre-Manhattan Project water table was at approximately 118 m above sea level in 200 East Area (BNWL-B-360, *Selected Water Table Contour Maps and Well Hydrographs for the Hanford Reservation, 1944-1973*). PNNL-13400, *Groundwater Flow and Transport Calculations Supporting the Immobilized Low-Activity Waste Disposal Facility Performance Assessment*, more recently modeled the elevation of the water table beneath the Hanford Site for the Immobilized Low-Activity Waste Performance Assessment. Their model resulted in a water-table elevation of about 116 to 118 m above sea level in the 200 East Area after all influences from the Hanford Site have dissipated.

All non-permitted discharges of liquid effluent to the ground were stopped in 1995. Since that time, continued changes have occurred in the water-table elevation. The average rate of decline, 0.6 m/yr, was obtained by averaging the rate of decline in each monitoring well in the RCRA monitoring network between March 2003 and March 2008 (DOE/RL-2008-66).

The data show that the water table beneath SST WMA A/AX is declining at a rate of about 0.06 m/year. At the current rate of decline, the water table will take between 30 and 50 years to reach the estimated post-Hanford water-table elevation (PNNL-13400).

Accompanying the changes in water level were changes in groundwater flow direction. Pre-Hanford Site groundwater flow direction was generally toward the east or southeast (BNWL-B-360). Since 1944, liquid disposal to the B Pond, Gable Mountain Pond, and other disposal facilities has changed the flow direction several times during Hanford Site operations.

Figure 5-7. Hydrographs from Selected Wells in the Area of Waste Management Area A/AX, 200 East Area

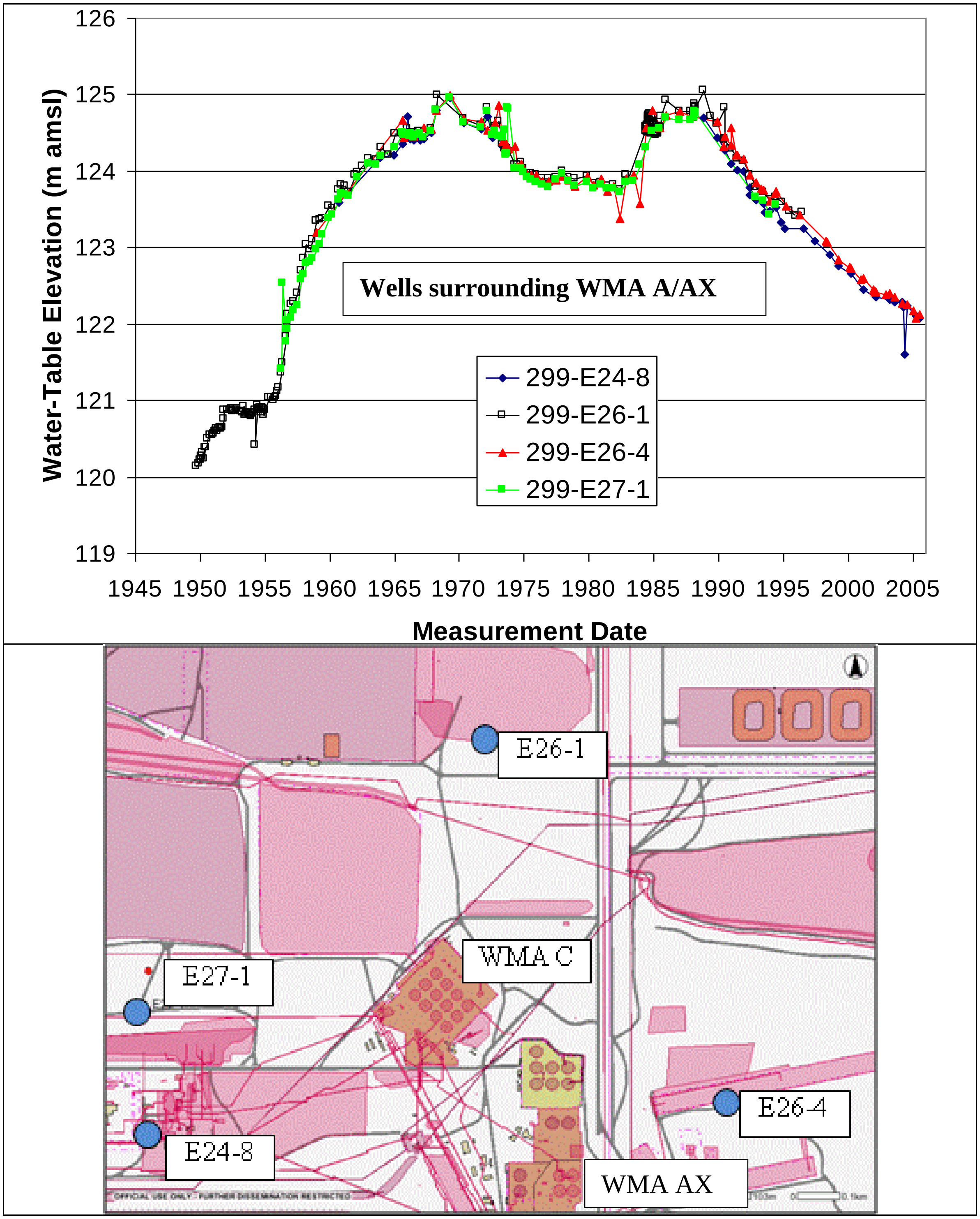

Table 5-3 gives historical groundwater flow directions and water-table gradients from the late 1950s to the year 2003 estimated from selected wells in close proximity to WMA A/AX. The flow directions and gradients were calculated in PNNL-15301 using the three-point analysis method and water level measurements in the HydroDat database (see data files on CD included in PNNL-15670). The earlier historical flow directions are determined from water levels collected on relatively far-field wells between 1958 and 1994 whereas the latter flow directions were determined from measurements in wells in the RCRA monitoring network at the WMA from 1990 to 2003. The apparent variations in estimated flow directions in the northern part of the 200 East Area, including the area of the WMA A/AX, may, in part, be influenced by the top of the basalt on the local-scale flow within the very thin unconfined aquifer. The top of the basalt, which forms the base of the unconfined aquifer in the area, is above the water table in the northeast corner of the 200 East Area and dips south to southwest. This surface is expected to influence local-scale flow directions especially near areas where the aquifer pinches out against the basalt. Also, the top of the basalt is an erosional surface with up to about 3.5 m of relief (PNNL-13404, *Hanford Site Groundwater Monitoring for Fiscal Year 2000*). Thus, local flow directions may differ greatly as water moves between high areas on the top of basalt.

The frequencies of historical groundwater flow directions in the area of WMA A/AX between 1958 and 1994 and, separately, more recent flow direction between 1990 and 2003, are shown graphically in Figure 5-8. Examination of the frequency of calculated directions of groundwater from the far-field (Figure 5-8a) and local-scale wells (Figure 5-8b), shows that, while varying considerably between 1958 through 2003, groundwater flow directions in the area of WMA A/AX have been generally toward the south over most of this period of time. Review of water-level measurements collected since 2003 and interpretations of plume migration during the past several years, discussed in Section 5.4.3, would continue to support the general observation of predominant groundwater flow direction to the south and southwest beneath the WMA A/AX.

Interpretation of changes in the direction of groundwater flow prior to the period shown in the rose diagrams is very limited because of the small number of groundwater wells that were available to define water table conditions. Because of these limitations, the specific direction of groundwater flow in the immediate area of WMA A/AX is difficult to determine and can only be inferred from the general regional interpretations of the water table provided prior to 1958.

Interpretations of water-table conditions prior to 1958 can be found in three documents:

- Maps of water-table conditions in 1951 and 1955 depicted in BNWL-B-360
- Maps of water table conditions from 1951 through 1955 in HW-40469, *Changes in the Hanford Ground Water Table 1944-1955*
- A map of water-table conditions from 1948 in USGS-W-P-7, *Geologic and Hydrologic Features of the Richland Area, Washington, Relevant to the Disposal of Waste at the Hanford Operations of the Atomic Energy Commission; Interim Report No. 1*.

Table 5-3. Water Levels, Groundwater Flow Directions, and Water-Table Gradients in the Area of Waste Management Area A/AX from 1958 to 2003 (from RPP-23748) (2 sheets)

Duration[(a)] (day)	Start Date	End Date	Water Levels (m amsl)			Groundwater Flow Direction[(b)]	Water-Table Gradient
			299-E26-1	299-E26-4	299-E27-1		
4	12/09/58	12/12/58	123.343	123.194	122.973	212.673	0.000433
1	08/18/65	08/18/65	124.48	124.660	124.500	328.459	0.000203
1	10/20/65	10/20/65	124.492	124.495	124.485	258.557	0.000009
4	01/03/66	01/06/66	124.559	124.486	124.485	188.628	0.000113
11	04/04/66	04/14/66	124.498	124.474	124.488	164.863	0.000029
1	05/20/66	05/20/66	124.498	124.474	124.463	199.422	0.000046
2	11/02/66	11/03/66	124.514	124.510	124.463	230.877	0.000056
11	03/28/67	04/07/67	124.462	124.568	124.436	308.904	0.000125
5	10/19/67	10/23/67	124.553	124.556	124.512	239.716	0.000046
1	05/18/70	05/18/70	124.675	124.678	124.631	239.428	0.000049
1	09/14/71	09/14/71	124.608	124.641	124.573	277.811	0.000055
6	03/15/72	03/20/72	124.824	124.538	124.771	152.595	0.000325
1	07/11/72	07/11/72	124.526	124.541	124.463	248.930	0.000073
5	10/03/72	10/07/72	124.59	124.635	124.518	267.052	0.000097
1	01/08/73	01/08/73	124.642	124.855	124.448	281.927	0.000331
1	08/13/73	08/13/73	124.279	124.352	124.210	280.928	0.000115
1	09/10/73	09/10/73	124.291	124.309	124.226	250.994	0.000076
1	04/11/74	04/11/74	124.078	124.328	124.037	313.189	0.000288
1	10/18/74	10/18/74	124.111	124.096	124.030	224.666	0.000090
1	01/08/75	01/08/75	124.038	124.026	123.988	221.536	0.000056
1	04/14/75	04/14/75	123.962	123.943	123.909	215.007	0.000061
1	07/07/75	07/07/75	123.965	123.950	123.884	224.666	0.000090
1	12/03/75	12/03/75	123.944	123.947	123.857	237.477	0.000096
1	06/15/76	06/15/76	123.904	123.870	123.814	213.979	0.000105
1	12/08/76	12/08/76	123.907	123.873	123.793	218.279	0.000130
1	07/01/77	07/01/77	123.916	123.876	123.878	186.664	0.000060
1	12/07/77	12/07/77	123.995	123.931	123.966	166.661	0.000077
1	06/01/78	06/01/78	123.91	123.886	123.869	203.768	0.000051
1	12/01/78	12/01/78	123.904	123.806	123.802	189.428	0.000153
1	12/01/79	12/01/79	123.928	123.931	123.857	237.928	0.000079
1	06/01/80	06/01/80	123.828	123.825	123.774	232.217	0.000060
1	12/01/80	12/01/80	123.852	123.907	123.826	297.966	0.000070
1	06/01/81	06/01/81	123.809	123.745	123.762	179.040	0.000087
1	12/01/81	12/01/81	123.819	123.800	123.762	216.359	0.000065
1	06/01/82	06/01/82	123.749	123.386	123.720	146.706	0.000409
1	12/01/82	12/01/82	123.944	123.904	123.845	212.603	0.000116
1	06/01/84	06/01/84	124.562	124.562	124.314	235.468	0.000274

Table 5-3. Water Levels, Groundwater Flow Directions, and Water-Table Gradients in the Area of Waste Management Area A/AX from 1958 to 2003 (from RPP-23748) (2 sheets)

Duration[(a)] (day)	Start Date	End Date	Water Levels (m amsl)			Groundwater Flow Direction[(b)]	Water-Table Gradient
			299-E26-1	299-E26-4	299-E27-1		
1	12/01/84	12/01/84	124.709	124.788	124.515	257.542	0.000237
9	06/12/85	06/20/85	124.588	124.565	124.549	203.569	0.000049
2	12/17/85	12/18/85	124.924	124.723	124.695	192.163	0.000330
4	12/08/87	12/11/87	124.771	124.711	124.671	203.112	0.000126
2	12/03/92	12/04/92	123.793	123.845	123.650	255.420	0.000172
2	06/09/93	06/10/93	123.729	123.760	123.607	249.787	0.000141
2	12/01/93	12/02/93	123.619	123.613	123.427	233.640	0.000212
1	06/03/94	06/03/94	123.653	123.735	123.558	275.430	0.000144
			299-E27-12	**299-E27-14**	**299-E27-7**		
1	06/28/90	06/28/90	124.297	124.312	124.331	228.635	0.000229
1	12/17/90	12/17/90	124.187	124.224	124.240	247.203	0.000316
1	06/17/91	06/17/91	124.056	124.117	124.097	301.756	0.000332
2	08/19/91	08/19/91	124.132	124.148	124.167	229.649	0.000233
2	03/04/92	03/05/92	123.76	123.953	123.990	258.790	0.001348
2	06/17/92	06/18/92	123.839	123.846	123.886	213.439	0.000388
1	12/16/92	12/16/92	123.733	123.749	123.777	223.989	0.000312
1	03/25/93	03/25/93	123.675	123.718	123.743	242.040	0.000415
1	12/15/93	12/15/93	123.516	123.532	123.551	229.649	0.000233
1	05/11/94	05/11/94	123.516	123.544	123.566	236.657	0.000315
1	12/09/94	12/09/94	123.498	123.523	123.545	234.665	0.000300
1	06/23/95	06/23/95	123.385	123.392	123.429	213.868	0.000360
2	10/30/95	10/30/95	123.398	123.395	123.432	205.009	0.000332
1	01/16/97	01/16/97	123.23	123.212	123.255	192.115	0.000361
1	06/10/97	06/10/97	123.199	123.249	123.225	315.891	0.000285
1	12/04/97	12/04/97	123.12	123.163	123.167	265.054	0.000277
1	06/08/98	06/08/98	123.065	123.020	123.033	117.982	0.000244
2	12/07/98	12/08/98	122.953	122.898	122.914	118.178	0.000298
1	06/03/99	06/03/99	122.843	122.831	123.728	207.362	0.008207
1	12/18/00	12/18/00	122.629	122.621	122.627	155.890	0.000055
1	06/20/01	06/20/01	122.571	122.574	122.574	271.893	0.000018
1	03/14/02	03/14/02	122.388	122.391	122.389	330.530	0.000019
1	12/16/02	12/16/02	122.442	122.410	122.520	197.195	0.000942
3	06/02/03	06/04/03	122.309	122.328	126.511	207.970	0.038467

Reference: RPP-23748, *Geology, Hydrogeology, Geochemistry, and Mineralogy Data Package for the Single-Shell Tank Waste Management Areas at the Hanford Site*.

(a) Duration is the length of time between the start and end dates.
(b) Groundwater flow direction is degrees azimuth clockwise from north (0º).

amsl = above mean sea level

Figure 5-8. Range of Groundwater Flow Directions in the Vicinity of 241-A Tank Farm Based on Analyses of Water-Level Measurements Made in Selected Wells between 1958 and 2003 (from RPP-23748)

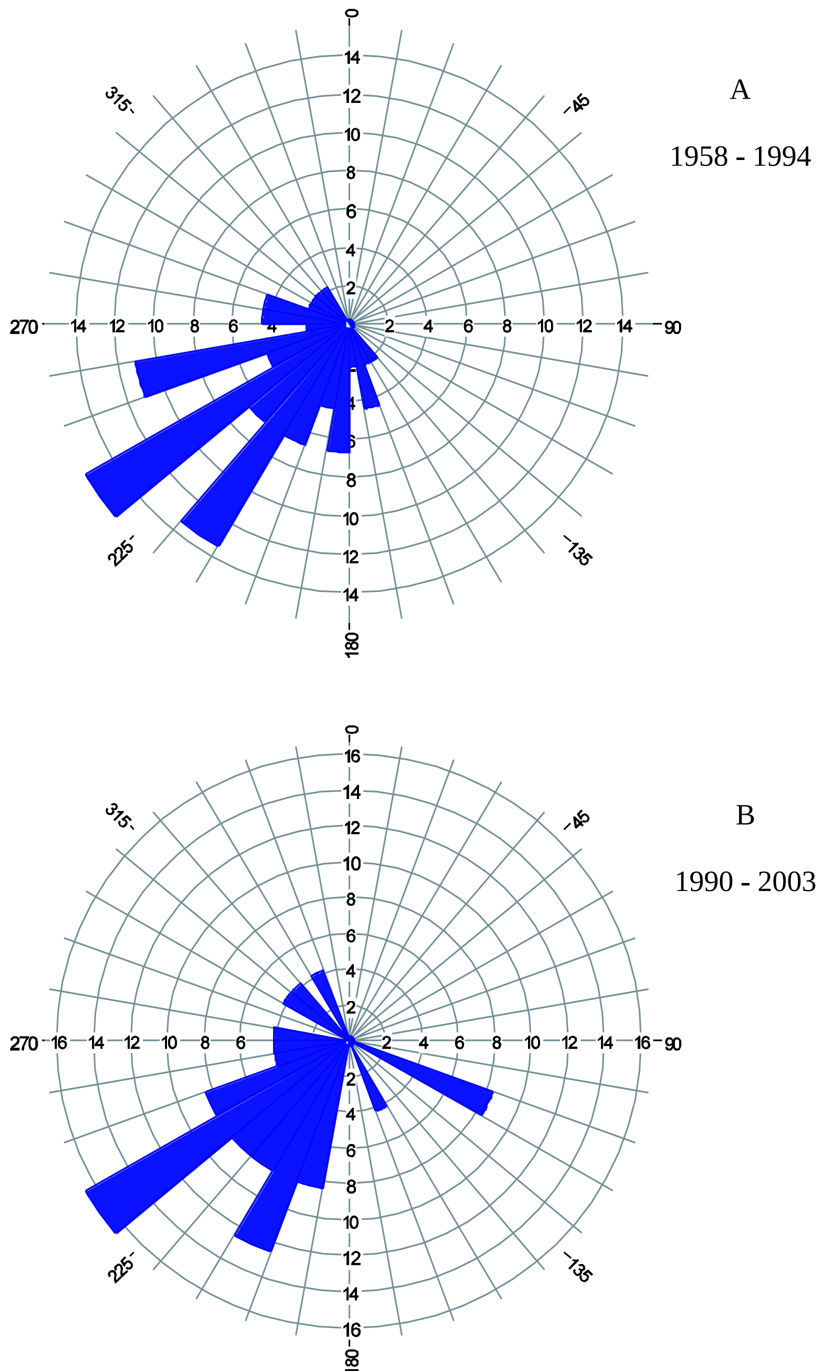

A. 1958 to 1994, wells 299-E26-1, 299-E26-4, and 299-E27-1, 45 measurements.
B. 1990 to 2003, wells 299-E27-12, 299-E27-14, and 299-E27-7, 24 measurements.
Reference: RPP-23748, *Geology, Hydrogeology, Geochemistry, and Mineralogy Data Package for the Single-Shell Tank Waste Management Areas at the Hanford Site*.

Because of the limited number of well measurements, the interpretations provided in these documents are appropriate for establishing a regional picture of water table conditions and would not be appropriate for resolving local-scale conditions. Interpretations of water table conditions from these maps would suggest that discharges at B Pond had a dominant influence on the unconfined aquifer in the late 1940s through the mid-1950s in 200 East Area. The discharges to B-pond created a saddle in the water table in 200 East Area. Based on the local-scale water table interpretation, groundwater flow in the area of WMA A/AX is generally to the southeast; in an area north of WMA A/AX, the flow direction appears to be to the south, and in the area south of WMA A/AX, the flow direction appears to be to the east (Figure 5-3). The interpretation of southeast flow underneath WMA A/AX is based on the slightly higher hydraulic head to the northwest, the orientation of a southeast trending paleochannel below WMA A/AX, and the configuration of the major contamination plumes.

5.4 GROUNDWATER GEOCHEMISTRY

This section is to describe the groundwater geochemistry beneath SST WMA A/AX.
A complete description of groundwater geochemistry beneath the 200 East Area WMAs is in RPP-23748 and PNNL-15301. This discussion is based on previous work at WMA C described in RPP-RPT-46088, Rev. 1. General background chemistry for the Hanford Site is provided.

5.4.1 Background Groundwater Chemistry on Hanford Site

Natural chemical background for the Hanford Site is given from the work in DOE/RL-96-61. Hanford Site background is also described in terms of the water chemistry from samples of two up gradient wells used to monitor Hanford Site background.

U.S. Department of Energy published a study of Hanford Site groundwater background in 1997 (DOE/RL-96-61). The study included historical groundwater monitoring data collected between 1989 and 1993 and new data collected specifically for the purpose of evaluating groundwater background.

An initial screening of the historical data eliminated all data from wells that (1) did not sample the unconfined aquifer, (2) were located within or proximal to known contaminated sites or contaminant plumes, and (3) contained halogenated hydrocarbons. Data from each well were then screened against a list of target constituents most likely to reflect concentration variations in response to contamination events. Wells were eliminated if they yielded samples with concentrations greater than a threshold concentration for the target constituents. The threshold values were obtained from a preliminary background determination in 1992 (DOE/RL-92-23, *Hanford Site Groundwater Background*). The remaining data were then put through a final screening by eliminating outliers (i.e., data that did not conform to the pattern established by other observations) (DOE/RL-96-61).

New groundwater data were collected from 45 wells located mostly in gaps in the geographic coverage of the historical data. There are several important differences between the historical data and the new data.

- The historical data were collected to monitor groundwater whereas the new data were collected specifically to determine background. Therefore, the historical data lack constituents important in considerations of background composition.
- The historical data have a temporal coverage that is lacking from the new data.
- The detection limits are substantially different for the two data sets. The detection limits for metals and radionuclides are significantly lower for the new data.
- The new data represent an internally consistent data set resulting from using the same laboratories and methods for all samples. This is not necessarily true for the older data.

The resulting Hanford Site groundwater background concentrations are given in Table 5-4. Data reported as equal to or less than the detection limit were assigned a value of one-half the detection limit for purposes of calculating the mean. In general, filtered samples were used for analyses of metals and radionuclides and unfiltered samples were used for anions.

Several variables affect the chemical composition of groundwater used for the Hanford Site groundwater background study. These variables are discussed in detail in DOE/RL-92-23 and include well construction, lithology of the sediment in the screened (or perforated) interval, the length of the screened or perforated interval, and recharge.

The concentrations of major cations and anions in groundwater samples give a good indication of the quality of the groundwater and offer a useful tool for comparing groundwater samples. One useful way to depict major ion concentrations in groundwater is with Stiff diagrams. Stiff diagrams are a graphical means of representing the chemical analysis of major cations and anions in water samples ("The Interpretation of Chemical Water Analysis by Means of Patterns" [Stiff 1983]). Figure 5-9 shows the mean composition of the major cations and anions, as determined in the Hanford Site groundwater background study (DOE/RL-96-61), as a modified Stiff diagram. Nitrate has been added to the conventional Stiff diagram because nitrate is a major anion in much of the Hanford Site's contaminated groundwater. Although average groundwater compositions do not represent actual groundwater compositions, the charge balance for the average composition depicted in Figure 5-9 is +3.3%, which suggests that the representation in the figure describes Hanford Site background groundwater composition. Figure 5-9 shows that the Hanford Site's background groundwater is a calcium-bicarbonate dominated groundwater.

Wells 699-19-88 and 699-49-100C were chosen because they are up gradient of all operating facilities at the Hanford Site and they are believed to be free of any Hanford Site contamination. As such, they are monitored as part of the Hanford Site Groundwater Monitoring Project and represent background conditions for Hanford Site groundwater.

Table 5-4. Hanford Site Groundwater Background Concentrations[a] (from DOE/RL-96-61) (3 sheets)

Analyte[b]	Data Set	Reason for Selection	Units	Geo-metric Mean	Geometric Standard Deviation	Number of Samples	Min	Max
Alkalinity as $CaCO_3$	New	More data	µg/L	118,650	1,183	30	80,000	170,000
Aluminum	*New*	*Lower DL*	*µg/L*	*1.23*	*3.92*	*32*	*0.5*	*187*
Americium-241	*New*	*Lower DL*	*fCi/L*	*0.732*	*2.11*	*16*	*0.05*	*1*
Ammonia	*New*	*Lower DL*	*µg/L*	*26.2*	*3,120*	*32*	*5*	*882*
Antimony	*Historical*	*No new*	*µg/L*	*23.8*	*1.92*	*15*	*9.47*	*53.9*
Antimony-125	*New*	*Lower DL*	*fCi/L*	*3.77*	*1.61*	*17*	*1.73*	*8.97*
Arsenic	New	Lower DL	µg/L	1.83	3.11	29	0.5	8.81
Barium	New	Lower DL	µg/L	31.2	2.58	32	0.5	94.1
Beryllium	*Historical*	*Lower DL*	*µg/L*	*0.583*	*2.91*	*17*	*0.2*	*2.5*
Beryllium-7	*Historical*	*No new*	*pCi/L*	*6.42*	*1.26*	*4*	*5.25*	*8.3*
Boron	Historical	No new	µg/L	20.3	1.56	7	12.6	45
Bromide	New	Lower DL	µg/L	61.9	1,721	32	15	235
Cadmium	*New*	*Lower DL*	*µg/L*	*0.274*	*2.57*	*32*	*0.05*	*0.5*
Calcium	Historical	More data	µg/L	36,518	1.33	25	19,200	79,683
Cesium-134	*Historical*	*No new*	*pCi/L*	*0.747*	*1.39*	*4*	*0.496*	*1.06*
Cesium-137	*New*	*Lower DL*	*fCi/L*	*2.26*	*2.79*	*17*	*0.643*	*29.5*
Chloride	Historical	More data	mg/L	7.05	0.0019	27	1.14	21.95
Chromium	*New*	*Lower DL*	*µg/L*	*0.893*	*2.16*	*27*	*0.5*	*4.41*
Cobalt	*New*	*Lower DL*	*µg/L*	*0.274*	*2.57*	*32*	*0.05*	*0.5*
Cobalt-60	*New*	*Lower DL*	*fCi/L*	*1.09*	*2.43*	*17*	*0.404*	*23*
Conductivity	Historical	More data	µS/cm	348,000	1,410	35	150,000	1,361,000
Copper	*New*	*Lower DL*	*µg/L*	*0.332*	*2.01*	*32*	*0.05*	*0.5*
Cyanide	*New*	*No Historical*	*µg/L*	*5.43*	*1,407*	*25*	*5*	*26.7*
Dissolved oxygen	New	No Historical	µg/L	5,306	2,117	31	380	9,440
Eh	New	No Historical	mv	315	1.38	31	91	510
Europium-152	*New*	*Lower DL*	*fCi/L*	*12.9*	*1.51*	*17*	*5.39*	*24.1*
Europium-154	*New*	*Lower DL*	*fCi/L*	*8*	*1.52*	*17*	*3.43*	*18.3*
Europium-155	*New*	*Lower DL*	*fCi/L*	*2.33*	*1.87*	*17*	*0.969*	*11.7*

Table 5-4. Hanford Site Groundwater Background Concentrations[a] (from DOE/RL-96-61) (3 sheets)

Analyte[b]	Data Set	Reason for Selection	Units	Geo-metric Mean	Geometric Standard Deviation	Number of Samples	Min	Max
Fluoride	Historical	More data	mg/L	0.491	0.0018	28	0.267	5.85
Gross alpha	New	More data	pCi/L	1.09	2.03	19	0.25	3.02
Gross beta	New	More data	pCi/L	5.5	1.33	19	3.39	9.45
Iodine	*New*	*No Historical*	*µg/L*	*250*	*1,000*	*25*	*250*	*250*
Iodine-129	New	Lower DL	aCi/L	28.8	2.51	9	6.3	96.1
Iron	Historical	More data	µg/L	55.3	6.17	22	6	7,225
Lead	*New*	*Lower DL*	*µg/L*	*0.271*	*2.59*	*31*	*0.05*	*0.5*
Lithium	New	More data	µg/L	5,729	1,701	30	2,380	19,000
Magnesium	New	More data	µg/L	11,245	1.85	25	825	39,600
Manganese	New	More data	µg/L	2.22	9.25	32	0.05	94.4
Mercury	New	Lower DL	µg/L	0	5.34	27	0	0.012
Molybdenum	*New*	*Lower DL*	*µg/L*	*0.862*	*2.79*	*25*	*0.5*	*11.6*
Nickel	New	Lower DL	µg/L	0.686	1.9	31	0.27	2.56
Nitrate	New	More data	mg/L	5.68	3.36	26	0.085	28.063
Nitrite	*New*	*More data*	*mg/L*	*0.03*	*2.48*	*32*	*0.01*	*0.63*
Oxalate	*New*	*No Historical*	*µg/L*	*161*	*1,566*	*32*	*95*	*280*
pH	Historical	More data	pH units	7.78	1.04	35	6.94	8.79
Phosphate	*New*	*Lower DL*	*µg/L*	*102*	*1,432*	*32*	*65*	*293*
Plutonium	*New*	*No Historical*	*µg/L*	*0.0038*	*2.15*	*25*	*0.001*	*0.005*
Plutonium-238	*New*	*Lower DL*	*fCi/L*	*0.064*	*2.64*	*16*	*0.015*	*0.485*
Plutonium-239/240	New	Lower DL	fCi/L	0.398	1.97	16	0.04	0.762
Potassium	Historical	No new	µg/L	4,578	1.71	25	768	10,000
Potassium-40	Historical	No new	pCi/L	77.3	2.12	10	12	188
Radium-226	New	Lower DL	fCi/L	18.2	1.6	17	7	41.5
Radium-228	New	Lower DL	fCi/L	32.3	1.72	17	12.8	75.6
Ruthenium-106	*New*	*Lower DL*	*fCi/L*	*1.63*	*1.89*	*17*	*0.607*	*5.92*
Selenium	New	Lower DL	µg/L	0.96	6.47	32	0.5	11.6
Silicon	Historical	No new	µg/L	13,691	2.03	7	2,966	23,900

Table 5-4. Hanford Site Groundwater Background Concentrations[a] (from DOE/RL-96-61) (3 sheets)

Analyte[b]	Data Set	Reason for Selection	Units	Geo-metric Mean	Geometric Standard Deviation	Number of Samples	Min	Max
Silver	*Historical*	*No new*	*µg/L*	*3.42*	*1.41*	*15*	*1.93*	*5*
Sodium	Historical	More data	µg/L	13,402	1.73	25	2,360	32,000
Strontium (elemental)	New	More data	µg/L	158	1.75	32	13.1	402
Strontium-90	New	Lower DL	fCi/L	4.78	2.39	14	0.641	15.6
Sulfate	New	More data	mg/L	27.1	1.54	28	11.19	71.21
Sulfide	*New*	*More data*	*µg/L*	*1.71*	*1.21*	*32*	*1.6*	*3.21*
Technetium-99	*Historical*	*No new*	*pCi/L*	*0.447*	*1.62*	*5*	*0.271*	*0.752*
Thallium	*Historical*	*No new*	*µg/L*	*1.14*	*1.35*	*4*	*0.883*	*1.73*
Thorium	*New*	*No Historical*	*µg/L*	*0.5*	*1*	*25*	*0.5*	*0.5*
Tin	*Historical*	*No new*	*µg/L*	*15.9*	*1.27*	*12*	*11.8*	*31.3*
Titanium	*Historical*	*No new*	*µg/L*	*30*	*1*	*7*	*30*	*30*
Total carbon	New	No Historical	µg/L	30,325	1,174	32	20,990	43,175
Total dissolved solids	New	No Historical	µg/L	200,919	1.22	30	140,000	295,000
Total inorganic carbon	New	More data	µg/L	28,722	1,166	32	19,550	39,020
Total organic carbon	New	No Historical	µg/L	1,293	1,779	32	560	6,720
Tritium	*Historical*	*More data*	*pCi/L*	*63.9*	*1.63*	*15*	*27.8*	*131*
Uranium	New	More data	µg/L	2.57	2.85	25	0.5	12.8
Uranium-234	Historical	No new	pCi/L	0.75	1.1	2	0.7	0.803
Uranium-235	New	Lower DL	fCi/L	23.1	3.34	17	1.55	114
Uranium-238	New	Lower DL	fCi/L	721	1.89	17	150	2,440
Vanadium	*New*	*Lower DL*	*µg/L*	*1.83*	*4.19*	*32*	*0.5*	*16.7*
Zinc	*New*	*Lower DL*	*µg/L*	*1.27*	*9.22*	*32*	*0.05*	*1,270*
Zirconium	*Historical*	*No new*	*µg/L*	*25*	*1*	*7*	*25*	*25*

Reference: DOE/RL-96-61, *Hanford Site Background: Part 3, Groundwater Background*.

(a) Data rows entered in italics signify that >50% of the data were below the detection limit.

(b) Radionuclides with half-lives less than 1,000 years are decayed to June 1, 1997.

DL = detection limit.

Figure 5-9. Modified Stiff Diagram Depicting Major Cation and Anion Compositions for Background Groundwater, Top of the Aquifer in the Hanford Site's Unconfined Aquifer

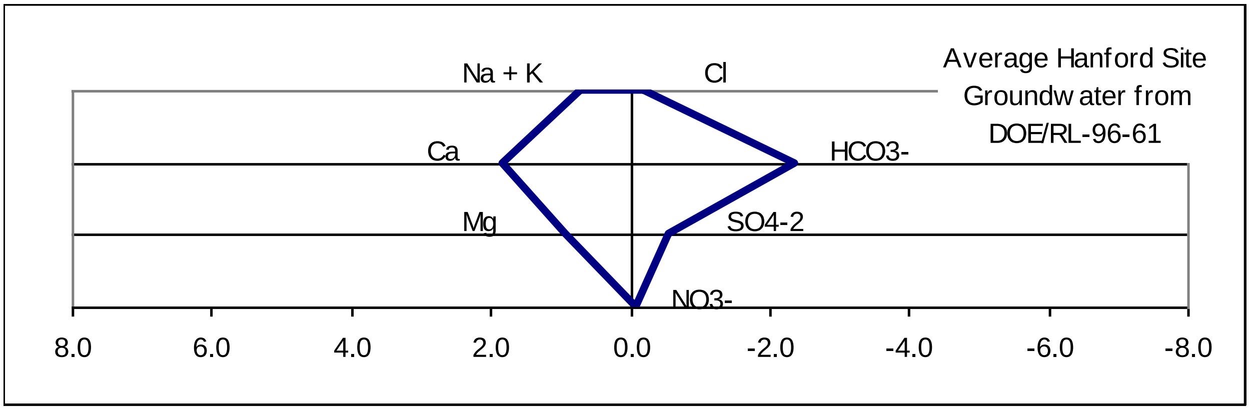

Note: Units for the x-axis are milliequivalents/liter with cations on the left and anions on the right.

Well 699-49-100C is located at the Yakima barricade. The well was drilled 2.4 m into basalt (total depth was 124.3 m bgs), completed with carbon steel casing in 1976, and perforated from 91.4 to 124.3 m bgs. The only records available for this well are an as-built diagram with driller's log that suggest that the water sampled from this well is from silty sandy gravels and sandy gravels of the Ringold Formation, member of Wooded Island of BHI-00184 or hydrogeologic units 5, 8, and 9 of PNL-8971.

Well 699-19-88 is located in the Dry Creek Valley, southwest of Highway 240. The well was drilled 8.5 m into basalt (total depth was 118.3 m bgs), completed with carbon steel casing in 1957, and perforated from 21.3 to 51.8 m bgs. The aquifer sampled is the Hanford formation and consists of unconsolidated gravel from 21.3 to 30.5 m bgs, very hard cemented gravel from 30.5 to 39.6 m bgs, and sand, silt and gravel from 39.6 to 51.8 m bgs.

Neither of these wells samples the same formation as up gradient wells at any SST WMAs. However, monitoring wells in 200 East Area, and thus the WMA A/AX, are screened in similar Hanford formation gravels. Also, both wells are located west of the 200 Areas and closer to the natural recharge area for the unconfined aquifer. The groundwater in that part of the aquifer is younger than the natural groundwater beneath the SST WMAs and is less altered by reaction with aquifer sediments. Up-gradient groundwater at most SST farms has been impacted by liquid disposal to cribs, ditches, and trenches. However, a few up-gradient wells at some tank farms are only slightly impacted and the general water composition from those wells resembles the groundwater composition of the background wells 699-49-100C and 699-19-88. Regardless of impacts from past-practice disposal facilities, groundwater from up-gradient wells at each SST farm is used as background for the tank farms when making up-gradient and down-gradient comparisons.

The average FY 2005 groundwater composition from the two up-gradient wells is given in Table 5-5 and a depiction of the major cations and anions is shown in Figure 5-10. The charge balances for the two analyses in Figure 5-10 are +3.5% for the 699-19-88 analysis and +1.9% for the well 699-49-100C analysis. Just as for the site-wide background groundwater, the up-gradient well groundwater is a calcium-bicarbonate dominated water type. Also, the groundwater from well 699-49-100C contains 12 mg/L nitrate suggesting that the groundwater at this location contains some nitrate contamination from up-gradient, probably agricultural, sources.

Table 5-5. Average FY 2013 Groundwater Composition in Up-gradient Wells at Waste Management Area A/AX

Constituent (units)	Concentration	
	Well 299-E24-20	Well 299-E24-22
Alkalinity as $CaCO_3$ (µg/L)	93,250	94,800
Calcium (µg/L)	53,913	52,390
Cesium-137 (pCi/L)	Not analyzed	Not analyzed
Chloride (mg/L)	20.35	18.08
Chromium (µg/L)	10.0	Not detected
Cobalt-60 (pCi/L)	Not analyzed	Not analyzed
Cyanide (µg/L)	Not analyzed	Not analyzed
Fluoride (mg/L)	0.20	0.22
Gross alpha (pCi/L)	2.10	2.00
Gross beta (pCi/L)	170	500
Iodine-129 (pCi/L)	3.04	3.20
Iron (µg/L)	30.8	19.2
Magnesium (µg/L)	16,075	14,970
Nitrate (mg/L)	47.63	20.84
pH Measurement (pH units)	8.0	8.0
Potassium (µg/L)	6,935	7,420
Sodium (µg/L)	23,713	25,660
Specific Conductance (µS/cm)	518	494.25
Sulfate (mg/L)	82.8	96.94
Technetium-99 (pCi/L)	260	887.5
Total organic carbon (µg/L)	320.25	760
Tritium (pCi/L)	7,200	1,600
Uranium (µg/L)	3.20	4.70

5.4.2 Background Groundwater Chemistry beneath Waste Management Area A/AX

Up-gradient groundwater composition for WMA A/AX is shown in Table 5-5. The data in the table are the average FY 2013 concentrations in each up-gradient well at the WMA, available on the Hanford Virtual Library. Data for the metals are from filtered samples; all other data are from unfiltered samples. Data flagged as suspect in the HEIS database have been excluded from the calculated averages.

The groundwater at WMA A/AX is characterized as a calcium-sulfate water that is different than groundwater at SST WMAs in other areas. Sulfate is also elevated in a few wells in the area of low-level burial ground WMA 2, north of WMA A/AX, suggesting that the high sulfate found at WMA A/AX is fairly regional in extent. The reason for the high sulfate is not known, but it does not reflect natural background conditions and may be related to leaching of the vadose zone caused by increased water levels associated with disposal at B Pond. Calcium, chloride, magnesium, and nitrate are also elevated relative to Hanford Site background groundwater.

5.5 CONCEPTUAL MODEL FOR THE GROUNDWATER PATHWAY AT WASTE MANAGEMENT AREA C

Following is a brief summary of the conceptual model of groundwater system relevant to the WMA A/AX that addresses 1) key characteristics of unconfined aquifer system, 2) hydraulic and water quality impacts from historic past operations, and 3) projected future hydraulic and water quality impacts.

5.5.1 Key Characteristics of Unconfined Aquifer System

Groundwater is present in both unconfined and confined aquifers at the Hanford Site. The unconfined aquifer is contained in the unconsolidated to semi-consolidated Ringold and Hanford formations that overlie the basalt bedrock. In some areas, low permeability mud layers form aquitards that create confined hydraulic conditions in the underlying sediment.

Within 200 East and specifically in vicinity of the WMA A/AX, depth to groundwater in December 2014 was between 88 and 90 m. The uppermost unconfined aquifer is made of undifferentiated sands and gravels of the lower part of Hanford formation, the Cold Creek Unit, and the Ringold Formation that collectively range from 8 to 27 m thick.

Natural sources of recharge to the unconfined aquifer system occur due to the following.

- Infiltration of runoff from elevated regions along the western boundary of the Hanford Site.

- Infiltration of spring water along the flanks the unconfined aquifer bordering upland areas.

- Upwelling of groundwater that originates from the basalt-confined aquifer system (Note: There have been situations in the past where the head in the unconfined system has been greater than that in the confined system leading to discharge of groundwater along with contaminants from the unconfined aquifer to the confined system).

- Infiltration of precipitation falling across the Hanford Site (Note: Infiltration from precipitation is temporally dependent; i.e., infiltration from precipitation is greater during the winter months because of greater precipitation and reduced evapotranspiration when plants are dormant, and much less during other times of the year primarily because of increased evapotranspiration due to plant activity).

- Some recharge also takes place along the Yakima River.

Recharge from precipitation is highly variable, both spatially and temporally. It ranges from near zero to greater than 100 millimeters per year, depending on climate, vegetation, and soil texture ("Variations in Recharge at the Hanford Site" [Gee et al. 1992], PNL-10285, *Estimated Recharge Rates at the Hanford Site*). The highest rates of recharge from precipitation are associated with areas for which surface conditions are dominated by coarse-textured soil with little or no vegetation; such conditions are found in all SST WMAs, including the area in and around WMA A/AX.

Regionally, groundwater in the unconfined aquifer flows toward and discharges to the Columbia River across most of the Hanford Site. Some variation to this generalization occurs in some operation areas along the river where artificial recharge mounds are present or during times of high river stage.

Waste Management Area A/AX is located in an area where the underlying water-table is very flat. The gradient in the vicinity of WMA A/AX is consistent with the regional gradient on the order of magnitude of 1E-5 and the existence of extremely permeable sands and gravels associated with the Hanford formation.

5.5.2 Hydraulic Impacts from Past Operations

Since the start of Hanford Site operations in the mid-1940s, artificial recharge from wastewater disposal facilities has been several times greater than the estimated recharge from natural sources. This caused an increase in the water-table elevation over most of the Hanford Site and the formation of groundwater mounds beneath major wastewater disposal facilities. In the vicinity of WMA A/AX, long-term hydrographs of water-level measurements suggest that unconfined aquifer has risen as much as 5 m and the direction of local-scale groundwater flow has changed in response to the artificial recharge for nearby wastewater disposal facilities.

The water table declined somewhat in the late 1960s and early 1970s, then increased again in the early 1980s before a final decline beginning in 1988 and continuing throughout the 1990s when wastewater discharges in the 200 East Area were significantly reduced. At WMA A/AX, water-table elevations have declined about 3m since the early 1990s.

In the vicinity of the WMA A/AX, the average flow direction is currently inferred based in part on water-level measurements and in evaluation and interpretation of local-scale plume migration to be to the south and southwest. Groundwater flow rates in the area are on the order of 0.2 to 0.4 m/day with flow direction historically to the south or southeast but difficult to confirm.

5.5.3 Project Future Impacts

In the future, hydraulic and water quality conditions found beneath the WMA A/AX are expected to change in the following manner.

- The effect of the historical wastewater discharges on the water table would dissipate and the water-level elevation in the unconfined aquifer would return to lower pre-Hanford conditions. Without any significant changes in land or water use either on site or up-gradient of the site, the current water-table at WMA A/AX could likely decline another 3 to 5 m over the next 50 to 100 yrs before reaching this new lower equilibrium water table condition (see Table 5-4).

- Current interpreted directions of flow would be anticipated to change from the current south to southwesterly direction to a more south and southeasterly direction.

- Water-table and groundwater flow conditions could be influences with significant changes in land or water use nearby or up-gradient of the site.

- Water quality impacts from past contaminant releases to groundwater from the vadose zone or up-gradient sources could increase or decline locally as sources in the vadose zone continue to release to groundwater or up-gradient source pass beneath the site. Results of the SST PA suggest that existing sources of mobile contaminants within the vadose zone could continue to migrate downward and impact groundwater over the next 200 to 300 years.

- Eventually, mobile contaminants released from grouted residuals left in tanks and ancillary equipment would be first expected to impact groundwater about years 4000 to 6000 and peak in years 8000 to 10000.

5.6 RECOMMENDED FLOW AND TRANSPORT PROPERTIES

The following discussion presents recommended flow and transport properties that will be used to support an integrated, saturated and unsaturated, local-scale model that will be used to flow and transport simulations in the immediate vicinity of the WMA A/AX. Results of these model simulation results will be used as input to regional-scale of groundwater flow and transport to evaluate water quality and risk impacts between the WMA A/AX and points of regional discharge along the Columbia River.

The flow and transport properties that will be used in the regional-scale modeling efforts are based on the estimated parameters utilized in the site-wide groundwater model that has been developed and implemented within the framework of the TC&WM EIS (DOE/EIS-0391, *Draft Tank Closure and Waste Management Environmental Impact Statement for the Hanford Site, Richland, Washington*). The flow and transport properties used in the regional-scale modeling will not be specifically discussed as a part of this report. The reader is referred to the Appendices L (*Groundwater Flow Field Development*) and O (*Groundwater Transport Analysis*) in the TC&WM EIS for specific details of the development, calibration, and implementation of this site-wide groundwater flow and transport model.

Flow parameters such as saturated hydraulic conductivity, effective porosity, hydraulic gradient, and depth to water table are needed for the unconfined aquifer part of the integrated, saturated-unsaturated, local-scale model analysis up to the WMA A/AX fence line. Recommendations for these specific parameters are provided in RPP-13310 for the SST PA, and specific detailed discussions of the basis for these parameters are provided in Section 5 of RPP-13310. These parameter estimates have undergone revisions based on initial modeling efforts for the WMA C PA. The revised estimates of flow parameters and related documentation will likely form the basis for the initial estimates of these parameters in the WMA A/AX PA.

Constituent-specific distribution coefficients that were recommended for use in the vadose zone pathway and summarized in RPP-RPT-46088, Rev. 1. These distribution coefficients have also undergone revisions based on initial modeling efforts for the WMA C PA, and the revised estimates of distribution coefficients and related documentation will likely form the basis for the initial estimates of the parameters in the WMA A/AX PA.

6.0 REFERENCES

ARH-LD-127, 1976, *Geology of the 241-A Tank Farm*, Atlantic Richfield Hanford Company, Richland, Washington.

ARH-LD-128, 1976, *Geology of the 241-AX Tank Farm*, Atlantic Richfield Hanford Company, Richland, Washington.

ARH-LD-132, 1976, *Geology of the 241-C Tank Farm*, Atlantic Richfield Hanford Company, Richland, Washington.

Atomic Energy Act of 1954, 42 USC 2011, et seq.

Baker V. R., B. N. Bjornstad, A. J. Busacca, K. R. Fecht, E. P. Kiver, U. L. Moddy, J. G. Rigby, D. F. Stradling, and A. M. Tallman, 1991, "Quaternary Geology of the Columbia Plateau," *The Geology of North America, Quaternary Nonglacial Geology: Conterminous U.S.*, Vol. K-2, Chapter 8, pp. 215-250.

Bedient, P. B., H. S. Rifai, and C. J. Newell, 1994, *Ground Water Contamination – Transport and Remediation*, PTR Prentice Hall, Englewood Cliffs, New Jersey.

BHI-00184, 1995, *Miocene- to Pliocene-Aged Suprabasalt Sediments of the Hanford Site, South-Central Washington*, Rev. 00, Bechtel Hanford, Inc., Richland, Washington.

BHI-01103, 1999, *Clastic Injection Dikes of the Pasco Basin and Vicinity: Geologic Atlas Series*, Rev. 0, Bechtel Hanford, Inc., Richland, Washington.

BNWL-B-360, 1974, *Selected Water Table Contour Maps and Well Hydrographs for the Hanford Reservation, 1944-1973*, Pacific Northwest Laboratories, Richland, Washington.

BNWL-243, 1966, *Soil Survey Hanford Project in Benton County Washington*, Pacific Northwest Laboratory, Richland, Washington.

Campbell N. P, 1989, "Structural and Stratigraphic Interpretation of Rocks under the Yakima Fold Belt, Columbia Basin, Based on Recent Surface Mapping and Well Data," in *Volcanism and Tectonism on the Columbia River Flood-Basalt Province*, Geological Society of America, Special Paper 239.

Comprehensive Environmental Response, Compensation, and Liability Act of 1980, 42 USC 9601 et seq., as amended.

De Smedt, F. and P. J. Wierenga, 1984, "Solute Transfer through Columns of Glass Beads," *Water Resources Research*, Vol. 20, No. 2, pp. 225–232.

DOE/EIS-0391, 2009, *Draft Tank Closure and Waste Management Environmental Impact Statement for the Hanford Site, Richland, Washington*, U.S. Department of Energy, Richland, Washington.

DOE/ORP-2000-24, 2001, *Hanford Immobilized Low-Activity Tank Waste Performance Assessment: 2001 Version*, Rev. 0, U.S. Department of Energy, Office of River Protection, Richland, Washington.

DOE/ORP-2005-01, 2005, *Initial Single-Shell Tank System Performance Assessment for the Hanford Site*, Rev. 0, U.S. Department of Energy, Office of River Protection, Richland, Washington.

DOE/RL-92-05, 1993, *B Plant Source Aggregate Area Management Study Report*, Rev. 0, U.S. Department of Energy, Richland, Washington.

DOE/RL-92-23, 1992, *Hanford Site Groundwater Background*, U.S. Department of Energy, Richland, Washington.

DOE/RL-96-17, 2009, *Remedial Design Report/Remedial Action Work Plan for the 100 Area*, Rev. 6, U.S. Department of Energy, Richland Operations Office, Richland, Washington.

DOE/RL-96-61, 1997, *Hanford Site Background: Part 3, Groundwater Background*, Rev. 0, U.S. Department of Energy, Richland, Washington.

DOE/RL-98-72, 1999, *Retrieval Performance Evaluation Methodology for the AX Tank Farm*, U.S. Department of Energy, Richland Operations Office, Richland, Washington.

DOE/RL-2002-39, 2002, *Standardized Stratigraphic Nomenclature for Post-Ringold-Formation Sediments Within the Central Pasco Basin*, Rev. 0, U.S. Department of Energy, Richland Operations Office, Richland, Washington.

DOE/RL-2008-66, 2009, *Hanford Site Groundwater Monitoring for Fiscal Year 2008*, CH2M Hill Plateau Remediation Contractor, Richland, Washington.

DOE/RL-2014-32, *Hanford Site Groundwater Monitoring Report for 2013*, Rev. 0, CH2M HILL Plateau Remediation Company, Inc., Richland, Washington.

DOE/RW-0164, 1988, *Consultation Draft Site Characterization Plan. Reference Repository Location, Hanford Site, Washington*, U.S. Department of Energy, Office of Civilian Radioactive Waste Management, Washington, D.C.

Ecology, EPA, and DOE, 1989, *Hanford Federal Facility Agreement and Consent Order – Tri-Party Agreement*, 2 vols., as amended, State of Washington Department of Ecology, U.S. Environmental Protection Agency, and U.S. Department of Energy, Olympia, Washington.

Ecology Publication No. 94-145, 1994, *Model Toxics Control Act Cleanup Levels & Risk Calculations (CLARC) Version 3.1*, Washington State Department of Ecology Toxics Clean-up Program, Olympia, Washington.

EDF-ER-275, 2004, *Engineering Design File – Fate and Transport Modeling Results and Summary Report*, Rev. 3, Idaho National Engineering and Environmental Laboratory, Idaho Falls, Idaho.

EM-ER-01-115, 2001, "Kd Values for INTEC Groundwater Modeling" (letter from T. Jenkins to M. Doornbos, BBWI, dated July 3), U.S. Department of Energy, Idaho Operations Office Idaho Falls, Idaho.

EPA 402-R-99-004A, 1999, *Understanding Variation in Partition Coefficient, Kd, Values*, U.S. Environmental Protection Agency, Washington, D.C.

EPA/540/R-95/128, 1996, *Soil Screening Guidance: Technical Background Document*, Second Edition, U.S. Environmental Protection Agency, Washington, D.C.

EPA/600/2-91/065, 1991, *The RETC Code for Quantifying the Hydraulic Functions of Unsaturated Soils*, U.S. Environmental Protection Agency, Washington, D.C.

Fecht K. R., S. P. Reidel, and A. M. Tallman, 1987, "Paleodrainage of the Columbia River System on the Columbia Plateau of Washington State – A Summary," *Selected Papers on the Geology of Washington*, Washington Division of Geology and Earth Resources, Bulletin 77, pp. 219-248.

Flury, M., J. B. Mathison, and J. B. Harsh, 2002, "In Situ Mobilization of Colloids and Transport of Cesium in Hanford Sediments," *Environmental Science & Technology*, Vol. 36, No. 24, pp. 5335–5341.

Freeze, R. A. and J. A. Cherry, 1979, *Groundwater*, Prentice-Hall, Inc., Englewood Cliffs, New Jersey.

Gee, G. W., M. J. Fayer, M. L. Rockhold, and M. D. Campbell, 1992, "Variations in Recharge at the Hanford Site," *Northwest Science*, Vol. 66, pp. 237-250.

Gelhar, L. W., 1993, *Stochastic Subsurface Hydrology*, Prentice Hall, New York, New York.

Gelhar, L. W., C. Welty, and K. R. Rehfeldt, 1992, "A Critical Review of Data on Field Scale Dispersion in Aquifers," *Water Resources Research*, Vol. 28, pp. 1955-1974.

HNF-2603, 1998, *A Summary and Evaluation of Hanford Site Tank Farm Subsurface Contamination*, Rev. 0, Lockheed Martin Hanford Corporation, Richland, Washington.

HNF-4936, 1999, *Subsurface Physical Conditions Description of the S-SX Waste Management Area*, Rev. 0, Lockheed Martin Hanford Corporation, Richland, Washington.

HNF-5507, 2000, *Subsurface Conditions Description of the B-BX-BY Waste Management Area*, Rev. 0A, CH2M HILL Hanford Group, Inc., Richland, Washington.

HNF-EP-0182, 2007, *Waste Tank Summary Report for Month Ending October 31, 2006*, Rev. 223, CH2M HILL Hanford Group, Inc., Richland, Washington.

HNF-EP-0182, 2009, *Waste Tank Summary Report for Month Ending April 30, 2009,* Rev. 253, Washington River Protection Solutions LLC, Richland, Washington.

Honeyman, B. D., 1984, *Cation and Anion Adsorption at the Oxide/Solution Interface in Systems Containing Binary Mixtures of Adsorbents: An Investigation of the Concept of Adsorptive Additivity*, Ph.D. Thesis, Stanford University, Stanford, California.

HW-40469, 1955, *Changes in the Hanford Ground Water Table 1944-1955*, Hanford Atomic Products Operation, Richland, Washington.

HW-61780, 1959, *Subsurface Geology of the Hanford Separation Areas,* Hanford Atomic Products Operation, General Electric Company, Richland, Washington.

Kersting, A. B., D. W. Efurd, D. L. Finnegan, D. J. Rokop, D. K. Smith, and J. L. Thompson, 1999, "Migration of Plutonium in Ground Water at the Nevada Test Site," *Nature*, Vol. 397, Issue 6714, pp. 56–59.

Khaleel, R. and J. F. Relyea, 1997, "Correcting Laboratory-Measured Moisture Retention Data for Gravels," in *Water Resources Research*, Vol. 33, Issue 8), pp. 1875-1878.

Khaleel, R., J. F. Relyea, and J. L. Conca, 1995, "Evaluation of van Genuchten-Mualem Relationships to Estimate Hydraulic Conductivity at Low Water Contents," *Water Resources Research*, Vol. 31, Issue 11, pp. 2659-2668.

Lindsey, K. A., S. P. Reidel, K. R. Fecht, J. L. Slate, A. G. Law, and A. M. Tallman, 1994, "Geohydrologic Setting of the Hanford Site, South-Central Washington," *Geologic Field Trips in the Pacific Northwest*, 1994 Geological Society of America Annual Meeting, Vol. 1, Chap. 1C, pp. 1-16.

McCaffrey, R., A. I. Qamar, R. W. King, R. Wells, G. Khazaradze, C. A. Williams, C. W. Stevens, J. J. Vollick and P. C. Zwick, 2007, "Fault locking, block rotation and crustal deformation in the Pacific Northwest," *Geophysical Journal International*, Vol. 169, Issue 3, pp. 1315–1340.

McCarthy, J. F. and J. M. Zachara, 1989, "Subsurface Transport of Contaminants," *Environmental Science & Technology*, Vol. 23, No. 5, pp. 496–502.

Millington, R. J. and J. P. Quirk, 1961, "Permeability of Porous Solids," *Transactions of the Faraday Society*, Vol. 57, pp. 1200-1207.

Mualem, Y., 1976, "A New Model for Predicting the Hydraulic Conductivity of Unsaturated Porous Media," *Water Resources Research*, Vol. 12, No. 3, pp. 513-522.

Murray, C. J., A. L. Ward, and J. Wilson, 2007, "Influence of Clastic Dikes on Vertical Migration of Contaminants at the Hanford Site," *Vadose Zone Journal*, Vol. 6, No. 4, pp. 959-970.

Newcomb, R. C., 1958, "Ringold Formation of Pleistocene Age in Type Locality, the White Bluffs, Washington," *American Journal of Science* Vol. 256, pp. 328-340.

Nkedi-Kizza, P., J. W. Biggar, M. T. van Genuchten, P. J. Wierenga, H. M. Selim, J. M. Davidson, and D. R. Nielsen, 1983, "Modeling Tritium and Chloride 36 Transport Through an Aggregated Oxisol," *Water Resources Research*, Vol. 19, Issue 3, pp. 691-700.

NUREG/CR-6114, 1994, *Auxiliary Analyses in Support of Performance Assessment of a Hypothetical Low-Level Waste Facility: Groundwater Flow and Transport Simulation*, Vol. 3, U.S. Nuclear Regulatory Commission, Washington, D.C.

Open File Report 94-8, 1994, *Geologic Map of the Richland 1:100,000 Quadrangle, Washington*, Washington State Department of Natural Resources, Olympia, Washington.

Pace, M. N., M. A. Hayes, P. M. Jardine, T. L. Mehlhorn, J. M. Zachara, B. N. Bjornstad, 2003, "Quantifying the Effects of Small-Scale Heterogeneities on Flow and Transport in Undisturbed Cores from the Hanford Formation," *Vadose Zone Journal*, Vol. 2, pp. 664-676.

Pluhar, C. J., 2003, "Paleomagnetic and Geochemical Applications to Tectonics and Quaternary Geology: Studies at Coso Volcanic Field, CA and the Channeled Scabland, WA," University of California, Santa Cruz, California.

Pluhar, C. J., B. N. Bjornstad, S. P. Reidel, R. S. Coe, and P. B. Nelson, 2006, "Magnetostratiphic Evidence from the Cold Creek Bar for Onset of Ice-Age Cataclysmic Floods in Eastern Washington During the Early Pleistocene," *Quaternary Research*, Vol. 65, pp. 123-135.

PNL-2899, 1979, *Radiological Status of the Ground-Water Beneath the Hanford Project January – December 1978*, Pacific Northwest Laboratory, Richland, Washington.

PNL-6415, 1996, *Hanford Site National Environmental Policy Act (NEPA) Characterization*, Rev. 8, Pacific Northwest National Laboratory, Richland, Washington.

PNL-6820, 1989, *Hydrogeology of the 200 Areas Low-Level Burial Grounds – An Interim Report, Volumes 1 and 2*, Pacific Northwest National Laboratory, Richland, Washington.

PNL-8337, 1992, *Summary and Evaluation of Available Hydraulic Property Data for the Hanford Site Unconfined Aquifer System*, Pacific Northwest Laboratory, Richland, Washington.

PNL-8971, 1993, *Three-Dimensional Conceptual Model for the Hanford Site Unconfined Aquifer System, FY 1993 Status Report*, Pacific Northwest Laboratory, Richland, Washington.

PNL-10285, 1995, *Estimated Recharge Rates at the Hanford Site*, Pacific Northwest Laboratory, Richland, Washington.

PNL-10886, 1995, *Development of a Three-Dimensional Ground-Water Model of the Hanford Site Unconfined Aquifer System: FY 1995 Status Report*, Pacific Northwest National Laboratory, Richland, Washington.

PNNL-12261, 2000, *Revised Hydrogeology for the Suprabasalt Aquifer System, 200-East Area and Vicinity, Hanford Site, Washington*, Pacific Northwest National Laboratory, Richland, Washington.

PNNL-13023, 2001, *RCRA Groundwater Monitoring Plan for Single-Shell Tank Waste Management Area A-AX at the Hanford Site*, Pacific Northwest National Laboratory, Richland, Washington.

PNNL-13024, 2001, *RCRA Groundwater Monitoring Plan for Single-Shell Tank Waste Management Area C at the Hanford Site*, Pacific Northwest National Laboratory, Richland, Washington.

PNNL-13037, 2004, *Geochemical Data Package for the 2005 Hanford Integrated Disposal Facility Performance Assessment*, Rev. 2, Pacific Northwest National Laboratory, Richland, Washington.

PNNL-13080, 2000, *Hanford Site Groundwater Monitoring: Setting, Sources, and Methods*, Pacific Northwest National Laboratory, Richland, Washington.

PNNL-13378, 2001, *Results of Detailed Hydrologic Characterization Tests – Fiscal Year 1999*, Pacific Northwest National Laboratory, Richland, Washington.

PNNL-13400, 2000, *Groundwater Flow and Transport Calculations Supporting the Immobilized Low-Activity Waste Disposal Facility Performance Assessment*, Pacific Northwest National Laboratory, Richland, Washington.

PNNL-13404, 2001, *Hanford Site Groundwater Monitoring for Fiscal Year 2000*, Pacific Northwest National Laboratory, Richland, Washington.

PNNL-13447, 2001, *Transient Inverse Calibration of Hanford Site-Wide Groundwater Model to Hanford Operational Impacts – 1943 to 1996*, Pacific Northwest National Laboratory, Richland, Washington.

PNNL-13514, 2001, *Results of Detailed Hydrologic Characterization Tests – Fiscal Year 2000*, Pacific Northwest National Laboratory, Richland, Washington.

PNNL-13672, 2001, *A Catalog of Vadose Zone Hydraulic Properties for the Hanford Site*, Pacific Northwest National Laboratory, Richland, Washington.

PNNL-13672, 2002, *A Catalog of Vadose Zone Hydraulic Properties for the Hanford Site*, Rev. 1, Pacific Northwest National Laboratory, Richland, Washington.

PNNL-13801, 2002, *Groundwater Quality Assessment Report for Waste Management Area S-SX (April 2000 through December 2001)*, Pacific Northwest National Laboratory, Richland Washington.

PNNL-13858, 2002, *Revised Hydrogeology for the Suprabasalt Aquifer System, 200-West Area and Vicinity, Hanford, Washington*, Pacific Northwest National Laboratory, Richland, Washington.

PNNL-13895, 2002, *Hanford Contaminant Distribution Coefficient Database and Users Guide*, Pacific Northwest National Laboratory, Richland, Washington.

PNNL-13895, 2003, *Hanford Contaminant Distribution Coefficient Database and Users Guide*, Rev. 1, Pacific Northwest National Laboratory, Richland, Washington.

PNNL-14186, 2003, *Results of Detailed Hydrologic Characterization Tests – Fiscal Year 2002*, Pacific Northwest National Laboratory, Richland, Washington.

PNNL-14286, 2003, *STOMP Subsurface Transport Over Multiple Phases Version 3.0 User's Guide*, Pacific Northwest National Laboratory, Richland, Washington.

PNNL-14538, 2003, *Borehole Data Package for R.C.R.A. Wells 299-E25-93 and 299-E24-22 at Single-Shell Tank Waste Management Area A-AX, Hanford Site, Washington*, Pacific Northwest National Laboratory, Richland, Washington.

PNNL-14594, 2004, *Characterization of Vadose Zone Sediments Below the TX Tank Farm: Boreholes C3830, C3831, C3832 and RCRA Borehole 299-W10-27*, Pacific Northwest National Laboratory, Richland, Washington.

PNNL-14656, 2004, *Borehole Data Package for Four CY 2003 RCRA Wells 299-E27-4, 299-E27-21, 299-E27-22, and 299-E27-23 at Single-Shell Tank, Waste Management Area C, Hanford Site, Washington*, Pacific Northwest National Laboratory, Richland, Washington.

PNNL-14702, 2006, *Vadose Zone Hydrogeology Data Package for Hanford Assessments*, Rev. 1, Pacific Northwest National Laboratory, Richland, Washington.

PNNL-14804, 2004, *Results of Detailed Hydrologic Characterization Tests – Fiscal Year 2003*, Pacific Northwest National Laboratory, Richland, Washington.

PNNL-14849, 2004, *Characterization of Vadose Zone Sediments Below the T Tank Farm: Boreholes C4104, C4105, 299-W10-196, and RCRA Borehole 299-W11-39*, Pacific Northwest National Laboratory, Richland, Washington.

PNNL-15301, 2006, *RCRA Assessment Plan for Single-Shell Tank Waste Management Area T*, Pacific Northwest National Laboratory, Richland, Washington.

PNNL-15503, 2008, *Characterization of Vadose Zone Sediments Below the C Tank Farm: Borehole C4297 and RCRA Borehole 299-E27-22*, Rev. 1, Pacific Northwest National Laboratory, Richland, Washington.

PNNL-15617, 2008, *Characterization of Vadose Zone Sediments from C Waste Management Area: Investigation of the C-152 Transfer Line Leak*, Rev. 1, Pacific Northwest National Laboratory, Richland, Washington.

PNNL-15670, 2006, *Hanford Site Groundwater Monitoring for Fiscal Year 2005*, Pacific Northwest National Laboratory, Richland, Washington.

PNNL-15670, 2006, *Hanford Site Groundwater Monitoring for Fiscal Year 2005*, Chapter 2.10, "200-BP-5 Operable Unit," Pacific Northwest National Laboratory, Richland, Washington.

PNNL-15837, 2007, *Data Package for Past and Current Groundwater Flow and Contamination Beneath Single-Shell Tank Waste Management Areas*, Pacific Northwest National Laboratory, Richland, Washington.

PNNL-15955, 2007, *Geology Data Package for the Single-Shell Tank Waste Management Areas at the Hanford Site*, Pacific Northwest National Laboratory, Richland, Washington.

PNNL-16407, 2007, *Geology of the Waste Treatment Plant Seismic Boreholes*, Rev. 1, Pacific Northwest National Laboratory, Richland, Washington.

PNNL-16663, 2007, *Geochemical Processes Data Package for the Vadose Zone in the Single-Shell Tank Waste Management Areas at the Hanford Site*, Pacific Northwest National Laboratory, Richland, Washington.

PNNl-17154, 2008, *Geochemical Characterization Data Package for the Vadose Zone in the Single-Shell Tank Waste Management Areas at The Hanford Site*, Pacific Northwest National Laboratory, Richland, Washington.

PNNL-19071, 2009, *Annual Hanford Seismic Report for Fiscal Year 2009*, Pacific Northwest National Laboratory, Richland, Washington.

Polmann, D. J., 1990, *Application of Stochastic Methods to Transient Flow and Transport in Heterogeneous Unsaturated Soils*, Ph.D. Thesis, Massachusetts Institute of Technology, Cambridge, Massachusetts.

PSPL, 1981, *Skagit/Hanford Nuclear Project, Preliminary Safety Analysis Report*, Vol. 1, Puget Sound Power and Light Company, Seattle, Washington.

Reidel S. P., N. P. Campbell, K. R. Fecht, and K. A. Lindsey, 1994, "Late Cenozoic Structure and Stratigraphy of South-Central Washington," *Regional Geology of Washington State*, Washington Division of Geology and Earth Resources, Bulletin 80, pp. 159-180.

Reidel, S. P. and T. L. Tolan, 2009, "Landscape Evolution in a Flood-Basalt Province: an Example from the Pacific Northwest," Paper No. 6-2 in Session No. 6, The Evolution of Basaltic Landscapes: Time and the River and Lava Flowing, 2009 Portland GSA Annual Meeting (18-21 October 2009), Portland, Oregon.

Reidel, S. P., T. L. Tolan, P. R. Hooper, M. H. Beeson, K. R. Fecht, R. D. Bentley, and J. L. Anderson, 1989, "The Grande Ronde Basalt, Columbia River Basalt Group; Stratigraphic Descriptions and Correlations in Washington, Oregon, and Idaho," In *Volcanism and Tectonism in the Columbia River Flood-Basalt Province*, Geological Society of America, Special Paper 239, pp. 21-53.

Resource Conservation and Recovery Act of 1976, 42 USC 6901 et seq.

RHO-BWI-ST-4, 1979, *Geologic Studies of the Columbia Plateau – A Status Report: October 1979*, Rockwell Hanford Operations, Richland, Washington.

RHO-BWI-ST-14, 1981, *Subsurface Geology of the Cold Creek Syncline*, "Chapter 3 – Wanapum and Saddle Mountains Basalts of the Cold Creek Syncline Area," Rockwell Hanford Operations, Richland, Washington.

RHO-ST-23, 1979, *Geology of the Separation Areas, Hanford Site, South-Central Washington*, Rockwell Hanford Operations, Richland, Washington.

Risk Assessment Information System, Queried 04/2010, http://rais.ornl.gov/

Roy, S. B., and D. A. Dzombak, 1997, "Chemical Factors Influencing Colloid-Facilitated Transport of Contaminants in Porous Media," *Environmental Science & Technology*, Vol. 31, No. 3, pp. 656–664.

RPP-6296, 2000, *Modeling Data Package for S-SX Field Investigation Report (FIR)*, Rev. 0, CH2M HILL Hanford Group, Inc., Richland, Washington.

RPP-7884, 2002, *Field Investigation Report for Waste Management Area S-SX*, Rev. 0, CH2M HILL Hanford Group, Inc., Richland, Washington.

RPP-8531, 2001, *Vadose Zone Geology of Boreholes 299-W10-27 and 299-W11-39 T-TX-TY Waste Management Area Hanford Site, South-Central Washington*, Rev. 0, CH2M HILL Hanford Group, Inc., Richland, Washington.

RPP-8681, 2001, *Vadose Zone Geology of Boreholes 299-E33-45 and 299-E33-46 B-BX-BY Waste Management Area Hanford Site, South-Central Washington*, Rev. 0, CH2M HILL Hanford Group, Inc., Richland, Washington.

RPP-9223, 2001, *Modeling Data Package for B-BX-BY Field Investigation Report (FIR)*, Rev. 0, CH2M HILL Hanford Group, Inc., Richland, Washington.

RPP-10435, 2002, *Single-Shell Tank System Integrity Assessment Report*, Rev. 0, CH2M HILL Hanford Group, Inc., Richland, Washington.

RPP-13310, 2006, *Modeling Data Package for an Initial Assessment of Closure of the C Tank Farm*, Rev. 1, CH2M HILL Hanford Group, Inc., Richland, Washington.

RPP-14430, 2003, *Subsurface Conditions Description of the C and A-AX Waste Management Area*, Rev. 0, CH2M HILL Hanford Group, Inc., Richland, Washington.

RPP-17209, 2006, *Modeling Data Package for an Initial Assessment of Closure of the S and SX Tank Farms*, Rev. 1, CH2M HILL Hanford Group, Inc., Richland, Washington.

RPP-20621, 2004, *Far-Field Hydrology Data Package for the Integrated Disposal Facility Performance Assessment*, Rev. 0, "Appendix F. Physical and Hydraulic Measurements of FY1998 Clastic Dike Samples," CH2M HILL Hanford Group, Inc., Richland, Washington.

RPP-23748, 2006, *Geology, Hydrogeology, Geochemistry, and Mineralogy Data Package for the Single-Shell Tank Waste Management Areas at the Hanford Site*, Rev. 0, CH2M HILL Hanford Group, Inc., Richland, Washington.

RPP-35484, 2008, *Field Investigation Report for Waste Management Areas C and A-AX*, Rev. 1, CH2M HILL Hanford Group, Inc., Richland, Washington.

RPP-ASMT-42278, 2009, *Tank 241-A-103 Leak Assessment Report,* Rev. 0, Washington River Protection Solutions, LLC, Richland, Washington.

RPP-ASMT-42628, 2014, *Tank 241-AX-102 Integrity Assessment Report*, Rev. 0, Washington River Protection Solutions, LLC, Richland, Washington.

RPP-ASMT-57574, 2014, *Tank 241-AX-104 Integrity Assessment Report*, Rev. 0, Washington River Protection Solutions, LLC, Richland, Washington.

RPP-PLAN-39114, 2009, *Phase 2 RCRA Facility Investigation/Corrective Measures Study Work Plan for Waste Management Area C*, Rev. 1, Washington River Protection Solutions LLC, Inc., Richland, Washington.

RPP-RPT-35222, 2007, *Far-Field Hydrology Data Package for the RCRA Facility Investigation (RFI) Report*, CH2M HILL Hanford Group, Inc., Richland, Washington.

RPP-RPT-38152, 2008, *Data Quality Objectives Report Phase 2 Characterization for Waste Management Area C RCRA Field Investigation/Corrective Measures Study*, Rev. 0, Cenibark International, Inc., Richland, Washington.

RPP-RPT-41918, 2010, *Assessment Context for Performance Assessment for Waste in C Tank Farm Facilities after Closure*, Rev. 0, Washington River Protection Solutions LLC, Inc., Richland, Washington.

RPP-RPT-42294, 2009, *Hanford Waste Management Area C Soil Contamination Inventory Estimates*, Rev. 0, Washington River Protection Solutions LLC, Richland, Washington.

RPP-RPT-44042, 2009, *Recharge and Waste Release within Engineered System in Waste Management Area C*, Rev. A, Washington River Protection Solutions LLC, Richland, Washington.

RPP-RPT-46088, *Flow and Transport in the Natural System at Waste Management Area C*, Rev. 1, Washington River Protection Solutions LLC, Inc., Richland, Washington.

Sen, T. K. and K. C. Khilar, 2006, "Review on Subsurface Colloids and Colloid-Associated Contaminant Transport in Saturated Porous Media," *Advances in Colloid and Interface Science*, Vol. 119, pp. 71–96.

Spitz, K. and J. Moreno, 1996, *A Practical Guide to Groundwater and Solute Transport Modeling*, John Wiley and Sons, Inc., New York, New York.

Stiff, H. A. Jr., 1983, "The Interpretation of Chemical Water Analysis by Means of Patterns," in *Chemical Hydrology*, W. Back and R. A. Freeze (eds.), Benchmark Papers in Geology, Volume 73, Hutchinson Ross Publishing Company, Stroudsburg, Pennsylvania.

Technical Guidance Document for Tank Closure Environmental Impact Statement Vadose Zone and Groundwater Revised Analyses (http://www.hanford.gov/orp/uploadfiles/TCEIS-Vadose.pdf)

Tolan, T. L., Martin, B. S., Reidel, S. P., Anderson, J. L., Lindsey, K. A., Burt, W. C., 2009, "An introduction to the stratigraphy, structural geology, and hydrogeology of the Columbia River Flood-Basalt Province: A primer for the GSA Columbia River Basalt Group field trips," *Volcanoes to Vineyards: Geologic Field Trips through the Dynamic Landscape of the Pacific Northwest*, Geological Society of America Field Guide 15, p. 599-643.

USGS Bulletin 1457-G, 1979, *Revisions in stratigraphic nomenclature of the Columbia River Basalt Group*, U.S. Geological Survey, Washington, D.C.

USGS-W-P-7, 1949, *Geologic and Hydrologic Features of the Richland Area, Washington, Relevant to the Disposal of Waste at the Hanford Operations of the Atomic Energy Commission; Interim Report No. 1*, U.S. Geological Survey, Department of Interior, Portland Oregon.

van Genuchten, M, Th. 1980, "A Closed-form Equation for Predicting the Hydraulic Conductivity of Unsaturated Soils," *Soil Science Society of America Journal*, Vol. 44, pp. 892-989

WAC 173-160, "Minimum Standards for the Construction and Maintenance of Wells," *Washington Administrative Code*, as amended.

WAC 173-340, "Model Toxics Control Act – Cleanup," *Washington Administrative Code*, as amended.

Wan, J. M., T. K. Tokunaga, E. Saiz, J. T. Larsen, Z. P. Zheng, and R. A. Couture, 2004a, "Colloid Formation at Waste Plume Fronts," *Environmental Science & Technology*, Vol. 38, No. 22, pp. 6066–6073.

Wan, J. M., T. K. Tokunaga, J. T. Larsen, and R. J. Serne, 2004b, "Geochemical Evolution of Highly Alkaline and Saline Tank Waste Plumes during Seepage through Vadose Zone Sediments," *Geochimica et Cosmochimica Acta*, Vol. 68, No. 3, pp. 491–502.

Waters, A. C., 1961, "Stratigraphic and Lithologic Variations in the Columbia River Basalt," *American Journal of Science* Vol. 259, pp. 583-611.

WHC-EP-0883, 1995, *Variability and Scaling of Hydraulic Properties of 200 Area Soils, Hanford Site*, Westinghouse Hanford Company, Richland, Washington.

WHC-MR-0391, 1992, *Field Trip Guide to the Hanford Site*, Westinghouse Hanford Company, Richland, Washington.

WHC-SD-EN-EE-004, 1991, *Revised Stratigraphy for the Ringold Formation, Hanford Site, South-Central Washington*, Rev. 0, Westinghouse Hanford Company, Richland, Washington.

WHC-SD-EN-TI-012, 1992, *Geologic Setting of the 200 East Area: An Update*, Rev. 0, Westinghouse Hanford Company, Richland, Washington.

WHC-SD-EN-TI-147, 1993, *Hydrologic Testing at the Single-Shell Tanks, 1989*, Rev. 0, Westinghouse Hanford Company, Richland, Washington.

WHC-SD-W236A-TI-002, 1996, *Probabilistic Seismic Hazard Analysis, DOE Hanford Site, Washington*, Rev. 1A, Westinghouse Hanford Company, Richland, Washington.

WHC-SD-WM-EE-004, 1995, *Performance Assessment of Grouted Double-Shell Tank Waste Disposal at Hanford*, Rev. 1, Westinghouse Hanford Company, Richland, Washington.

Wicks, C. W., J. S. Gomberg, and C. S. Weaver, 2009, "InSAR measurement of surface deformation at the Hanford Reservation associated with the 2009 Wooded Island earthquake swarm (Invited)," in *American Geophysical Union, Fall Meeting 2009*, San Francisco, California.

WMP-17524, 2003, *Vadose Zone Hydraulic Property Letter Reports*, Rev. 0, Fluor Hanford, Richland, Washington.

WMP-22817, 2004, *Geologic Contacts Database for the 200 Areas of the Hanford Site*, Rev. 0, Fluor Hanford, Inc., Richland, Washington.

Zachara, J. M., R. J. Serne, M. D. Freshley, F. M. Mann, F. J. Anderson, M. I. Wood, T. E. Jones, and D. A. Myers, 2007, "Geochemical Processes Controlling Migration of Tank Wastes in Hanford's Vadose Zone," *Vadose Zone Journal*, Vol. 6, No. 4, pp. 985–1003.